NRC Research and/or Technical Assistance Rept

PDR

EGG-NSMD-6182
February 1983

RELAP5/MOD1 CODE MANUAL

VOLUME 3: CHECKOUT PROBLEMS SUMMARY

R. A. Riemke
H. Chow
V. H. Ransom

Idaho National Engineering Laboratory
Operated by the U.S. Department of Energy

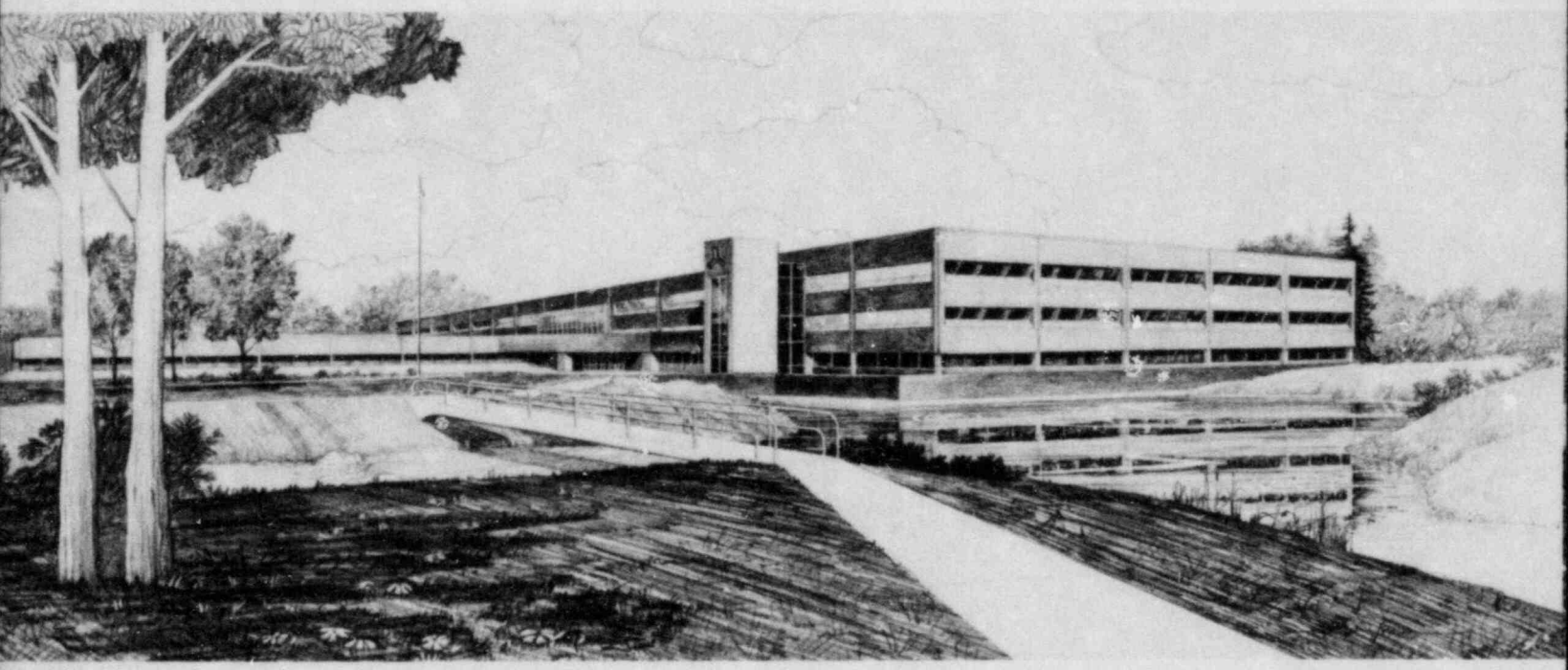

This is an informal report intended for use as a preliminary or working document

Prepared for the
U.S. NUCLEAR REGULATORY COMMISSION
Under DOE Contract No. DE-AC07-76ID01570
FIN No. A6330

EG&G Idaho

EG&G Idaho, Inc.

FORM EG&G-398
(Rev. 11-81)

INTERIM REPORT

Accession No. _____

Report No. EGG-NSMD-6182

Contract Program or Project Title: Nuclear Safety Methods Division

Subject of this Document: RELAP5/MOD1 CODE MANUAL
VOLUME 3: CHECKOUT PROBLEMS SUMMARY

Type of Document: Informal Technical Report

Author(s): R. A. Riemke, H. Chow, V. H. Ransom

Date of Document: February 1983

Responsible NRC/DOE Individual and NRC/DOE Office or Division:

This document was prepared primarily for preliminary or internal use. It has not received full review and approval. Since there may be substantive changes, this document should not be considered final.

EG&G Idaho, Inc.
Idaho Falls, Idaho 83415

Prepared for the
U.S. Nuclear Regulatory Commission
Washington, D.C.
Under DOE Contract No. DE-AC07-76ID01570
NRC FIN No. A6330

INTERIM REPORT

ABSTRACT

This report contains an account of five checkout problems which were used to test RELAP5/MOD1 during its development and refinement. The problems chosen are separate effects experiments, an electrically heated integral system experiment, and a nuclear heated integral system experiment. The code results are compared to data and the discussion contains information relative to the code's ability to simulate the physical phenomena seen in the tests. These problems are intended to provide examples of accepted modeling techniques.

SUMMARY

The RELAP5/MOD1 code is a Light Water Reactor transient analysis code featuring a nonhomogeneous and nonequilibrium two-phase flow model, a transient heat conduction model, control system models, and a reactor kinetics model. These models are integrated into a fast running and user convenient code which is designed for the CDC Cyber 176.

A series of checkout problems have been used to test the code during development. This report contains summaries for five selected problems. The summaries contain discussions of the test apparatus, the RELAP5/MOD1 model of the test, and a comparison of the code results to test data. The problems have been selected to be representative of Pressurized Water Reactor (PWR) separate effects and integral experiments. The particular tests which are summarized are: the General Electric small vessel level swell Test 1004-3, the Marviken III Test 24 which is a large vessel blowdown, the Wyle-LOFT orifice calibration experiment WSB03R, the Semiscale Test S-07-6 electrically heated simulation of a PWR large break blowdown, and the LOFT Test L3-7 which is a nuclear heated system small break loss-of-coolant accident simulation. Each of these test problems serve to illustrate the code's capability to model the phenomena of interest in PWR loss-of-coolant accidents (LOCAs), to illustrate accepted modeling practice, and to serve as a guide for use of the code.

In general, RELAP5/MOD1 provides an accurate model of the nuclear steam supply system transient behavior for the test applications. The known and potential limitations of the code are discussed in an effort to guide the user in application of the code. RELAP5/MOD1 represents a significant advance in the continued development of a very large and sophisticated system transient simulation code and the limitations and utility of the code are not entirely established. The material contained herein is a partial step toward quantifying the accuracy and usefulness of the RELAP5/MOD1 code.

ACKNOWLEDGMENTS

The authors wish to acknowledge the efforts of Dr. Han-Hsiung Kuo who performed the Semiscale S-07-6 calculations and assembled the initial draft of this report. The efforts of the remaining RELAP5 development team, Richard Wagner, Dr. John Trapp, Dr. Ju-Chuan Lin, Dennis Kiser, and Edna Johnson are also gratefully acknowledged.

CONTENTS

FIGURES

TABLES

RELAP5/MOD1 CODE MANUAL

VOLUME 3: CHECKOUT PROBLEMS SUMMARY

1. INTRODUCTION

The purpose of Volume 3 of the RELAP5/MOD1 Code Manual is to document checkout problem results. Five problems are included and range from single separate effects experiments to a nuclear integral experiment. These problems serve both as application examples and as a partial assessment of the code capability.

1.1 RELAP5/MOD1

The RELAP5/MOD1 computer program is the second version of the code to be released and has many improvements and added modeling capabilities compared with the earlier RELAP5/MOD0. RELAP5/MOD1 was released to the National Energy Software Center during December 1980 and is being maintained. The latest version of the code is RELAP5/MOD1/Cycle 19. Each new cycle represents error corrections and/or minor model improvements. Modeling deficiencies which are a result of models yet to be developed or which represent major improvement of constitutive models, will not be corrected in the MOD1 version, but rather will be installed in future versions of the code. RELAP5/MOD2 is currently under development and is scheduled for release during September 1983 through the U.S. Nuclear Regulatory Commission.

RELAP5/MOD1 is primarily intended for modeling of light water reactor blowdown transients, small break LOCAs and operational transients. For this application the generic MOD0 modeling capability for one-dimensional hydrodynamic and associated one-dimensional heat conduction and heat transfer has been extended by modeling additions and improvements. The thermal hydraulic additions include: an accumulator, a steam separator, an annulus component, a noncondensible gas field, and a boron solute field. The associated model improvements include: revised flow regime maps to include vertical and horizontal flow with a stratified regime in the horizontal map, a horizontal

stratified flow model, a stratified break flow model, an improved and more implicit break flow model, and additional heat transfer correlations for condensing heat transfer, natural circulation, and pool boiling.

The system time modeling capability has been expanded by addition of a reactor kinetics model, general control valves, and a control system model. The reactor kinetics model is a point or zero-dimensional model that includes gamma decay heat. Power from the kinetics model can be used as an internal heat source for fuel pins and direct moderator heating. Reactivity effects from the hydrodynamic and heat conduction solutions is provided, but the effect of boron on reactivity has not been included.

The added valve modeling capability includes a motor operated valve and a general servo controlled valve which can be controlled by trips or control system variables. The control system model allows the user to define control variables that are the results of addition, subtraction, multiplication, division, exponentiation, differentiation, and integration on any of the variables advanced in time, including control variables. The control system design allows simultaneous, nonlinear, algebraic and differential equations to be defined and advanced in time.

The RELAP5 capability is being further extended through the development of RELAP5/MOD2 for all pressurized water reactor transients including reflood. The added capability in RELAP5/MOD2 will include new modeling, improvements to existing models, and new user conveniences.

1.2 Intended Application of RELAP5/MOD1

RELAP5/MOD1 is intended for use in transient simulation of pressurized water reactor systems under operational conditions and postulated accident conditions for reactor safety analysis. The code features generic modeling capability for steam-water-thermal systems and can be used to represent both primary and to a limited extent, the secondary system of a reactor. Models are also included for the plant trips, control systems, and neutronic system.

The code is equally applicable for transient analysis of any steam-water thermal-hydraulic system within the limitations of the constitutive models. This generic modeling capability is a major strength of the code and permits modeling a very wide variety of system components. Other strengths are the fast execution capability and the user convenience features. These conveniences include SI/British input/output options, restart and renodalization capability, and extensive input checking for recognizable errors.

1.3 Known Limitations of RELAP5/MOD1

In general, the code applicability is limited to steam-water systems at pressures from 2000 Pa to the critical pressure of water. (The code may function at super critical pressures; however, no assessment under such conditions has been undertaken.) The hydraulic behavior of steam-water-noncondensible systems can be modeled, but the constitutive models, particularly the convective heat transfer models, do not include consideration of the noncondensible field and may fail under some conditions when noncondensibles are present.

The constitutive models for the temperature constraint and the interphase mass transfer model are applicable to depressurization with moderate heat transfer. These models are not suitable for repressurization with a stratified and stable interface or to post-CHF conditions where high vapor superheat may exist. Thus, the code may not predict the correct behavior of refill transients involving reflood and repressurization. The constitutive model for wall heat transfer is based on equilibrium boiling heat transfer correlations and as such does not apply to subcooled boiling and post-CHF regimes (the predicted heat transfer rates may be accurate but no net vapor generation will result until bulk saturation occurs and no superheating of the vapor will occur until total dryout occurs).

The models for density stratification in horizontal components have been developed and assessed using a very limited data base. These models include: stratified flow in horizontal components, vapor pull through/liquid entrainment at abrupt area changes under stratified flow conditions, and vapor pull through/liquid entrainment at locations of choked flow either internally or at external discharge points. The data used for development of these models were obtained using air-water mixtures and thus, the effect, if any, of interphase mass transfer is not included. Such stratification effects are known to be important in LWR systems operating in reflux cooling modes, at branch connections such as the pressurizer surge line connection to the hot leg, and at flow discharge points for small break LOCAs.

While there are no known limitations of the stratification models for horizontal components, the user should be cautioned that very limited data exist for testing of such models. Only the LOFT-Wyle blowdown orifice calibration experiment was used for developmental testing. The main objective of this test was orifice calibration and as such, the stratification data is limited. More specialized separate effects data is needed for an accurate assessment.

The interphase drag formulation has several known limitations. In general, the interphase drag at interfaces or steep spatial void gradients is difficult to model because it depends on many variables such as rates of flow, presence of heat transfer, component orientation, flow geometry, etc. The model used in the RELAP5 code does not include many of these dependencies. The present model tends to predict void oscillations occurring near points of large void gradient. This has generally been observed in vertical flow situations such as level swell associated with depressurization. The void oscillations are nonphysical and vary with nodalization and time step size. The cause of these void oscillations is not fully understood, but seems to be a result of basing the interphase drag on volume average conditions without explicit tracking of void discontinuities. Other factors may be the fact that only time average behavior of the interphase drag is modeled and in reality the factors

influencing interphase drag, such as flow regime, are dynamic and may exhibit hysteresis effects which is beyond present modeling capability. In many cases, the void oscillation does not materially affect the overall calculated result since the liquid inventory and hydrostatic head may not be affected. Careful inspection of calculated results in vertical components where voids are generated is recommended. Such situations include vessel depressurization, the secondary side of steam generators, etc.

Another potential problem related to the interphase drag model is the prediction of CCFL phenomena. No developmental assessment of the code against CCFL data has been carried out, but there have been indications from LOFT calculations under reflux cooling modes of operation, that the CCFL phenomena at the steam generator tube entrances may not be predicted accurately. This phenomenon is characterized by countercurrent flow of a liquid condensate film which becomes unstable and transitions to slug flow. Accurate prediction of such CCFL conditions may require an empirical model similar to the Wallis or Kutadaladze flooding correlation which can be used to determine the interphase drag or relative velocity.

Some general limitations of the code include the one-dimensional representation of flow passages, one-dimensional representation of heat conduction paths, and the point or zeroth-dimensional representation of the reactor kinetics model. These limitations are consistent with the intended application of the code, i.e., representation of overall system effects and component interactions rather than a detailed local representation.

Some limitations of the user conveniences are that the renodalization capability is incomplete for heat structures, general tables and material properties tables. The internal plot package is limited to plotting only the results generated on a particular run and cannot provide plots on a restart.

1.4 Checkout Problems for RELAP5/MOD1

The checkout problems which are summarized in this report do not include all the problems used for development of the code, but are

considered representative of the more significant tests. The problems included do not utilize all features of the code and thus, are of limited comprehensiveness. In particular, neither a control system nor a core neutronic system is modeled. These particular models have not been checked against data, but rather have been checked against analytical solutions and previous code results such as from RELAP4 in the case of neutronics.

The problems which are presented represent accepted modeling practice (with certain exceptions which are noted in the discussions) and have been found to yield simulations which fall within uncertainty bounds when both code model uncertainty (i.e., one-dimensional, node size, and system approximations) and data uncertainty are considered. Where the results fall outside these uncertainties, it is discussed in the text. Some insights with regard to the model development are discussed and the input decks are included as appendices in order to serve as examples.

All problems presented herein were run with RELAP5/MOD1/Cycle 17 with the updates contained in Appendix A. In addition, the two systems problems were run with the updates in Appendix F, since they both contain an accumulator component. The updates listed in Appendices A and F have been subsequently incorporated into Cycle 18 of RELAP5/MOD1. As noted in the text, some additional updates of a diagnostic nature were used to explore unphysical behavior. With regard to these updates, Appendix H (turns pump dissipation off) is strictly a diagnostic update and is not intended to be incorporated into any future versions of RELAP5/MOD1. Appendix I (multiplies VISC term by 1/2 $ARAT^2$), however, is considered to be a model correction and will be incorporated into Cycle 20. Other corrections have been made in Cycles 18 and 19. These are largely concerned with models not employed by the problems presented here, and they would be expected to have little or no impact on this work.

For each test problem the following sequence will be followed in the report: First, the purpose of the test along with the reason why it was selected will be presented; second, a description will be presented of the test facility along with the initial conditions for the test; third, a

description of the RELAP5 model along with the input deck will be presented; fourth, the reasons for many of the modeling practices used will be presented, and finally, calculated results will be compared to experimental results and discussed.

The separate effects tests are the General Electric (GE) Level Swell Test 1004-3, the Marviken III Test 24, and the Wyle Small Break Test WSB03R. The systems tests are the Semiscale MOD3 S-07-6 Posttest Analysis and the LOFT L3-7 Posttest Analysis.

2. TEST PROBLEMS

2.1 Separate Effects Tests

2.1.1 GE Level Swell Test 1004-3

2.1.1.1 Purpose. The GE level swell test 1004-3[1] involves a vertical vessel which is initially pressurized and partially filled with saturated water. The test is initiated by opening a simulated break near the top of the vessel. As the vessel depressurizes a two-phase mixture is formed in the vessel and the transient void distribution is measured to provide a test of two-phase interphase momentum interaction. The data are useful for testing the interphase drag formulation of two-phase mathematical descriptions.

2.1.1.2 Test Description. The GE level swell test facility consists of a 0.3048 m (1 ft) diameter, 4.2672 m (14 ft) long vertically oriented cylindrical pressure vessel, a blowdown line containing an orifice, and a suppression pool at atmospheric conditions. A schematic of the vessel and the portion of the blowdown line containing the orifice is shown in Figure 1. The vessel, which initially contains both liquid water and steam at saturation conditions, discharges to the atmosphere through the break orifice 0.009525 m (3/8 in.) I.D. located within the 0.0508 m (2 in.) Schedule 80 blowdown pipe at the top of the vessel. Measurements made during the test transient included system pressure obtained by means of a pressure transducer at the top of the vessel and differential pressure measurements over 0.6096 m (2 ft) vertical intervals along the vessel. The differential pressure measurements were converted to mean void fraction at each level by assuming hydrostatic conditions to exist at all times. Further information on the data reduction method can be obtained from Reference 1.

2.1.1.3 RELAP5 Model. The RELAP5 model of the GE test facility is shown in Figure 1. The vessel was approximated as a cylinder which had the same height as the vessel. It was modeled using a vertical 29 volume pipe component. The volumes in the pipe were 0.1524 m (0.5 ft) high, except for

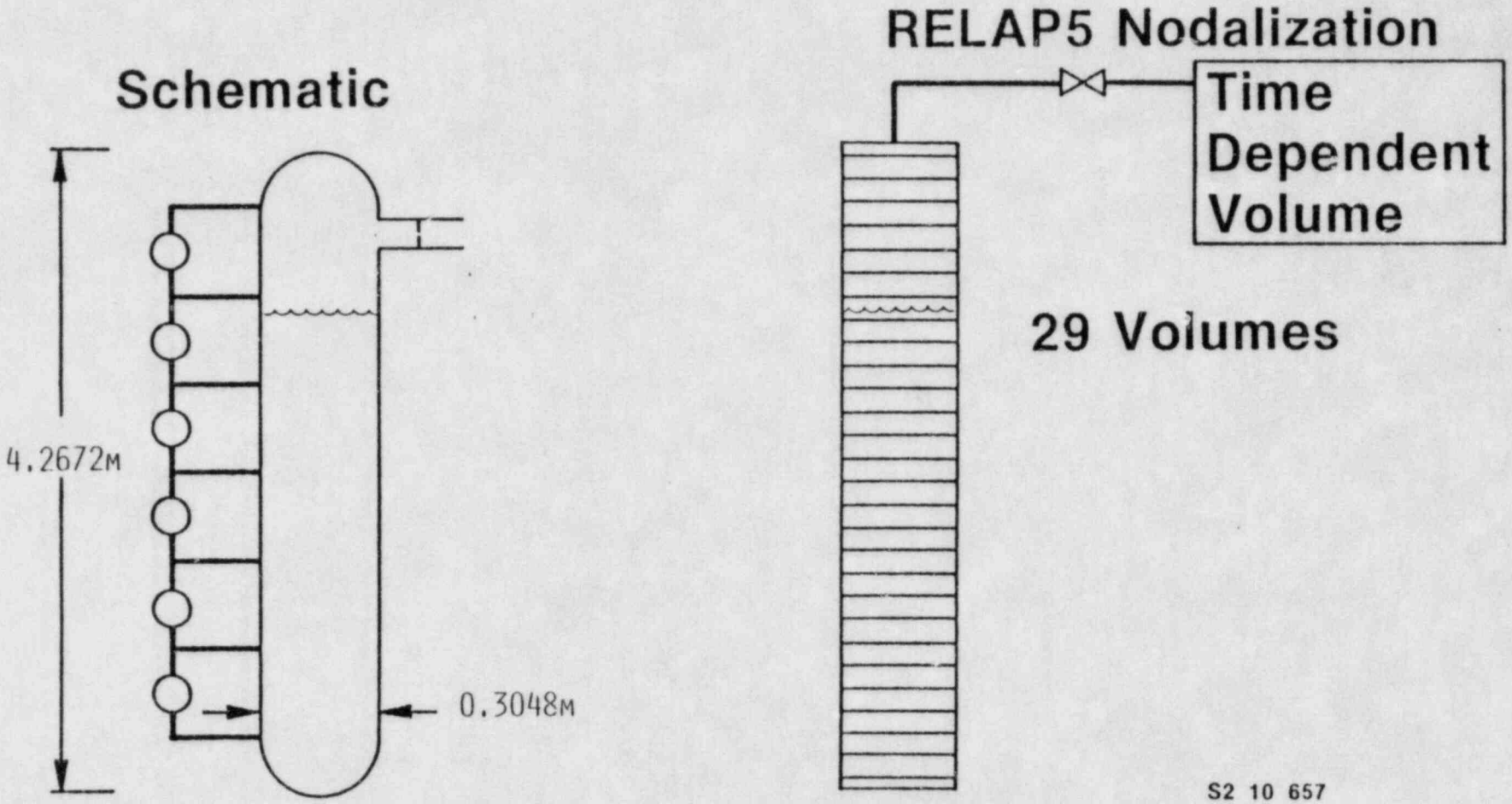

FIGURE 1. SCHEMATIC AND RELAP5/MOD1 NODALIZATION FOR GE LEVEL SWELL TEST 1004-3.

the volumes at the top and bottom. These volumes were 0.0762 m (0.25 ft) high and were made half the height of the other volumes in order that the 0.6096 m (2 ft) vertical intervals used for the void fraction comparisons would coincide with the volume centers.

The orifice in the blowdown pipe was modeled as a trip valve which was opened for times greater than 0.07 seconds. The abrupt area change option in code was used to model this orifice. In the calculation of this level swell problem, a two-phase discharge coefficient for the valve was taken to be 0.70. This value was used because it is approximately the value found for a discharge coefficient for orifices.[2]

The blowdown pipe was not modeled for this simulation since the discharge orifice is choked throughout the experiment. A time dependent volume component at atmospheric conditions was connected to the valve to represent the suppression pool at atmospheric conditions.

2.1.1.4 Simulation Results and Discussion. RELAP5/MOD1/CY=17, with the update listed in Appendix A, was used to simulate the experiment out to 200 seconds, which required 223 CPU seconds. As the deck in Appendix B shows, for the first one second, a user inputted maximum time step (Δt) of 0.01 seconds was specified, and from 1 to 200 seconds, a user inputted maximum Δt of 0.02 seconds was specified. The very small user inputted maximum Δt of 0.01 seconds from 0 to 1 seconds was used to assure accurate modeling of the trip valve which opened at 0.07 seconds. Figure 2 shows the comparison of data and the RELAP5 results for the pressure in the top of the vessel. The RELAP5 calculation is slightly below the data, but the trend is good. Figure 3 shows the comparison of data and RELAP5 for the void fraction at the 3.6576 m (12 ft) level. When the valve opened, the system depressurized and the water or two-phase mixture swelled as vapor was generated. The void at the top of the vessel dropped when water was carried to the top. This is followed by an increase in void as the system continues to blowdown and the mixture level recedes. Figure 3 shows that the RELAP5 calculation compares fairly well to the data for this process. The void comparisons at the lower elevations of 1.8288 m (6 ft) and

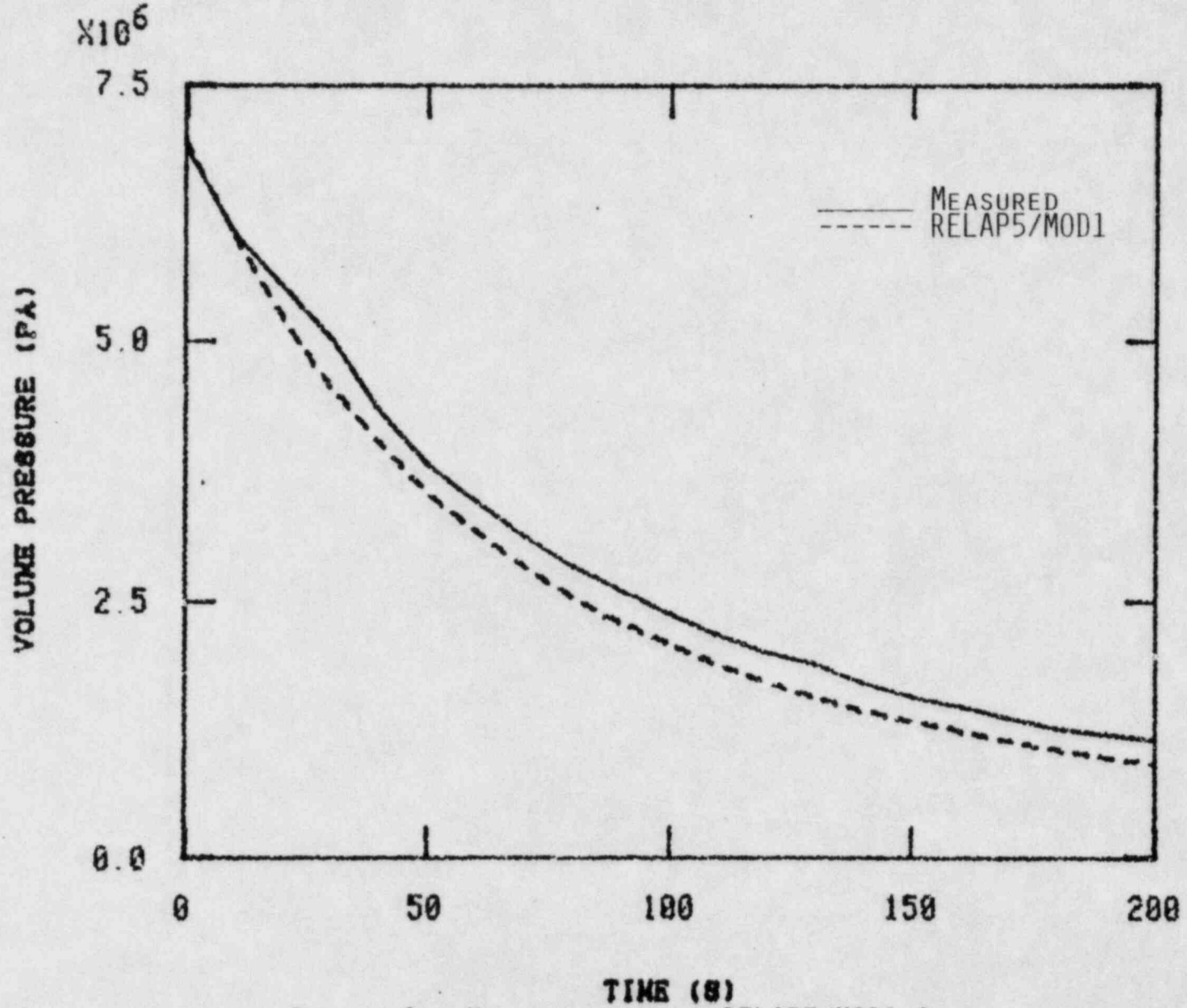

FIGURE 2. MEASUREMENT AND RELAP5/MOD1 CALCULATION OF GE LEVEL SWELL TEST 1004-3 PRESSURE IN THE TOP OF THE VESSEL (SMALL MAXIMUM Δt).

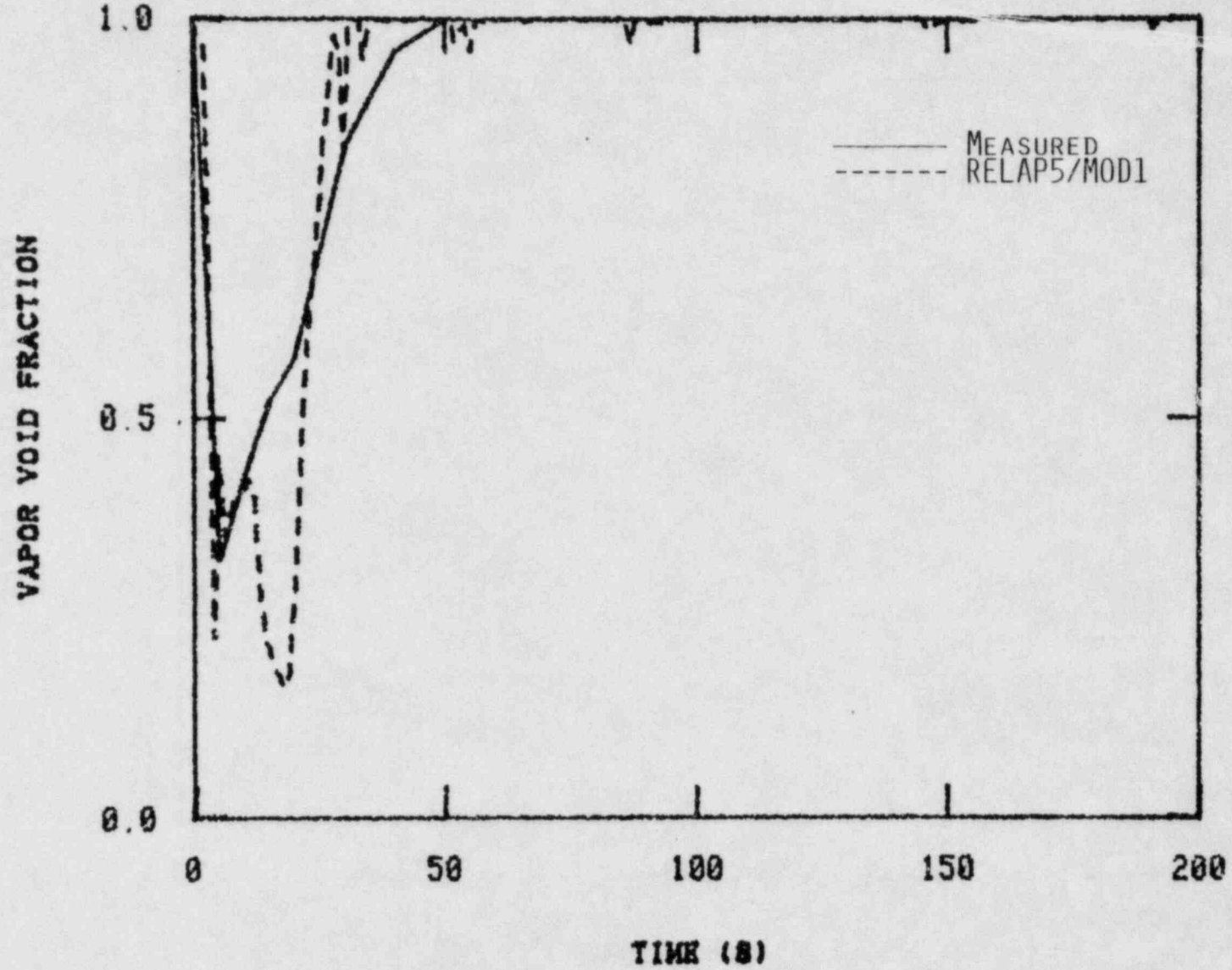

FIGURE 3. MEASUREMENT AND RELAP5/MOD1 CALCULATION OF GE LEVEL SWELL TEST 1004-3 VOID FRACTION AT 3.6576M (12 FT.) ABOVE THE BOTTOM OF THE VESSEL (SMALL MAXIMUM Δt).

0.6096 m (2 ft) are shown in Figures 4 and 5, and also compare well to the data. We have also recast the data and the RELAP5 calculation in terms of void fraction versus position in the vessel. Figures 6, 7, and 8 show these comparisons for times equal to 40, 100, and 180 seconds. These plots were obtained by a straight line connection of the data and RELAP5 calculation points from vessel levels 0.6096 m (2 ft), 1.2192 m (4 ft), 1.8288 m (6 ft), 2.4384 m (8 ft), 3.0480 m (10 ft) and 3.6576 m (12 ft). The results compare well for the two early times, but the later time shows that the calculation predicts too little void at the 2.4384 m (8 ft) level.

The input deck in Appendix B was changed to increase the user inputted maximum Δt to 0.1 seconds for 1 to 200 seconds. Again, using RELAP5/MOD1/CY=17 with the update listed in Appendix A, the simulation were carried out to 200 seconds and for this case only 79 CPU seconds were required. This fast running result was not without penalty, however, as the calculated system pressure was higher than the data (Figure 9), and the void fraction versus time plots showed considerable oscillation. Figures 10, 11, and 12 are shown for the 3.6576 m (12 ft), 1.8288 m (6 ft), and 0.6096 m (2 ft) levels. As a result of this problem, it is recommended that the user perform convergence studies in which the maximum permitted time step is increased and decreased. This is particularly important when two-phase conditions exist in vertical components.

The code currently uses an arithmetic time average for the interphase drag, that is, it sums one half the new and one half the old values. By using variable underrelaxation rather than a simple time average to calculate interphase drag, the code can be made to run at larger time steps without exhibiting large void fraction oscillations in time. More recently in the MOD2 development effort, a more mechanistic interphase drag model along with new flow regime maps has been added and this also improved the agreement with data for many problems. These features (underrelaxation, more mechanistic interphase drag, new flow regime maps) have not been added to RELAP5/MOD1, but will be available in RELAP5/MOD2.

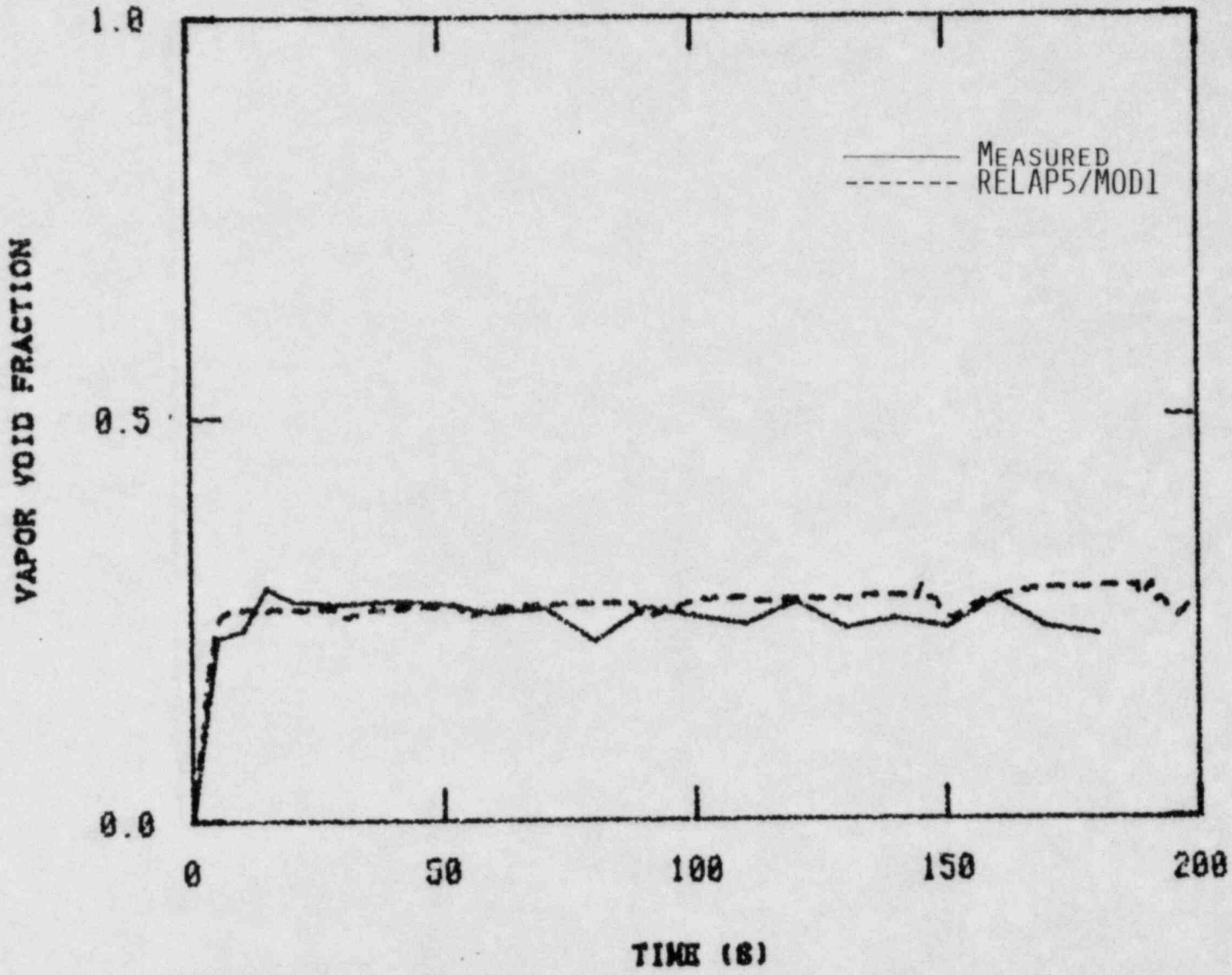

FIGURE 4. MEASUREMENT AND RELAP5/MOD1 CALCULATION OF GE LEVEL SWELL TEST 1004-3 VOID FRACTION AT 1.8288M (6 FT.) ABOVE THE BOTTOM OF THE VESSEL (SMALL MAXIMUM Δt).

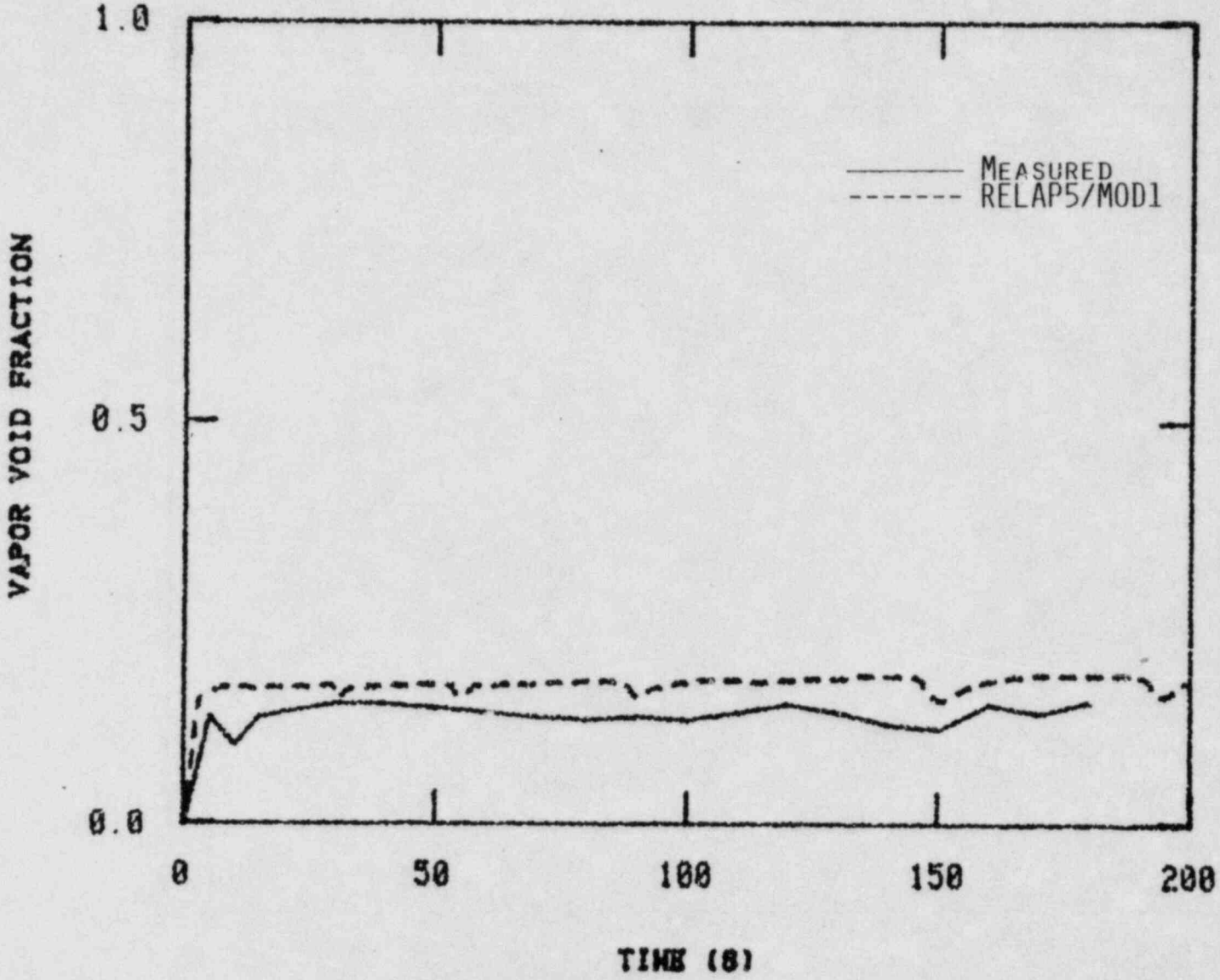

FIGURE 5. MEASUREMENT AND RELAP5/MOD1 CALCULATION OF GE LEVEL SWELL TEST 1004-3 VOID FRACTION AT 0.6096M (2 FT.) ABOVE THE BOTTOM OF THE VESSEL (SMALL MAXIMUM Δt).

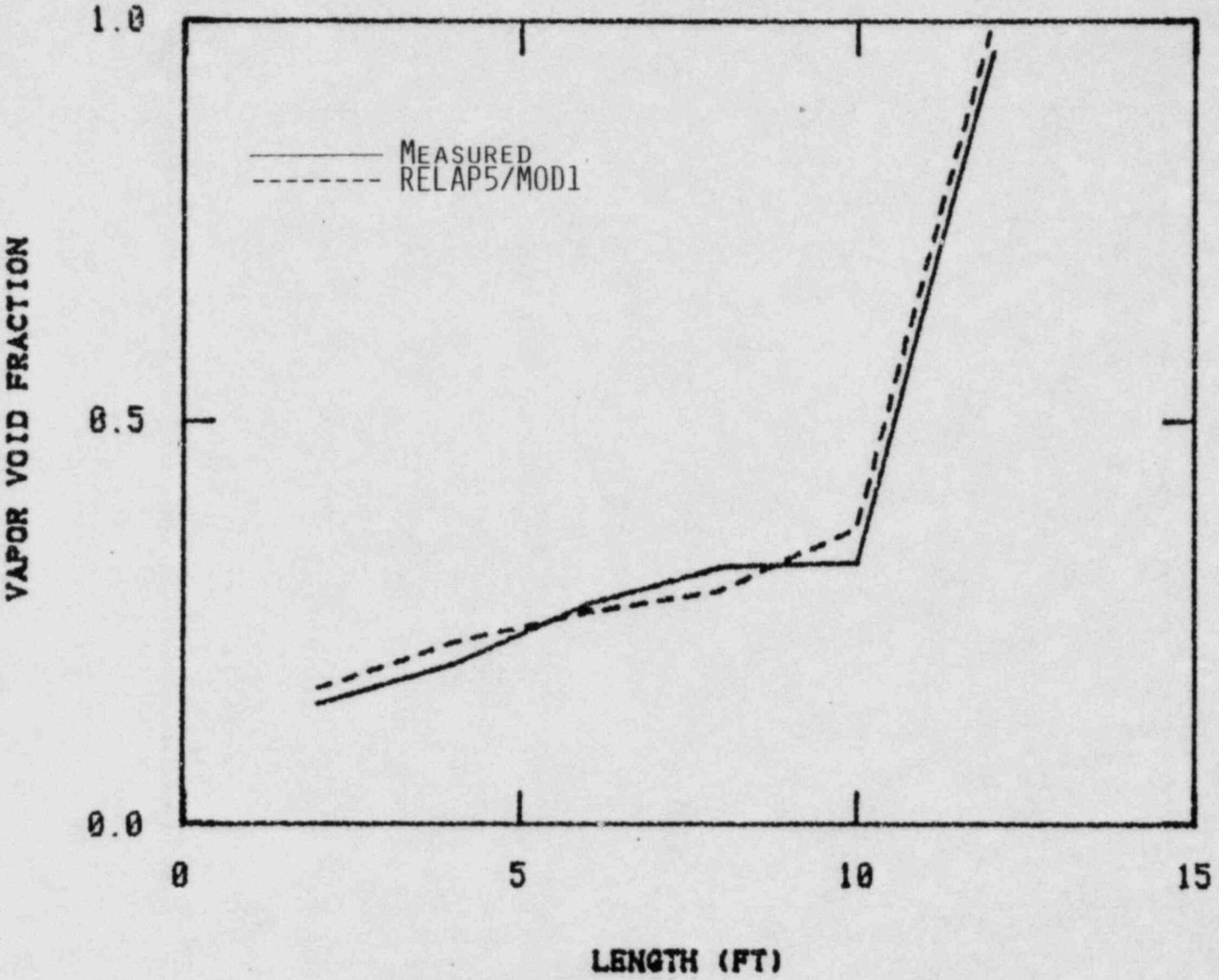

FIGURE 6. MEASUREMENT AND RELAP5/MOD1 CALCULATION OF GE LEVEL SWELL TEST 1004-3 VOID FRACTION PROFILE IN THE VESSEL AT 40 SECONDS (SMALL MAXIMUM Δt).

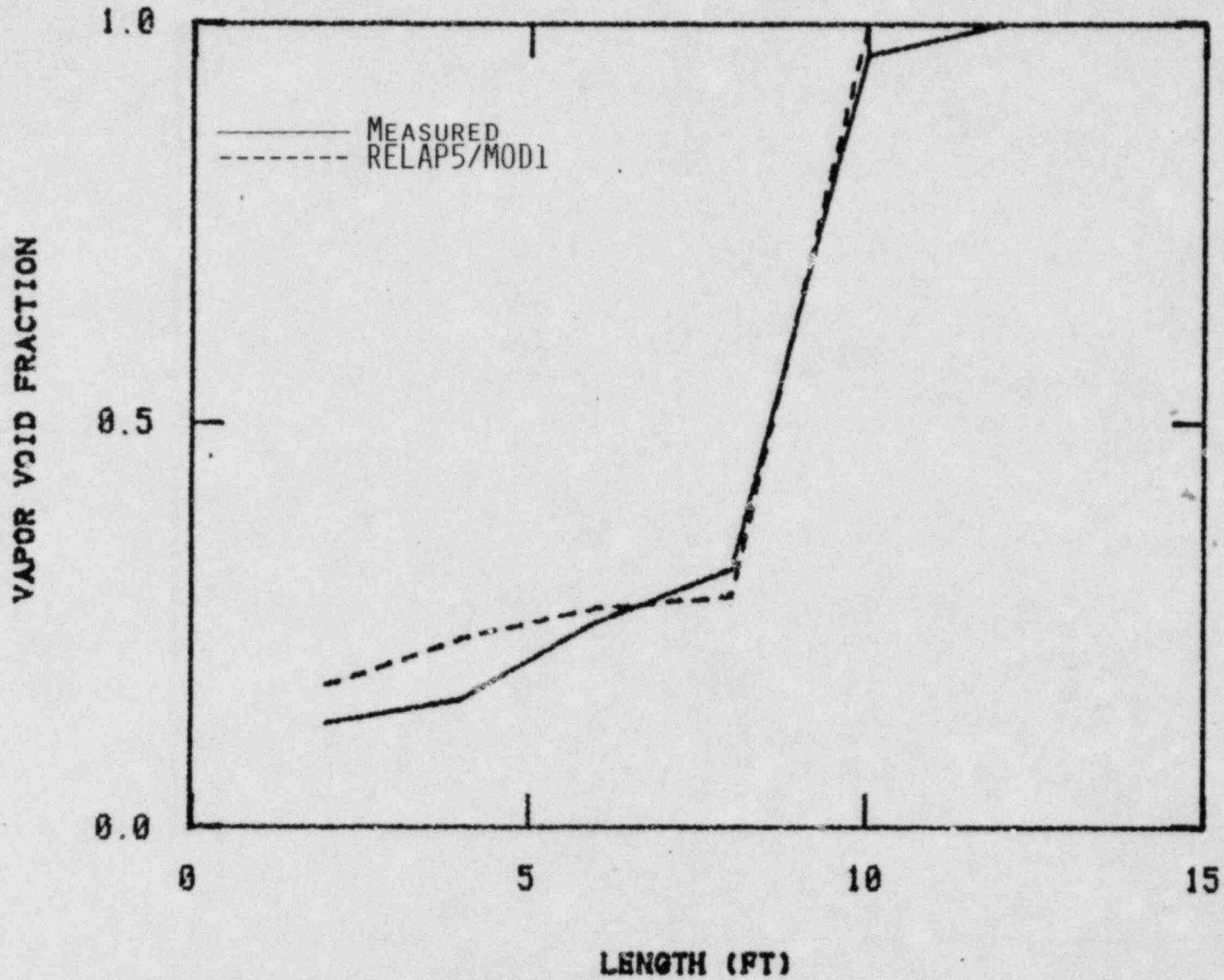

FIGURE 7. MEASUREMENT AND RELAP5/MOD1 CALCULATION OF GE LEVEL SWELL TEST 1004-3 VOID FRACTION PROFILE IN THE VESSEL AT 100 SECONDS (SMALL MAXIMUM Δt).

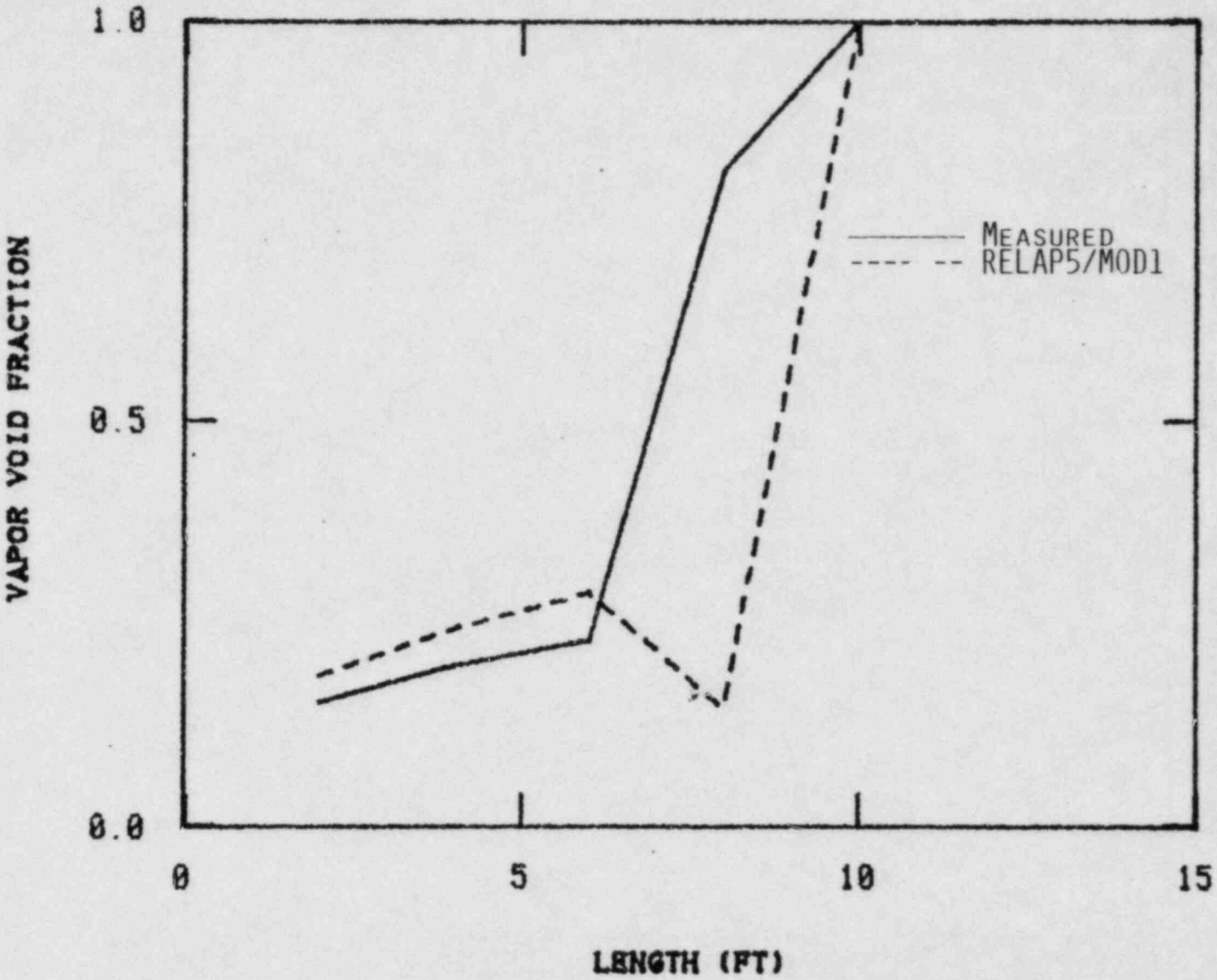

FIGURE 8. MEASUREMENT AND RELAP5/MOD1 CALCULATION OF GE LEVEL SWELL TEST 1004-3 VOID FRACTION PROFILE IN THE VESSEL AT 180 SECONDS (SMALL MAXIMUM Δt).

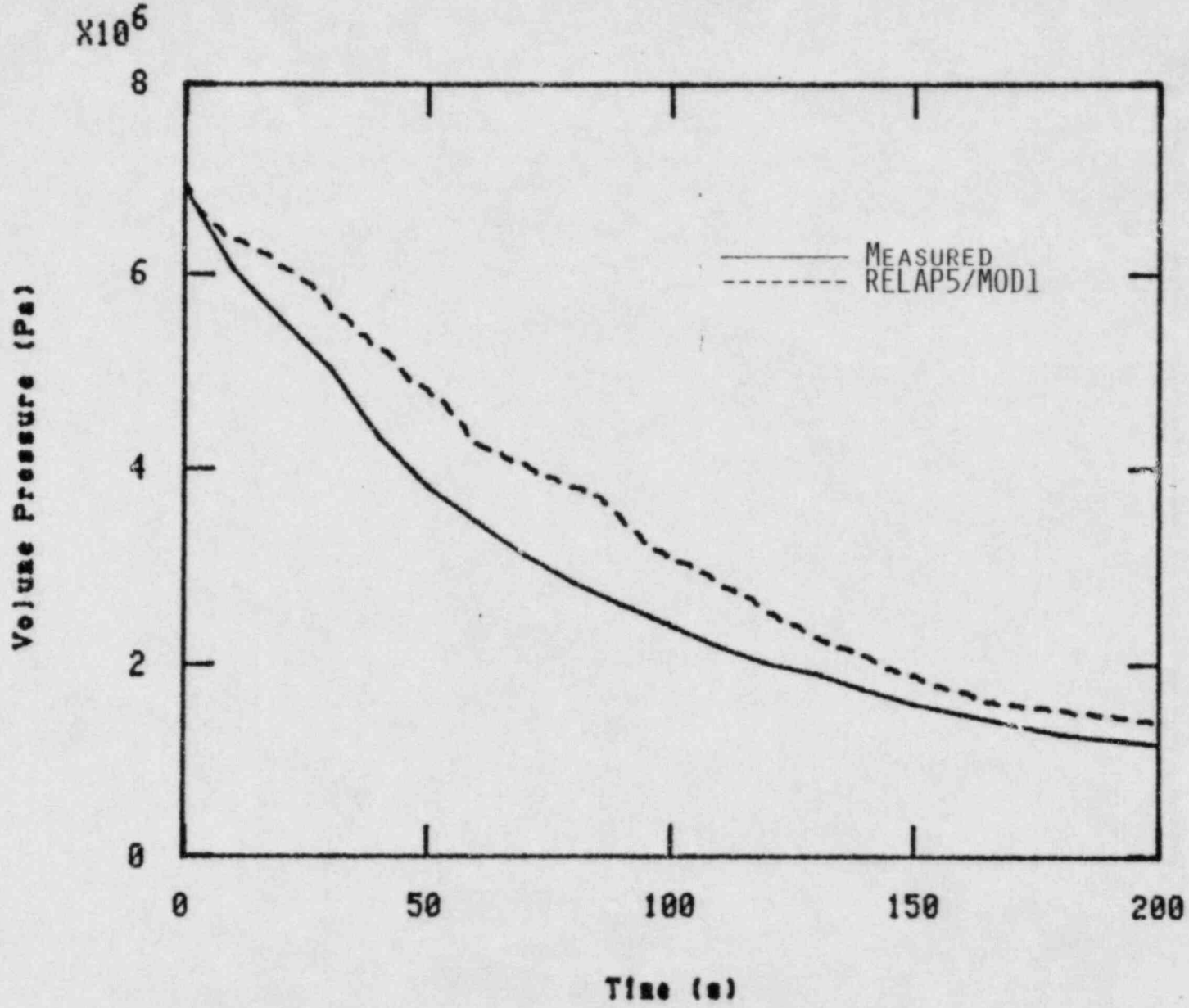

FIGURE 9. MEASUREMENT AND RELAP5/MOD1 CALCULATION OF GE LEVEL SWELL TEST 1004-3 PRESSURE IN THE TOP OF THE VESSEL (LARGE MAXIMUM Δt).

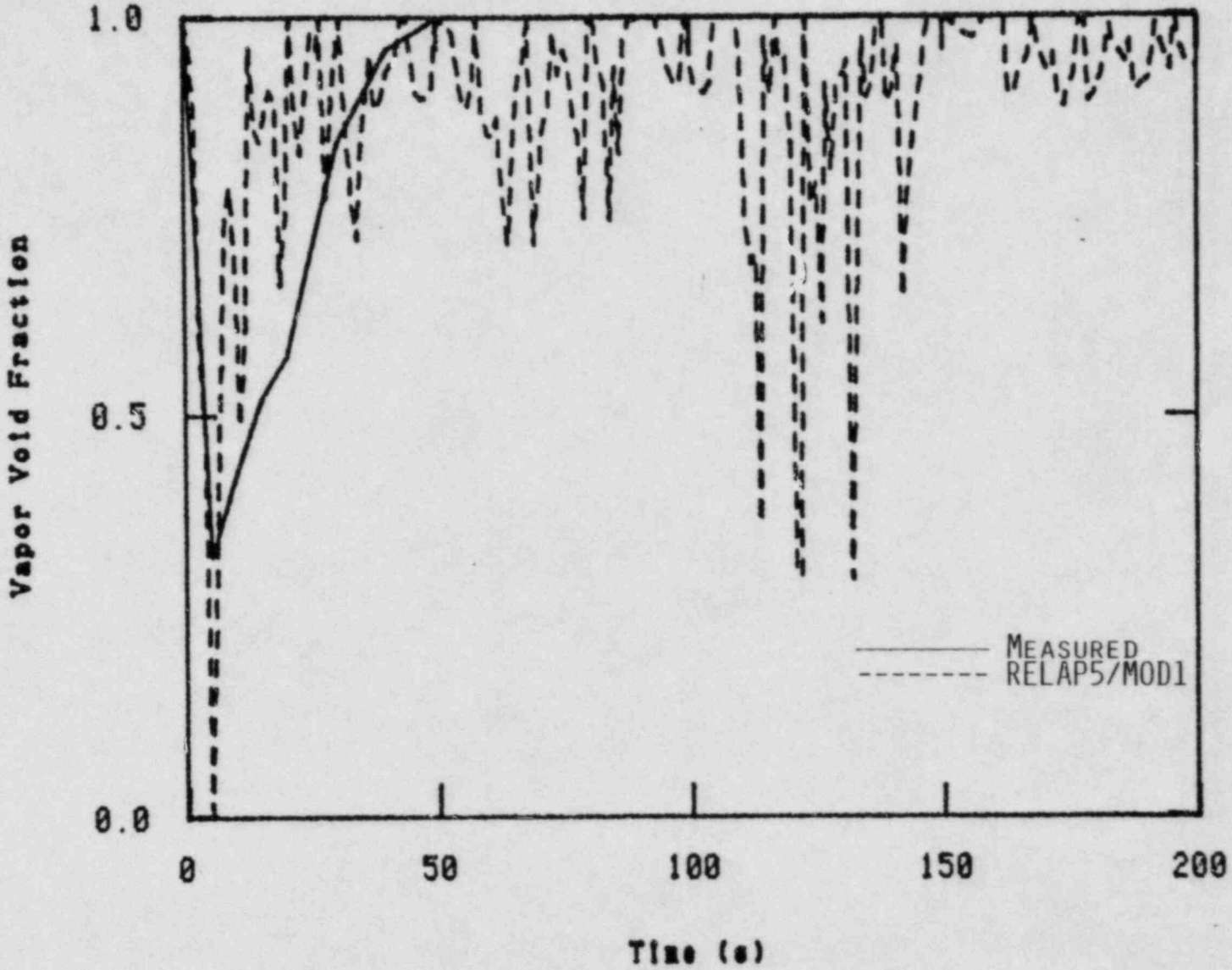

FIGURE 10. MEASUREMENT AND RELAP5/MOD1 CALCULATION OF GE LEVEL SWELL TEST 1004-3 VOID FRACTION AT 3.6576M (12 FT.) ABOVE THE BOTTOM OF THE VESSEL (LARGE MAXIMUM Δt).

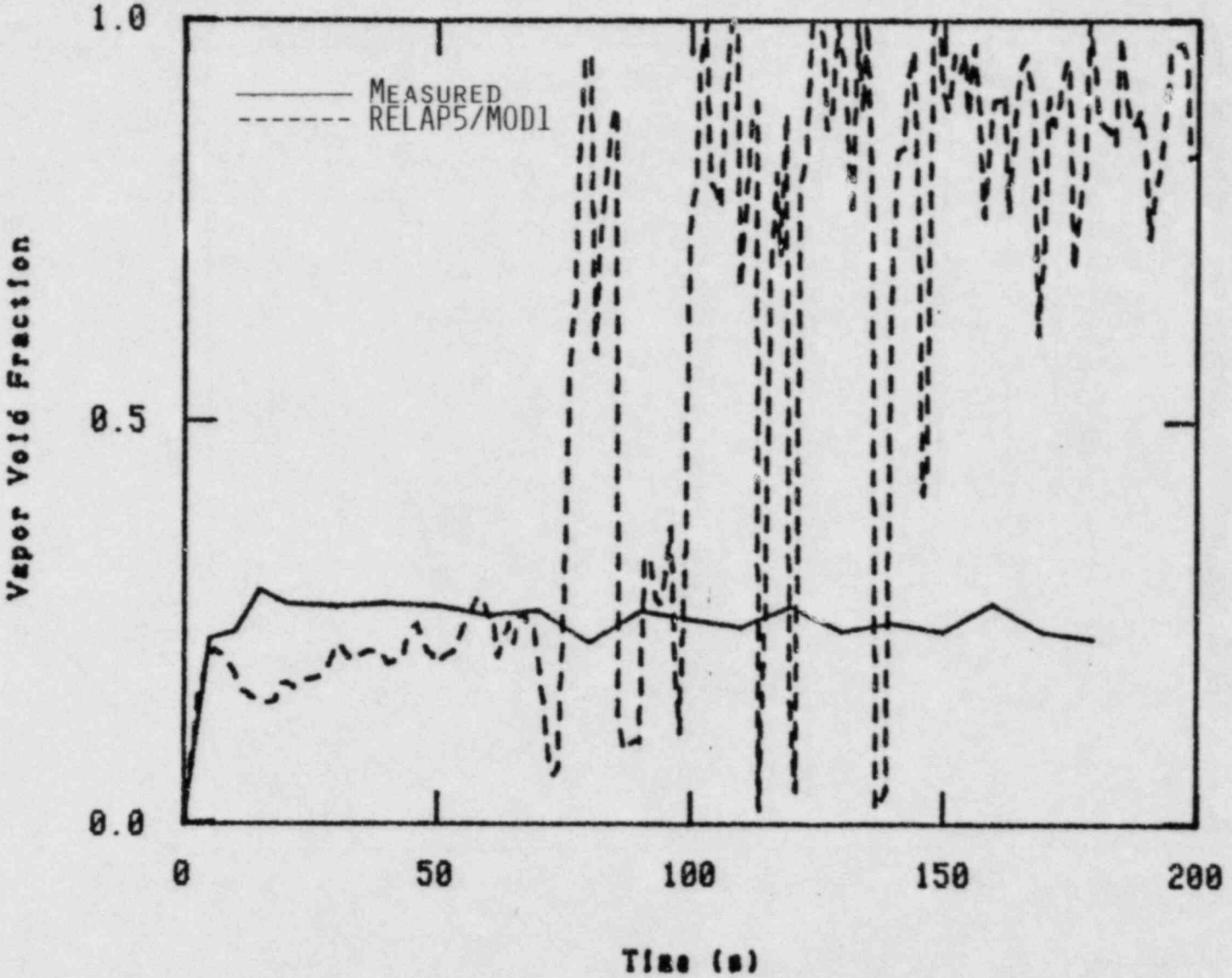

FIGURE 11. MEASUREMENT AND RELAP5/MOD1 CALCULATION OF GE LEVEL SWELL TEST 1004-3 VOID FRACTION AT 1.8288M (6 FT.) ABOVE THE BOTTOM OF THE VESSEL (LARGE MAXIMUM Δt).

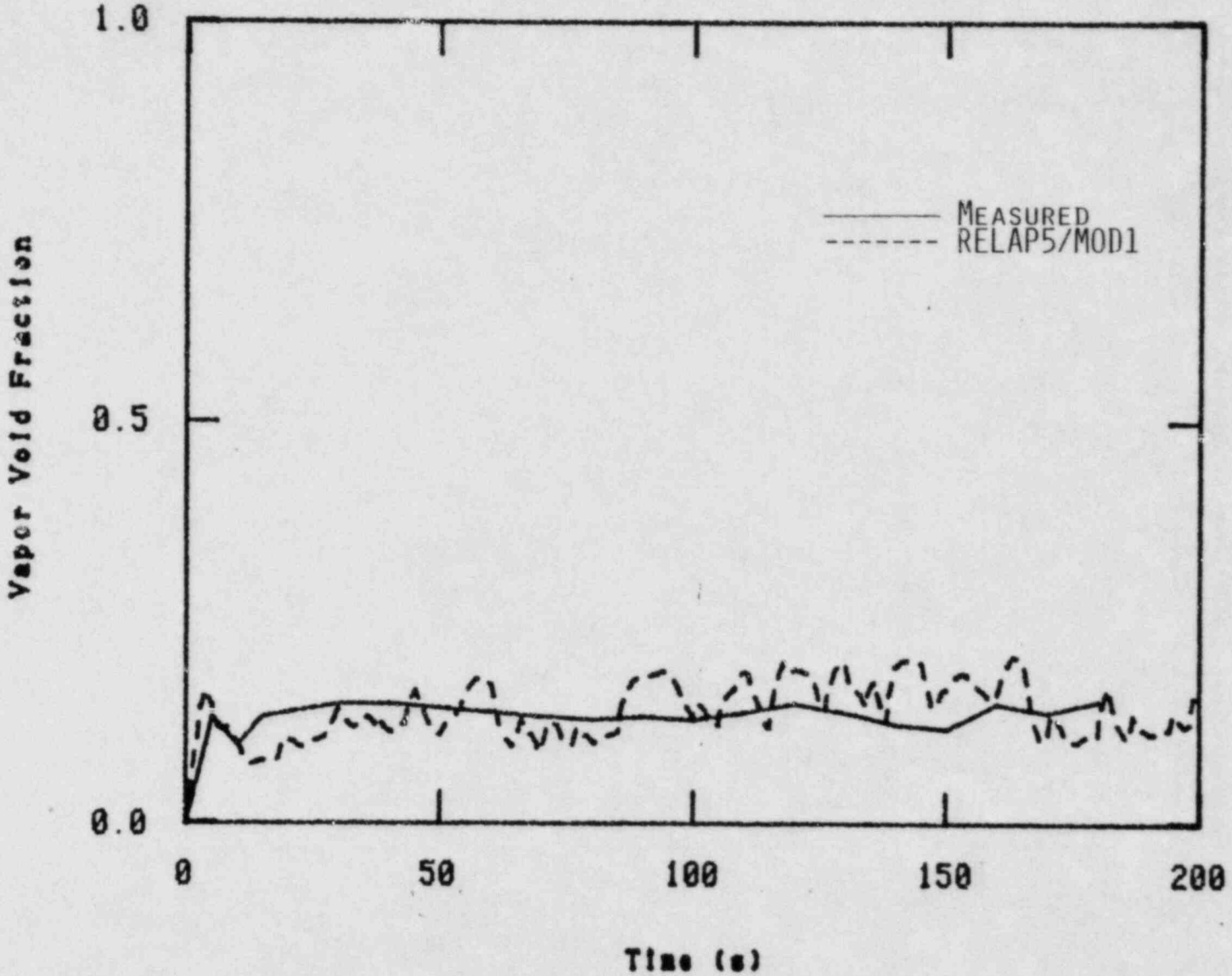

FIGURE 12. MEASUREMENT AND RELAP5/MOD1 CALCULATION OF GE LEVEL SWELL TEST 1004-3 VOID FRACTION AT 0.6096M (2 FT.) ABOVE THE BOTTOM OF THE VESSEL (LARGE MAXIMUM Δt).

In summary, the RELAP5/MOD1 simulation of GE Test 1004-3 shows good agreement with the data, suggesting that the interphase drag calculation is reasonable. If the user inputted maximum Δt is increased to reduce run time, oscillations in void versus time occur.

2.1.2 Marviken III Test 24

2.1.2.1 Purpose. Marviken III Test 24, a full-scale critical flow test, is selected to checkout and evaluate the RELAP5 choked flow model. Because of the short nozzle design (L/D = 0.33) and the long duration (about 20 seconds) of subcooling at the break, the test is particularly well-suited for establishing the applicability of the RELAP5 subcooled choking criterion, which is based on the Alamgir-Lienhard-Jones subcooled nucleation correlation.[2]

2.1.2.2 Test Description. Marviken III Test 24 is the twenty-fourth test in a series of full-scale critical flow tests performed as a multi-national project at the Marviken Power Station in Sweden.[3] The test equipment consisted of four major components: a pressure vessel, a discharge pipe, a test nozzle, and a rupture disc assembly.

The pressure vessel was originally a part of the Marviken nuclear power plant. Of the original vessel internals, only the peripheral part of the core superstructure, the cylindrical wall, and the bottom of the moderator tank remained. Gratings were installed at three levels in the lower part of the vessel to prevent the formation of vortices which might enter the discharge pipe. The vessel had an inside diameter of 5.22 m and was 24.55 m high from the vessel bottom to the top of the top-cupola. The net available internal volume was 420 m^3.

The discharge pipe consisted of seven elements including an axisymmetric inlet section, a connection piece, two pipe spools, two instrumentation rings, and an isolation ball valve. The internal diameters of the connection piece, pipe spools, and instrumentation rings were all 752 mm. The flow path through the ball valve contained fairly abrupt diameter

changes of 30 mm. The axial distance from the discharge pipe entrance to the end of the discharge pipe (nozzle entrance) was 6.3 m.

The test nozzle was connected to the lower end of the discharge pipe. The nozzle consisted of a rounded entrance section followed by a constant diameter test section, 500 mm in diameter with a length-to-diameter ratio (L/D) of 0.33 for Test 24.

A rupture disc assembly was attached to the downstream end of the test nozzle. The assembly contained two identical rupture discs, and the test was initiated by overpressurizing the volume between the discs. This overpressure caused the outer disc to fail, which subsequently resulted in the failure of the inner disc. Failure of the discs was designed to occur along the entire periphery so that they were completely removed from the nozzle exit.

A schematic of the pressure vessel and discharge pipe is shown in Figure 13 (see Reference 3 for detailed drawings). The initial water level in the vessel was at an elevation of 16.7 m above the discharge pipe inlet. A warm-up process was then applied to produce a temperature profile as shown in Figure 13. From the top of the vessel down, the fluid conditions were as follows: a steam dome (above 19.88 m) saturated at 4.96 MPa, a saturated liquid region extended for about 2 m, and a transition region where the temperature dropped rapidly down to 504 K at the discharge pipe inlet. The fluid at the bottom of the vessel was about 32 K subcooled relative to the steam dome temperature. The test was initiated at the above fluid conditions by releasing the rupture disc. The ball valve started to close after 55 seconds and was fully closed at 65 seconds.

2.1.2.3 RELAP5 Model. A sketch of the RELAP5 nodalization is shown in Figure 13. The vessel was represented by 39 volumes and was subdivided from the top as follows: 1 volume for the top-cupola, 1 volume for the steam dome, 1 volume for the two-phase interface region, 36 volumes of equal length (0.5 m) for the main portion of the vessel, and 1 volume for

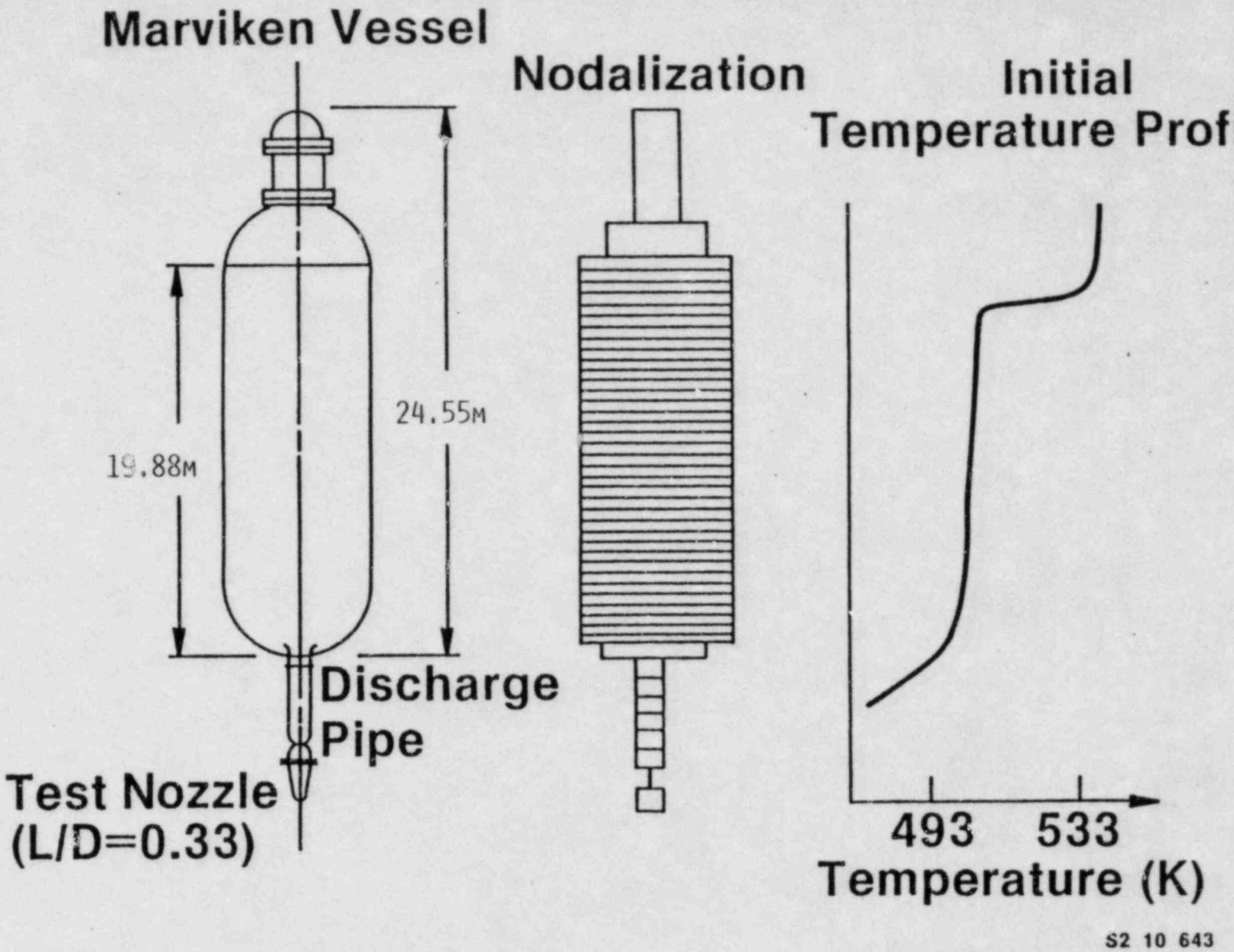

FIGURE 13. SCHEMATIC, RELAP5/MOD1 NODALICATION, AND INITIAL TEMPERATURE PROFILE FOR MARVIKEN TEST 24.

the bottom of the vessel which takes into account the standpipe entrance. All junctions in the vessel were modeled using the smooth option. The discharge pipe was modeled by 6 volumes. The third and fifth functions of the discharge pipe were modeled abrupt, while the rest were modeled smooth. The nozzle was modeled as a single junction with a smooth area change, and no special nodalization was used in the nozzle region. This was possible because RELAP5 includes an analytical choking criterion which is applied at the throat of the nozzle. Details of the geometry and initial conditions are shown in the input deck given in Appendix C. The time-step control cards used 0.05 seconds as the user inputted maximum time step from 0 to 5 seconds, and 0.25 seconds for the remainder of the run. The small time step in the early part was used to force the code to follow the rapid acceleration phenomena in the first part of the test.

2.1.2.4 Simulation Results and Discussion. The calculated blowdown transient began with the discharge outlet being opened to the ambient pressure. The calculation was carried out to 60 seconds using RELAP5/MOD1/CY=17 with the update listed in Appendix A. The measured data included pressures, differential pressures, temperatures, densities, and mass discharge rates inferred from pilot-static pressure data. The calculated results are generally in good agreement with the data. Some selected comparisons are shown in Figures 14 through 18. Note that the comparisons are presented only up to 50 seconds because the model does not include a ball valve which was part of the experimental set up. This valve was closed at 55 seconds, and thus the RELAP5 calculation cannot be expected to match the experiment from this time on. The simulation to 50 seconds required 44 CPU seconds.

Figure 17 shows a comparison of the calculation with the data for the mass flow rate at the nozzle. Subcooled critical flow exists for the first 20 seconds, and two-phase critical flow exists after that. The calculation compares well with the data except for the undershoot in the data at the beginning. The code does not model this undershoot well because the mass transfer model nucleation parameters were set for small systems (Edwards and Moby Dick experiments) rather than for the larger Marviken system. This nucleation delay is scale dependent, but because it exists for only a short time it is not of significance for large system blowdown calculations.

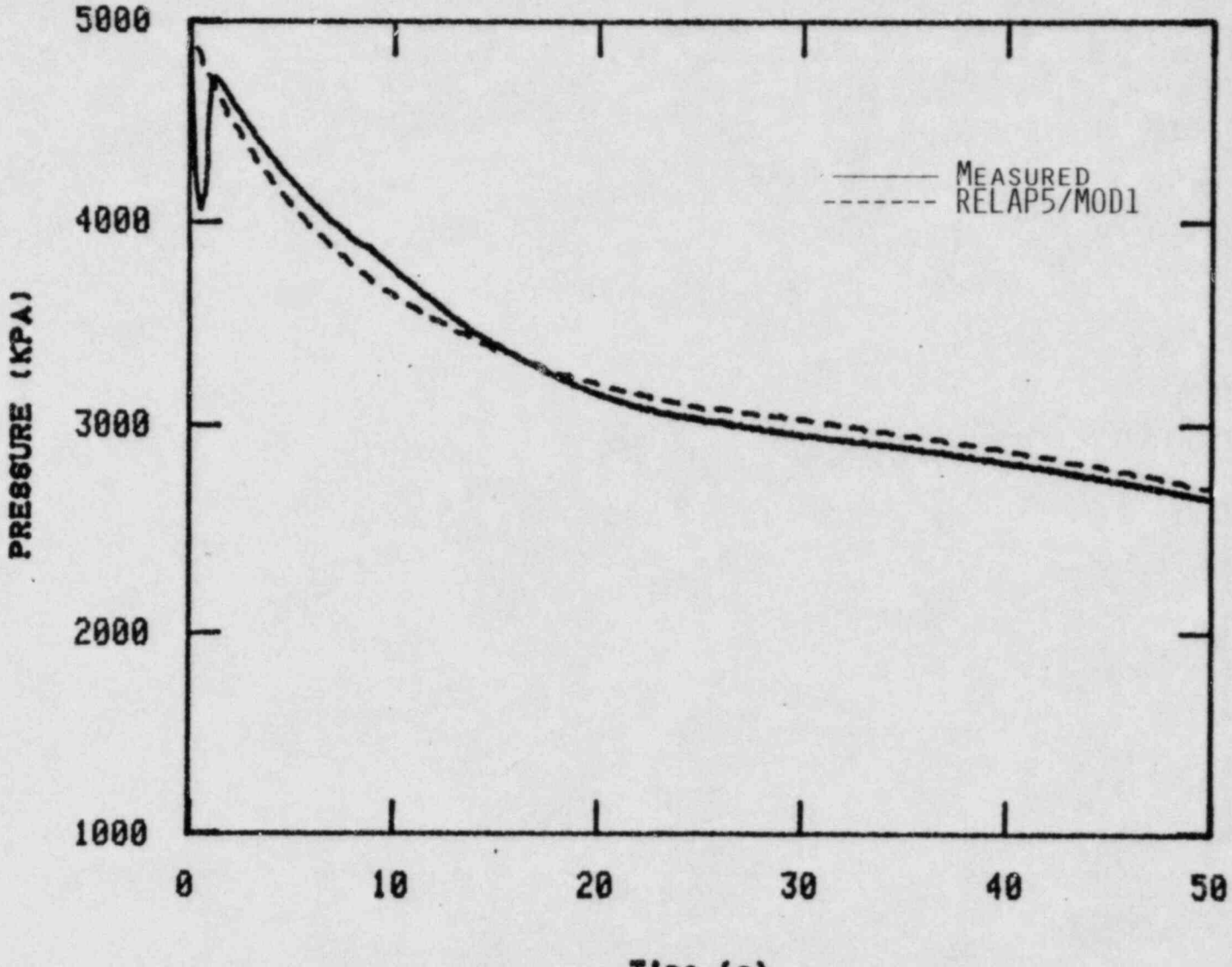

FIGURE 14. MEASUREMENT AND RELAP5/MOD1 CALCULATION OF MARVIKEN TEST 24 PRESSURE IN THE TOP OF THE VESSEL.

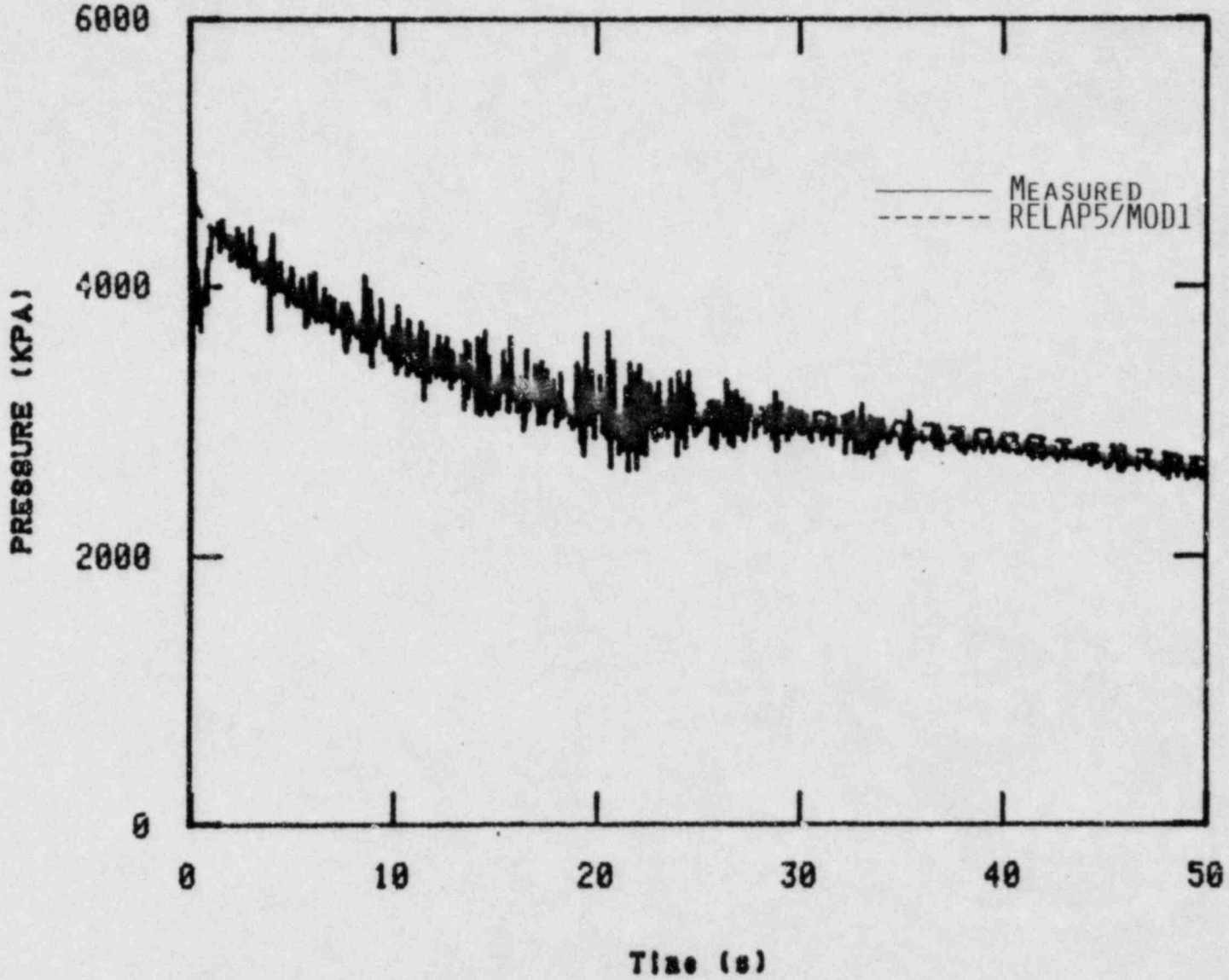

FIGURE 15. MEASUREMENT AND RELAP5/MOD1 CALCULATION OF MARVIKEN TEST 24 PRESSURE UPSTREAM OF THE NOZZLE.

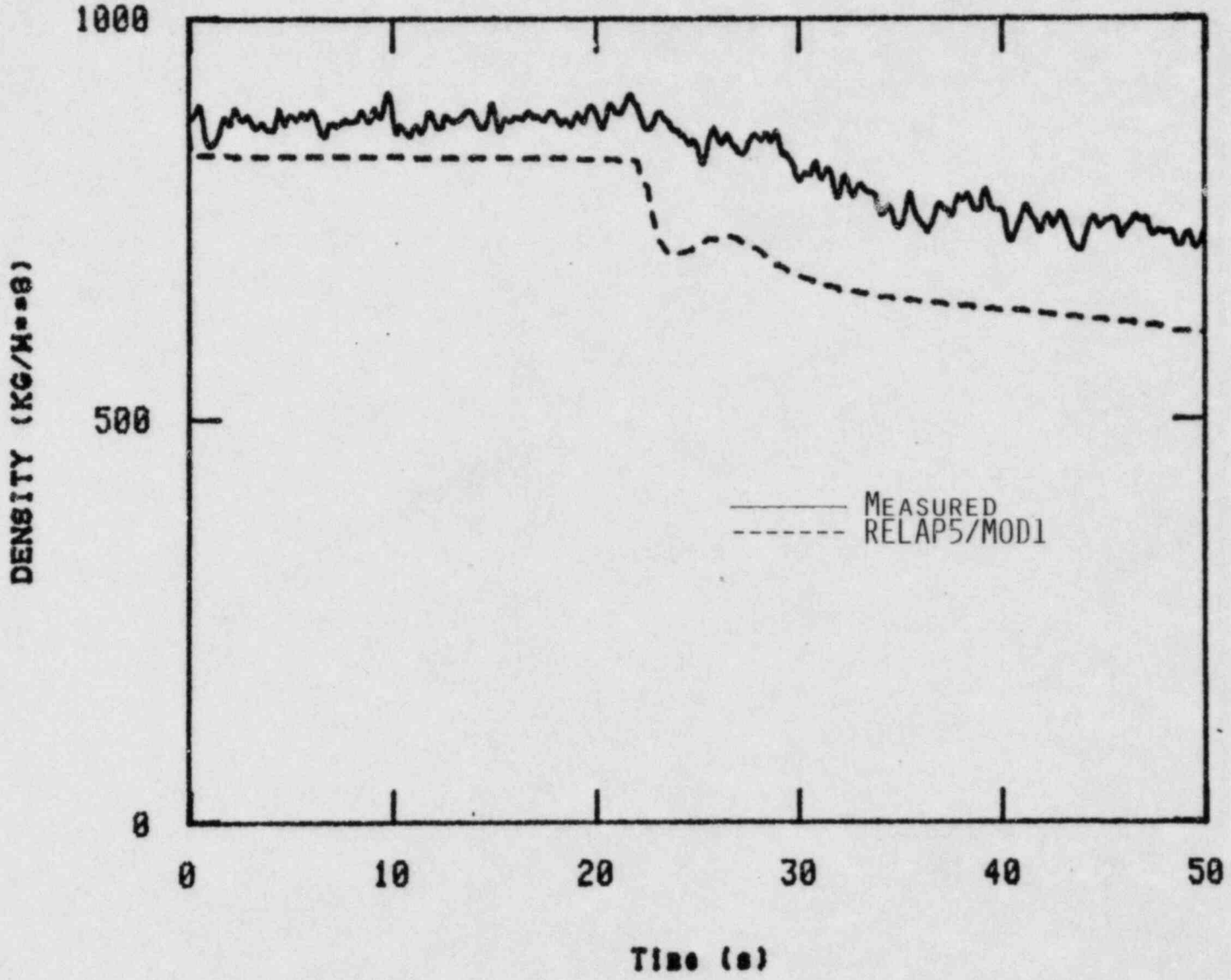

FIGURE 16. MEASUREMENT AND RELAP5/MOD1 CALCULATION OF MARVIKEN TEST 24 DENSITY IN THE MIDDLE OF THE DISCHARGE PIPE.

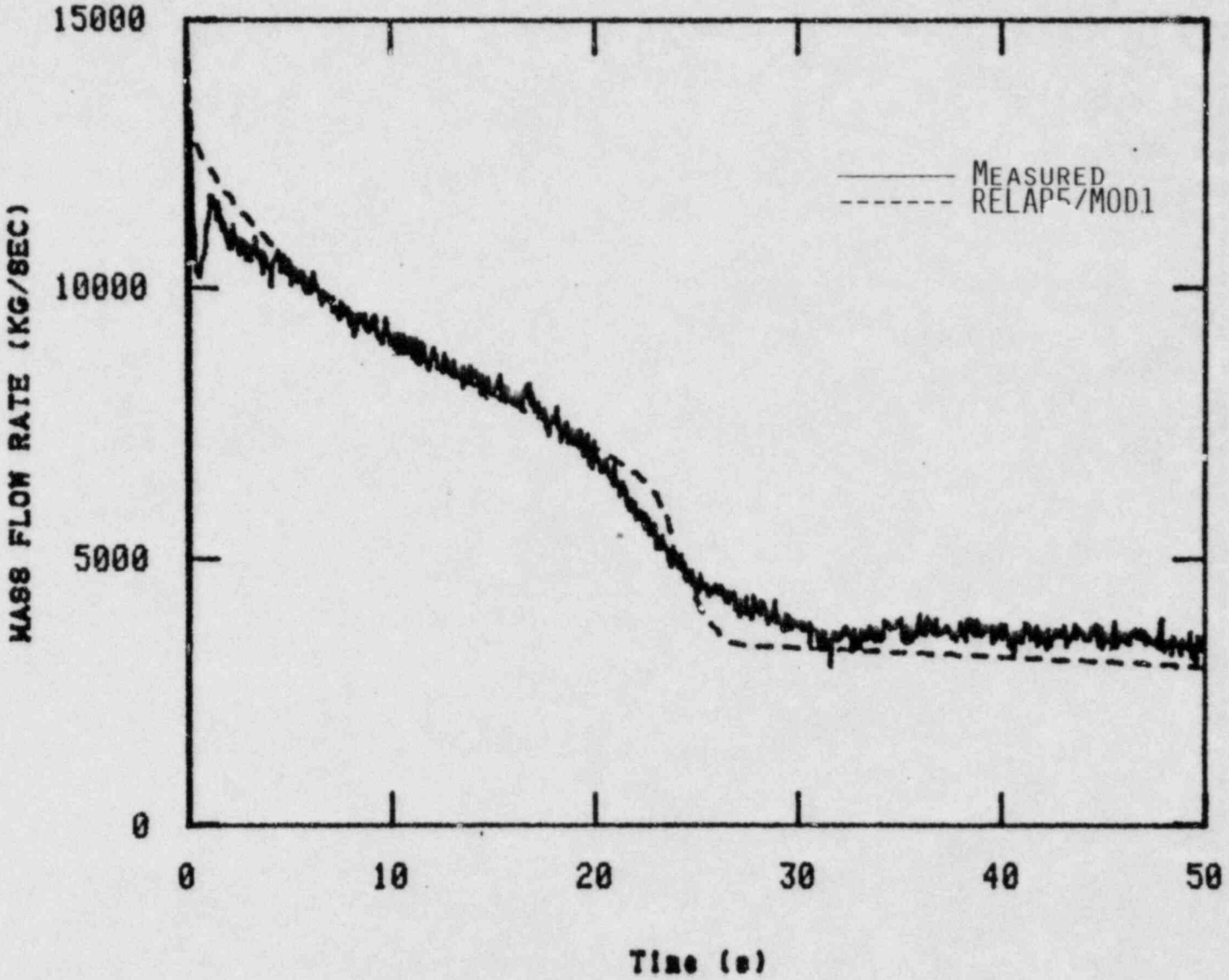

FIGURE 17. MEASUREMENT AND RELAP5/MOD1 CALCULATION OF MARVIKEN TEST 24 MASS FLOW RATE AT THE NOZZLE.

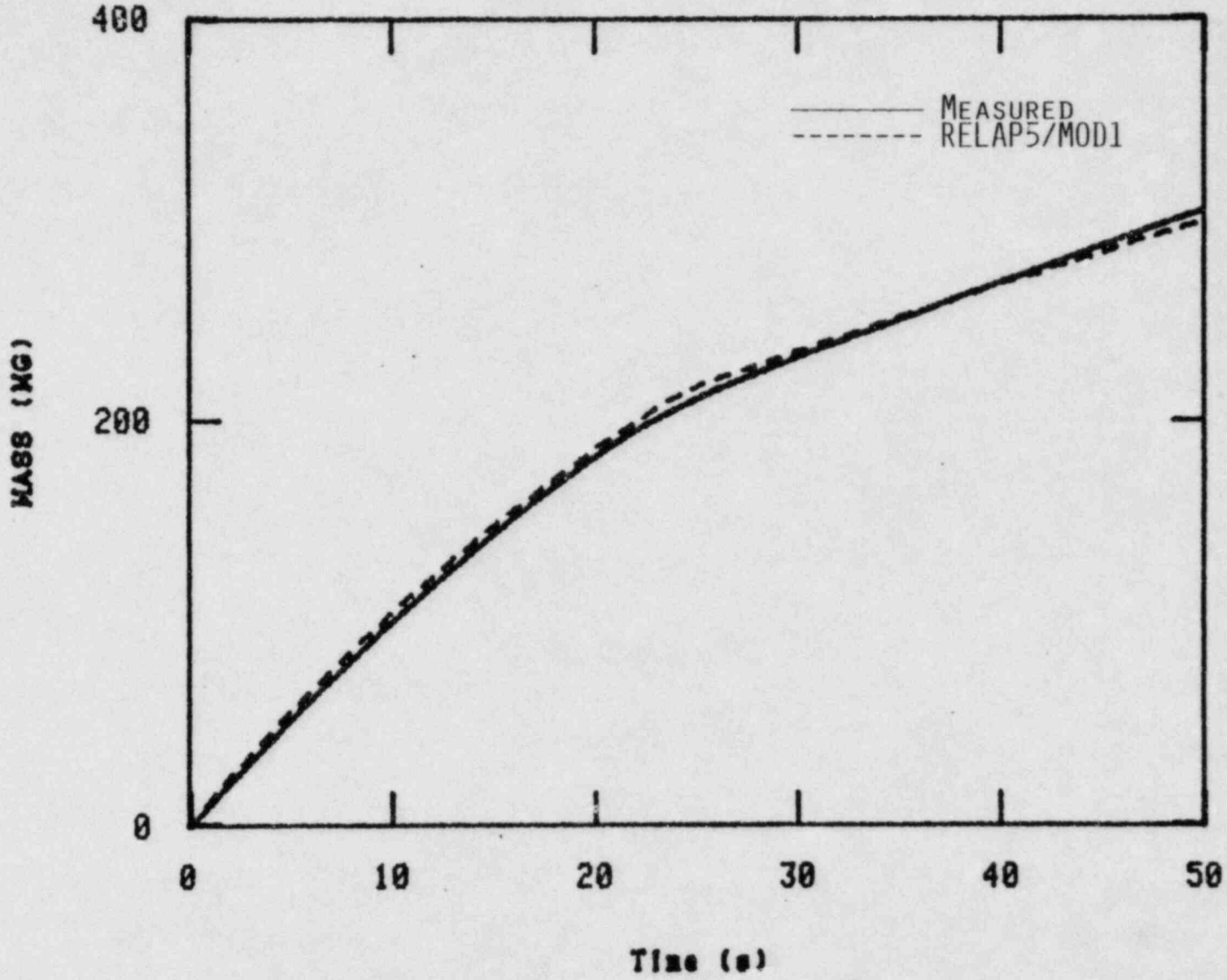

FIGURE 18. MEASUREMENT AND RELAP5/MOD1 CALCULATION OF MARVIKEN TEST 24 TOTAL DISCHARGE MASS FROM THE NOZZLE.

Figure 14 shows a comparison of the calculation with the data for the pressure at the top of the vessel. Neglecting the initial undershoot in the data, the code is underpredicting the pressure in the first 16 seconds of the calculation and overpredicting the pressure in the last part of the calculation. This result is somewhat disconcerting because the mass flow rate calculation agreed well with the data.

The system pressure disparity has been investigated and the reasons for it are quite interesting. In the Marviken experiment the vessel pressure is governed by the flashing of the saturated water layer as mass is discharged from the vessel and the volume occupied by the saturated mixture increases. In the experiment the thermal stratification is stable and very little mixing of the saturated water with the subcooled water occurs. In the numerical simulation of the experiment, however, numerical diffusion results in significant mixing of the saturated water layer with the subcooled water. The effect of this diffusion is to initially reduce the amount of saturated water and thus the ability of the system to repressurize is reduced. This causes an initial under prediction of the system pressure. As the pressure continues to fall, the saturation pressure of the thermally mixed fluid is reached and this contributes more saturated water which increases the calculated ability of the system to repressurize. This situation is illustrated in Figure 19 at 10 s in the blowdown. At this time the calculated pressure is lower than the measured system pressure, but the calculated amount of saturated water is now greater than in the experiment. As shown in Figure 14, the calculated pressure decreases more slowly beyond 10 s until the calculated and measured pressures are equal at 16 s. Beyond 16 s the calculated pressure is always higher than the measured pressure due to the greater quantity of water calculated to be at the saturation point.

The energy diffusion which occurs in the Marviken simulaton, and any other similar problem, is very nodalization sensitive. The initial model of the Marviken system used 20 volumes for the vessel, but the pressure under/overshoot was more extreme. At 39 volumes (the nodalization used for

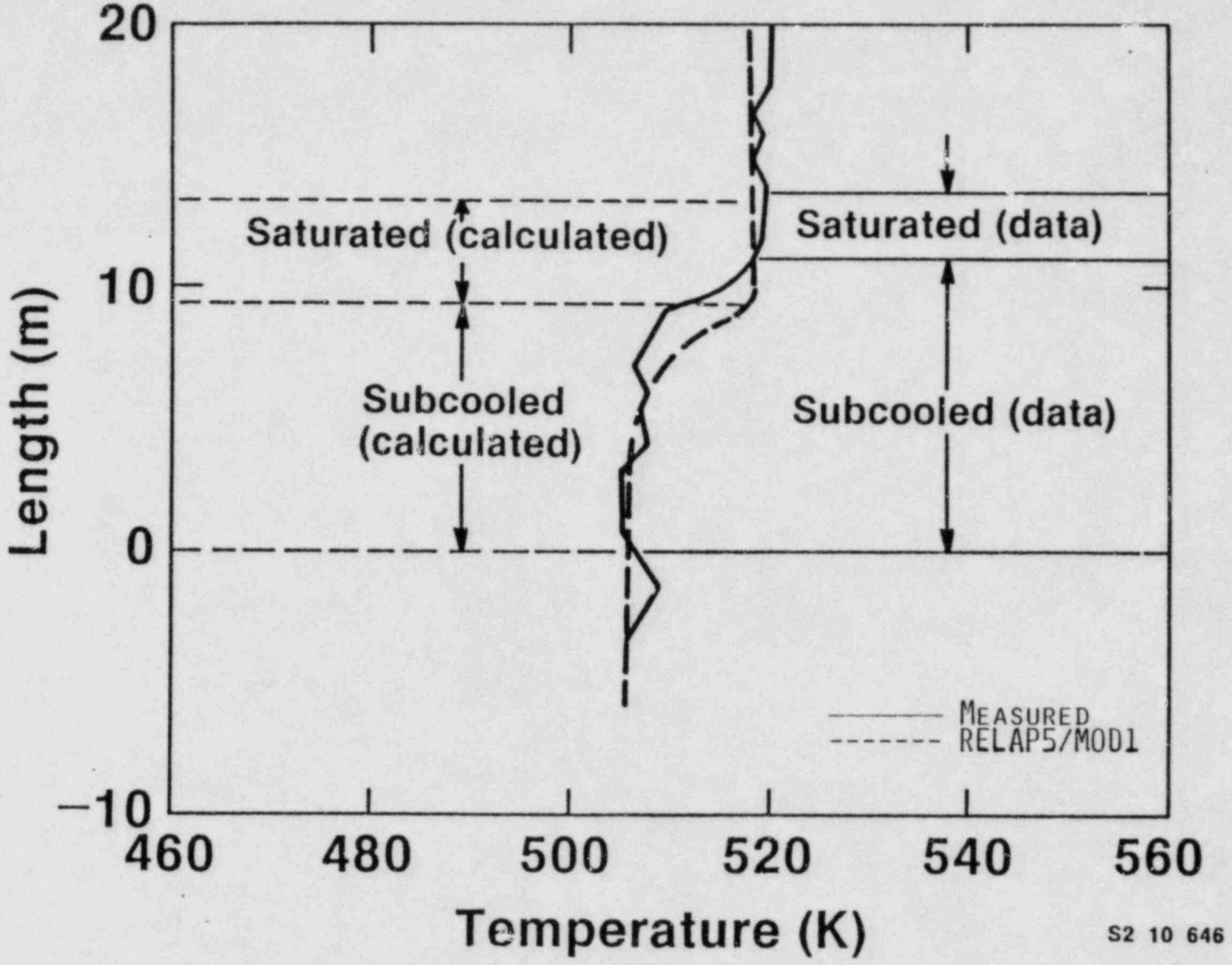

FIGURE 19. MEASUREMENT AND RELAP5/MOD1 CALCULATION OF MARVIKEN TEST 24 TEMPERATURE PROFILE IN THE VESSEL AT 10 SECONDS.

the results shown herein) the results were acceptable. Finer nodalization was not investigated in this study. However, the improvement in pressure prediction with increasingly fine nodalization reaches a point of diminishing return.

In summary, comparison of the RELAP5/MOD1 calculation with the Marviken III Test 24 provided a good evaluation of the ability of the two-phase thermal-hydraulic model to correctly predict mass discharge rates under choked flow conditions at a large scale. The code compares well to the data for the break mass flow rate, and this result substantiates the choked flow model. The presence of numerical energy diffusion in this simulation results in pressure underprediction and overprediction. This numerical energy diffusion problem can be reduced by using finer nodalization.

2.1.3 Wyle Small Break Test WSB03R

2.1.3.1 Purpose. In order to test the RELAP5 horizontal stratified flow model and its coupling to the choked flow model, a simulation of the Wyle small break test WSB03R[4] was performed. The RELAP5 simulation presented in this section has been previously presented.[5] Wyle Laboratories in Norco, California conducted transient tests of the LOFT break orifice using the LOFT Transient Fluid Calibration Facility. The objectives of the test were to obtain orifice calibration data at fluid conditions typical of small break Loss-of-Coolant Accidents (LOCA) and to provide a data base for critical flow model development.

2.1.3.2 Test Description. A schematic of the Wyle Test Facility is shown in Figure 20. The facility hardware consisted of a pressure vessel and a blowdown leg which are similar to the LOFT reactor vessel and broken cold leg. The pressure vessel was made from carbon steel, with a volume of approximately 5.4 m^3 (190 ft^3). The pressure vessel contained a carbon steel flow skirt to simulate the LOFT downcomer. The blowdown leg was connected to the vessel outlet flange. The flow skirt extended 0.8382 m (33 in.) above the connection. The blowdown leg consisted of a vessel

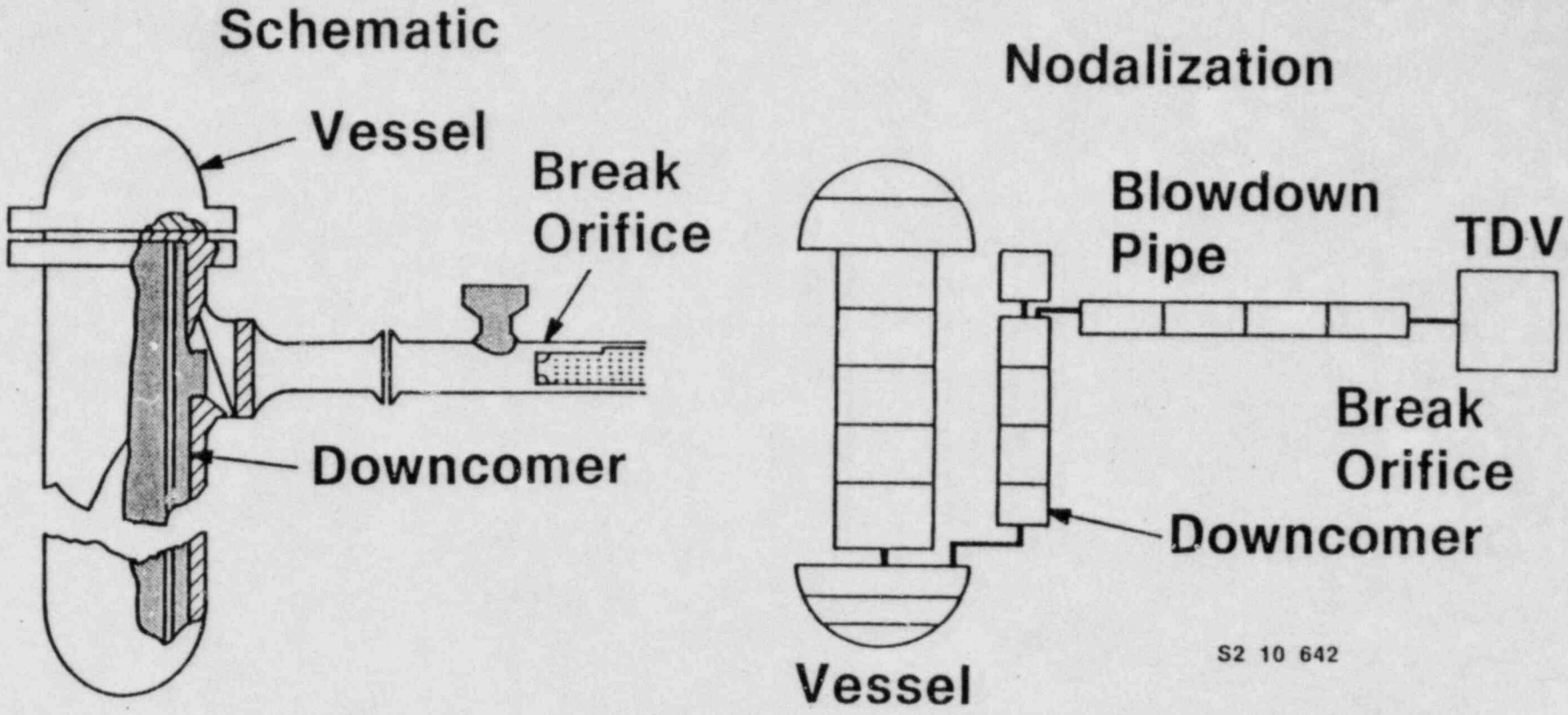

FIGURE 20. SCHEMATIC AND RELAP5/MOD1 NODALIZATION FOR WYLE SMALL BREAK TEST WSB03R.

outlet nozzle, an instrumentation test section, the break orifice, a shutoff gate valve, a burst disc assembly, and a discharge pipe. The test section was made from 35.56 cm (14 in) Schedule 160 stainless steel pipe. The break orifice was centered inside the test section.

Four load cells were used to support the vessel and blowdown leg. The pressure vessel was supported from three equally spaced cantilevered mounting lugs located at the outlet nozzle centerline. The lugs supported the full weight of the vessel through the load cells. The fourth load cell supported the blowdown leg above a concrete mass supported on air springs. The primary transducers for determining the system weight were the system load cells. The mass flow rate was calculated by differentiating the vessel weight measurement from the four load cells. A second reference vessel mass inventory measurement was provided by the top-to-bottom vessel differential pressure measurement.

A six-beam gamma densitometer, comprised of two three-beam densitometers mounted on opposite sides of the pipe, was used to determine the density upstream of the small break orifice. The fluid temperature upstream of the small break orifice and near the bottom of the vessel were measured by ISA Type K function thermocouples. The pressure upstream of the small break orifice was measured by a pressure transducer.

The test WSB03R was performed at an initial pressure of 15.0 MPa. The diameter of the break orifice was 16 mm (0.6374 in). This test was performed for the 16 mm diameter nozzle installed in the LOFT facility to control break flow during the LOFT small loss-of-coolant Experiment L3-1. The test duration was 1500 seconds.

2.1.3.3 RELAP5 Model. The RELAP5 model nodalization for the Wyle transient system is presented in Figure 20. The system configuration was nodalized so that system area changes and significant changes of piping are located at junctions. The pressure vessel, with core barrel in place was modeled by 10 volumes, using a 7 volume pipe, a branch, and 2 single volumes. All junctions were smooth, except for 2 abrupt junctions in the branch that connects to the 7 volume pipe and the downcomer. The downcomer

was modeled by a 4 volume pipe. The flow skirt extension above the blowdown pipe connection was modeled by a single volume pipe. All other junctions were modeled using the smooth option. The 4 volume vertical downcomer pipe was connected at the top to the blowdown pipe, which was modeled as a 4 volume horizontal pipe. This connection was modeled abrupt. It is possible to make this connection from the single volume top of the downcomer, but we have found this makes little difference in the results. In general, connections should be made along the lines of the main flow paths. The orifice was modeled as an abrupt single junction with the area equal to the actual orifice area. In the calculation, unity subcooled and the two-phase break flow multipliers were used. The unity multipliers were chosen because the measured values of density, pressure, and temperature were not consistent. This suggested that density was not known accurately, and thus, it was felt to be of little value to use any value other than the unit default values. There was insufficient data to determine the actual initial conditions for the whole system. Thus, some discrepancies in the comparisons of data and calculation may be due to the assumed initial conditions which might differ from the actual values. The RELAP5 deck for this test is given in Appendix D.

2.1.3.4 Simulation Results and Discussion. RELAP5/MOD1/CY=17, with the update listed in Appendix A, was used to simulate the experiment out to 1500 seconds, which required 450 CPU seconds. As the input deck in Appendix D shows, from 0 to 200 seconds, a user inputted maximum time step (Δt) of 0.20 seconds was allowed, and from 200 to 1500 seconds, a user inputted maximum Δt of 0.05 seconds was allowed. As with the GE level swell, this was done to provide a base run that had few oscillations. The calculated nozzle mass flow rate, upstream density, and upstream pressure are compared to the measured data in Figures 21, 22, and 23, respectively.

The calculated nozzle mass flow rate is compared to the measured value in Figure 21. The various regimes of choked discharge, evident from the results, are as follows: Subcooled liquid discharge exists from 0 to 10 seconds, saturated liquid discharge exists from 10 to 70 seconds, stratified two-phase discharge with void near the centerline from 70 to

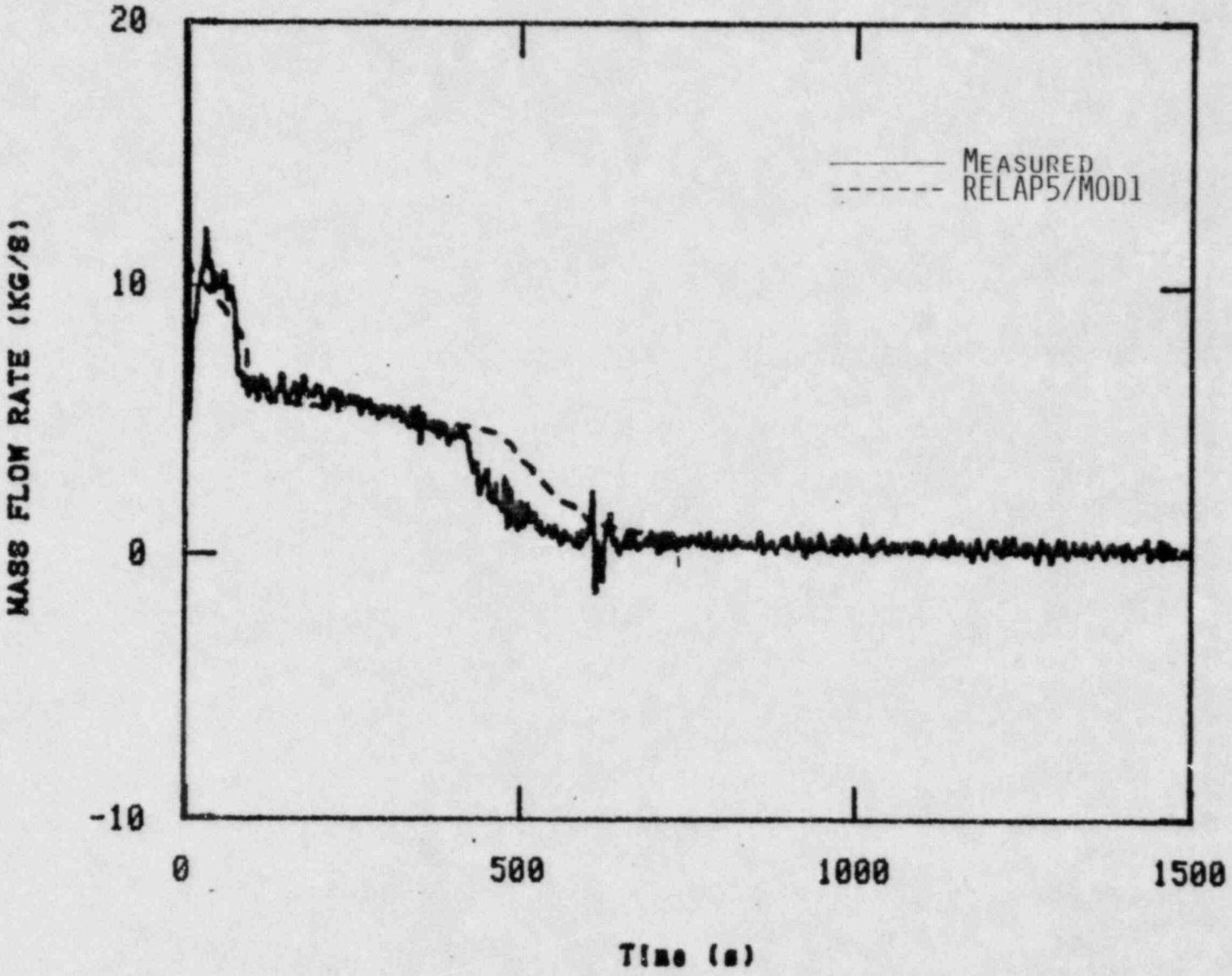

FIGURE 21. MEASUREMENT AND RELAP5/MOD1 CALCULATION OF WYLE SMALL BREAK TEST WSB03R MASS FLOW RATE AT THE BREAK ORIFICE (SMALL MAXIMUM Δt).

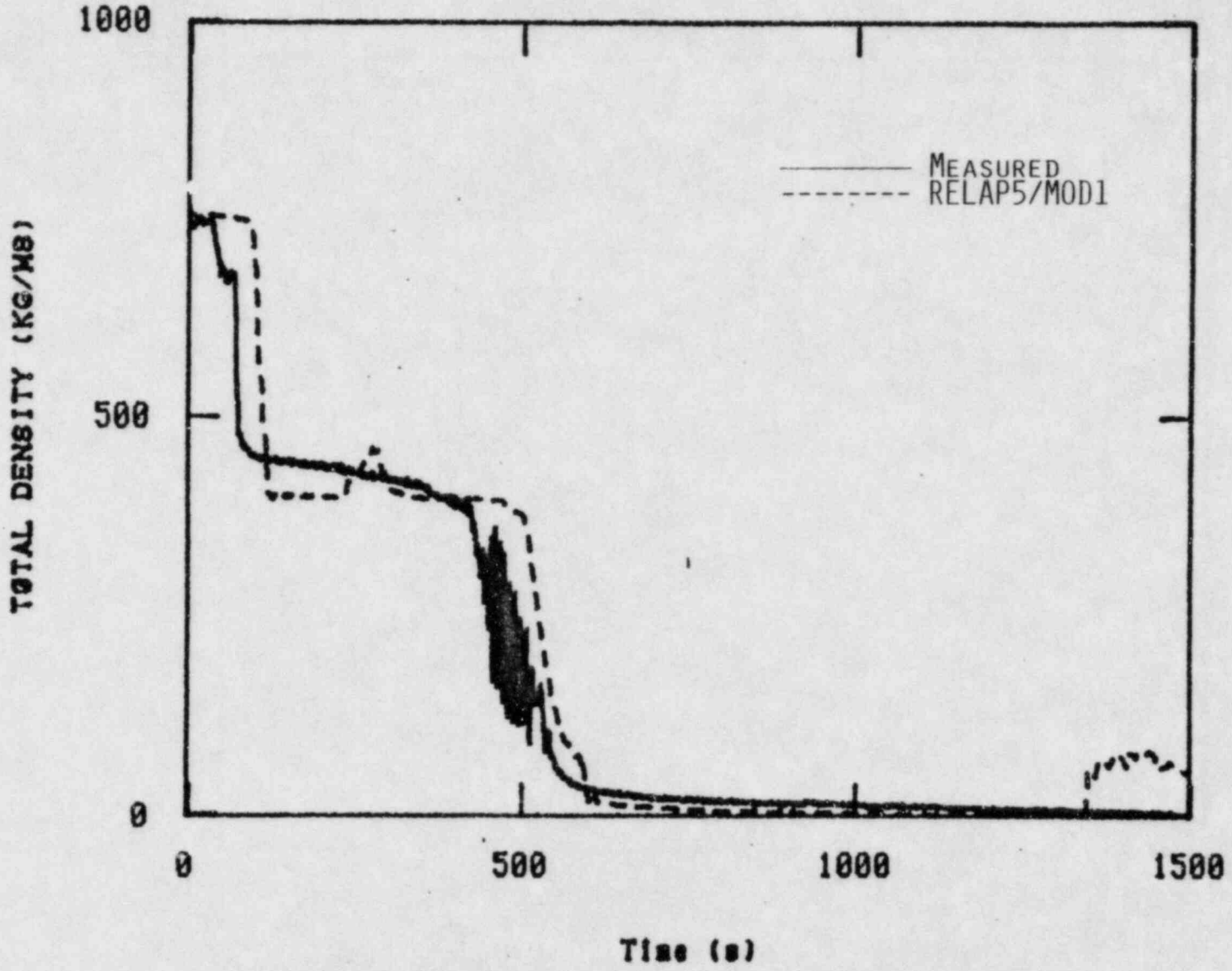

FIGURE 22. MEASUREMENT AND RELAP5/MOD1 CALCULATION OF WYLE SMALL BREAK TEST WSB03R DENSITY UPSTREAM OF THE BREAK ORIFICE (SMALL MAXIMUM Δt).

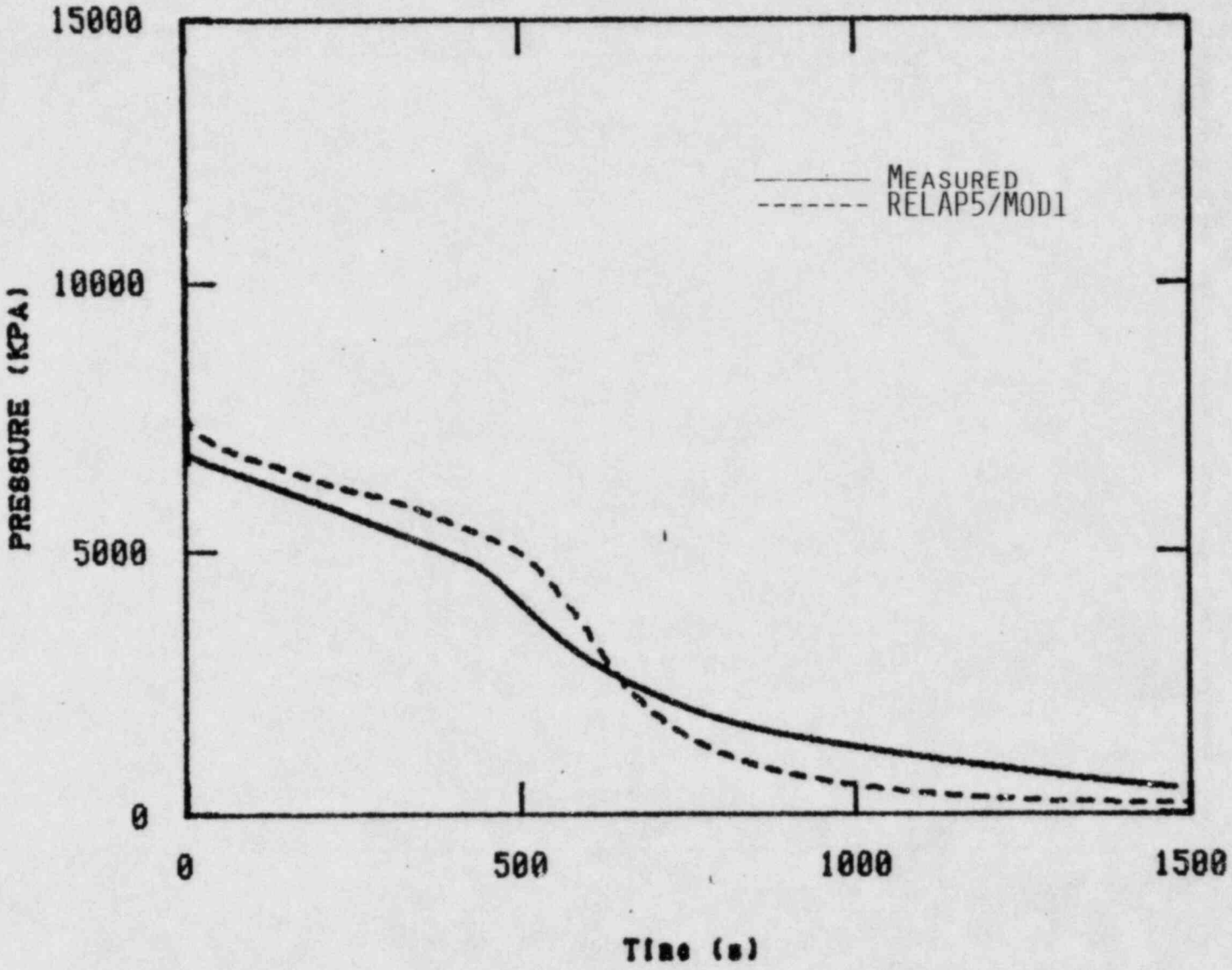

FIGURE 23. MEASUREMENT AND RELAP5/MOD1 CALCULATION OF WYLE SMALL BREAK TEST WSB03R PRESSURE UPSTREAM OF THE BREAK ORIFICE (SMALL MAXIMUM Δt).

420 seconds, and during the tail-off, steam discharges from 420 to 600 seconds. The model maintains a nearly constant level in the horizontal discharge pipe throughout the period of stratification while the data shows a gradual decline. This difference may indicate that greater vapor pull-through and liquid entrainment occur than that predicted by the correlations. The calculated and measured upstream densities are shown in Figure 22. The regimes of mass discharge are also evident from these density results. The pipe is liquid full up to 70 seconds, at which time the density drops to a value of about one half the liquid density. The liquid level drops approximately to the pipe centerline and remains stratified at near this value up to 420 seconds. The model predicts a slug of liquid (i.e., a slow increase followed by a decrease in density) during this period, which the data does not show. Beyond 420 seconds, the measured density initially fluctuates, while the calculated density remains smooth until near the end. Again, the code predicts a slug of liquid passes through which the data does not show. Finally, the calculated and measured upstream pressures are compared in Figure 23. The code predicts a high value early in the transient and a low value later on. The initial offset is due to the initial condition problem mentioned in Section 2.1.3.3. The depressurization rate is a strong function of the break volumetric discharge rate which is highest near the end of the blowdown, when mostly steam is discharging from the break. Accurate calculation of the system depressurization rate depends on a delicate balance between mass discharge rate and volumetric discharge rate. Under stratified flow conditions, large variations in the ratio or volumetric to mass discharge rate occur. Thus, the correctness of the predictions depends heavily on the stratified flow model. The pressure profile comparison in Figure 23 indicates that the stratified flow model in RELAP5 is a qualitative approximation to the physics of such flows, but the emperical correlations may need refinement as a larger data base becomes available.

In order to examine the horizontal stratification model at the break, the calculated void at the nozzle and the calculated void upstream of the nozzle are presented in Figure 24. During the first part of the stratification regime, where the pipe contains more liquid than vapor, the plot

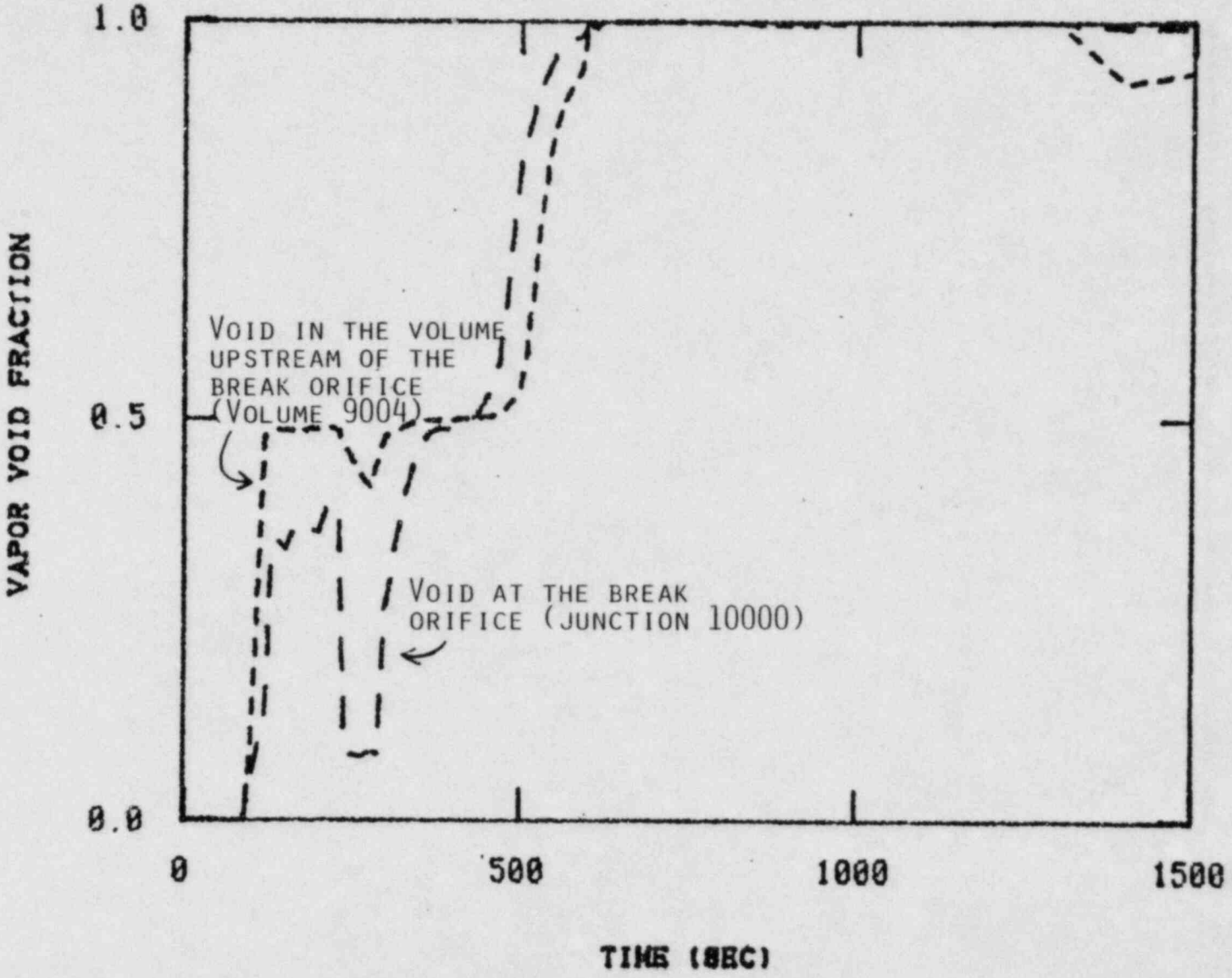

Figure 24. RELAP5/MOD1 calculation of Wyle small break test WSB03R void fraction at the break orifice and upstream of the break orifice (small maximum Δt).

shows that some vapor does pass through the break orifice, and even though it is somewhat less than the amount of vapor in the pipe. This correct vapor pull-through effect is provided for by the code's horizontal stratified choked flow model [see Equation (165) in RELAP5 manual,[6] Volume 1]. During the later part of the stratification regime, where the pipe contains more vapor than liquid, some liquid passes through the nozzle. this correct liquid entrainment is also provided for by the code's horizontal stratified choked flow model [see Equation (166) in RELAP5 manual, Volume 1].

An indication of the adequacy of the horizontal stratification model along the pipe is shown in Figure 25, which shows the calculated void fraction in the blowdown pipe versus length at times 100, 300, and 500 seconds. These plots were obtained by a straight line connection of the data and RELAP5 calculation points from the four volumes in the blowdown pipe. For liquid flowing out of the pipe, one would expect the profile to show a continuous increase along the pipe. The 100 second profile shows a slight increase and then a decrease in void along most of the pipe. The 300 second profile also shows a slight increase, but then a fairly constant profile for most of the pipe. The 500 second profile shows a slight decrease along most of the pipe but then an increase over the last part of the pipe. This suggests that void waves propagate back and forth in the pipe, however it could also be a peculiarity of the model and more detailed data will be required to resolve such questions.

The input deck in Appendix D was changed to increase the user inputted maximum Δt to 0.1 seconds from 200 to 1500 seconds (again, using RELAP5/MOD1/CY=17 with the update listed in Appendix A). The simulation was carried out to 1500 seconds and required 263 CPU seconds. The nozzle mass flow rate, upstream density, and upstream pressure are shown in Figures 26, 27, and 28. Oscillations develop in the calculated mass flow rate and density, particularly during the 500 to 600 second time frame. Thus, as in the case with GE level swell test, an attempt to improve the run time by increasing the user inputted maximum Δt results in faster run

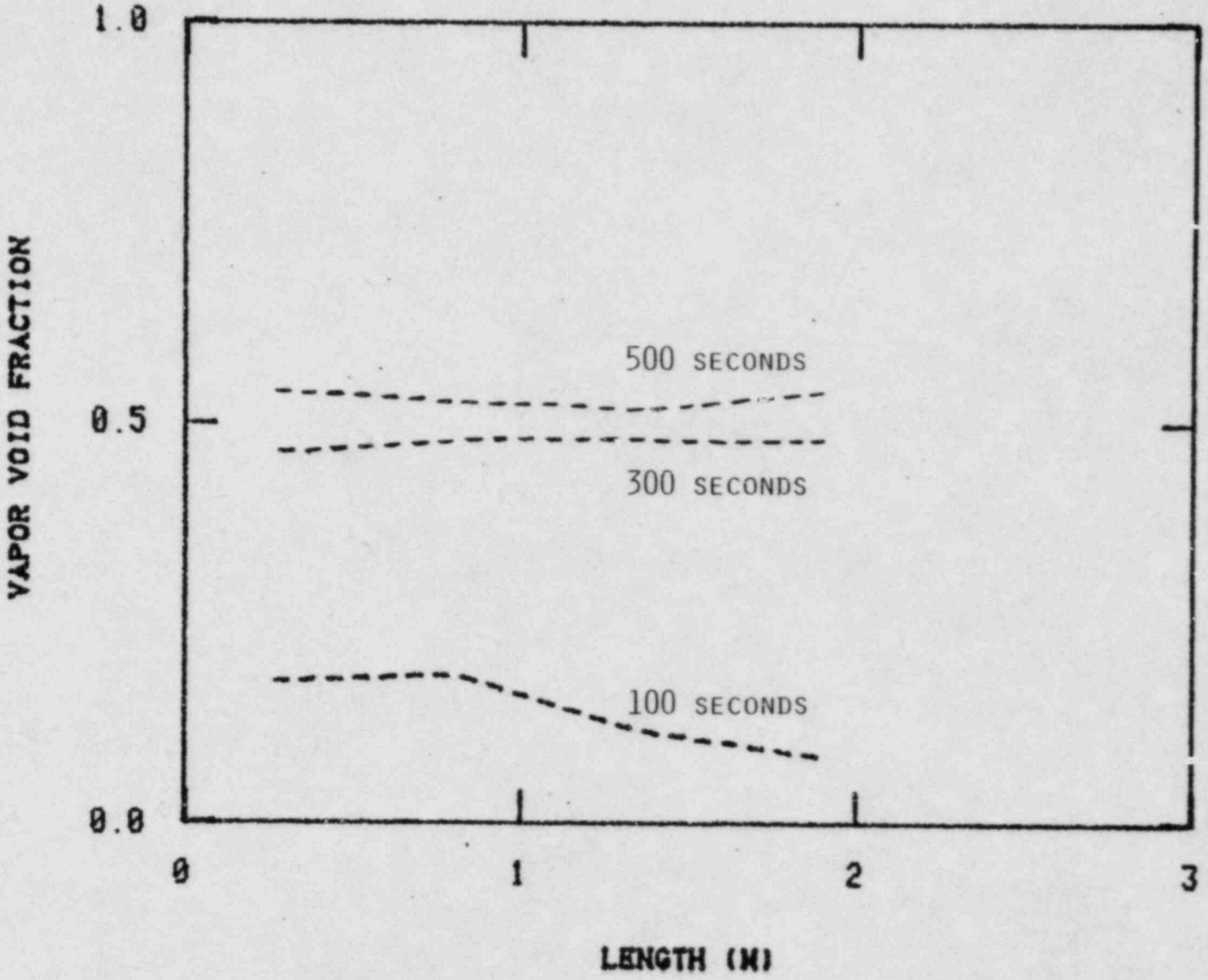

Figure 25. RELAP5/MOD1 calculation of Wyle small break Test WSB03R void fraction profiles in the blowdown pipe at 100, 300, and 500 seconds (small maximum Δt).

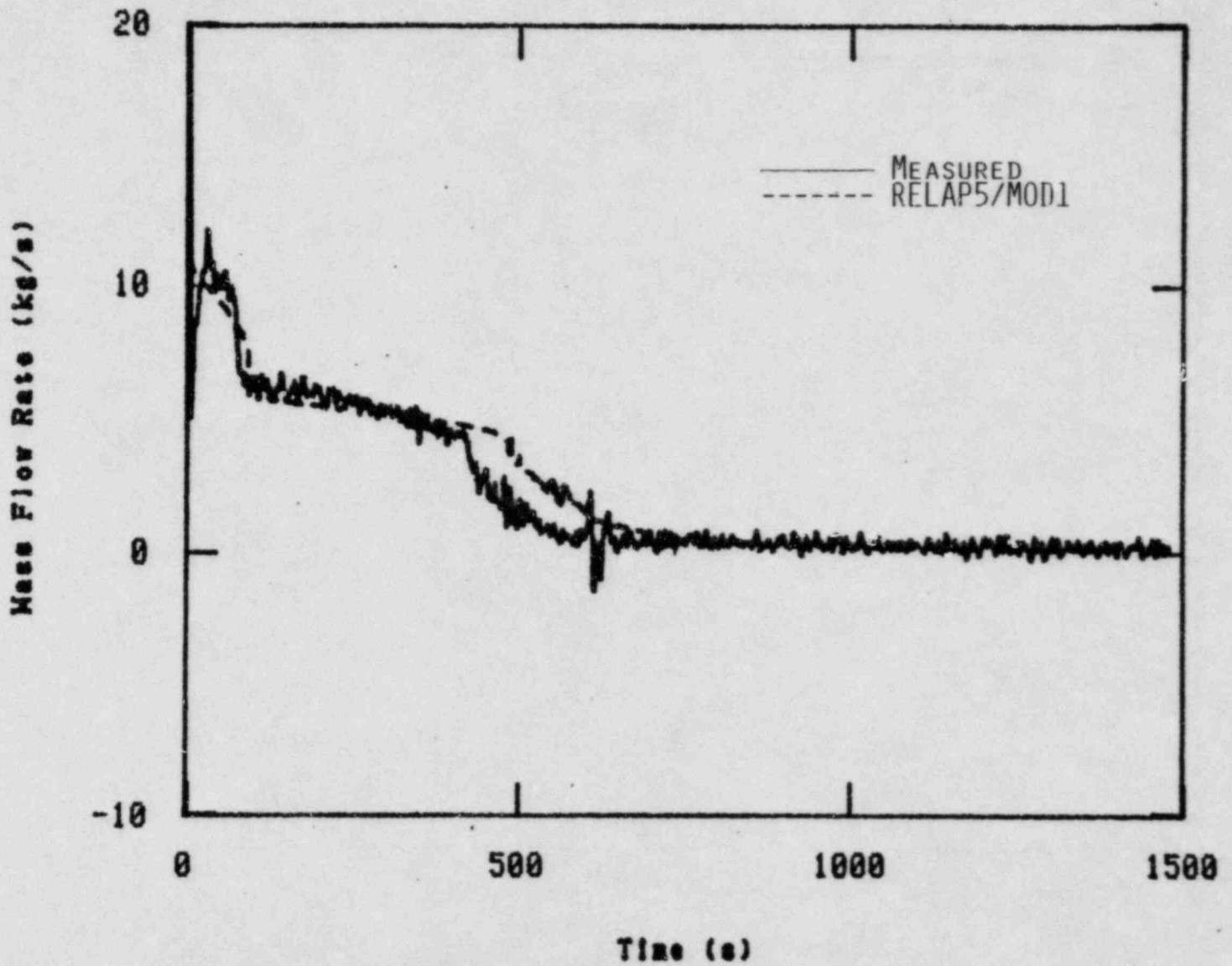

FIGURE 26. MEASUREMENT AND RELAP5/MOD1 CALCULATION OF WYLE SMALL BREAK TEST WSB03R MASS FLOW RATE AT THE BREAK ORIFICE (LARGE MAXIMUM Δt).

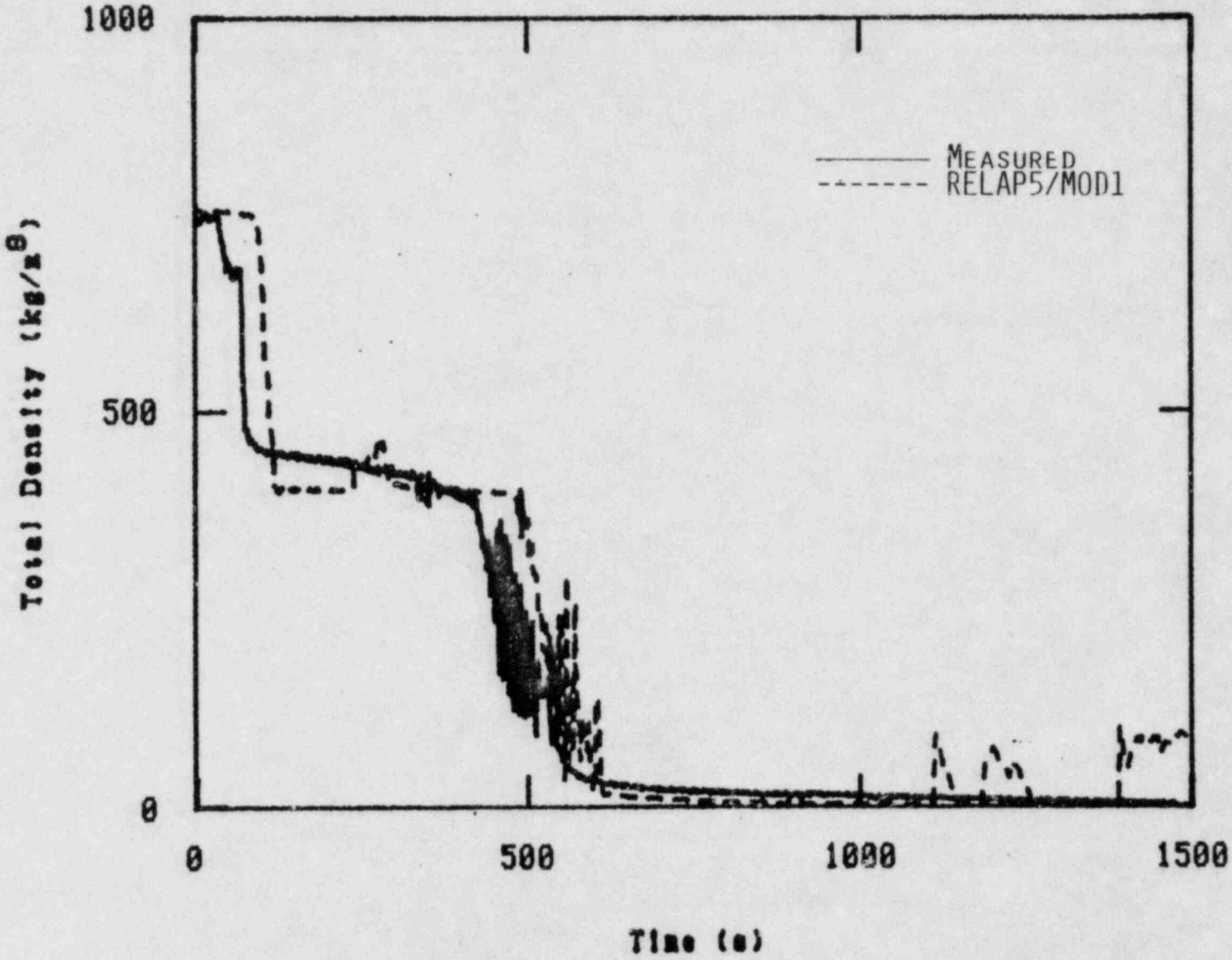

FIGURE 27. MEASUREMENT AND RELAP5/MOD1 CALCULATION OF WYLE SMALL BREAK TEST WSB03R DENSITY UPSTREAM OF THE BREAK ORIFICE (LARGE MAXIMUM Δt).

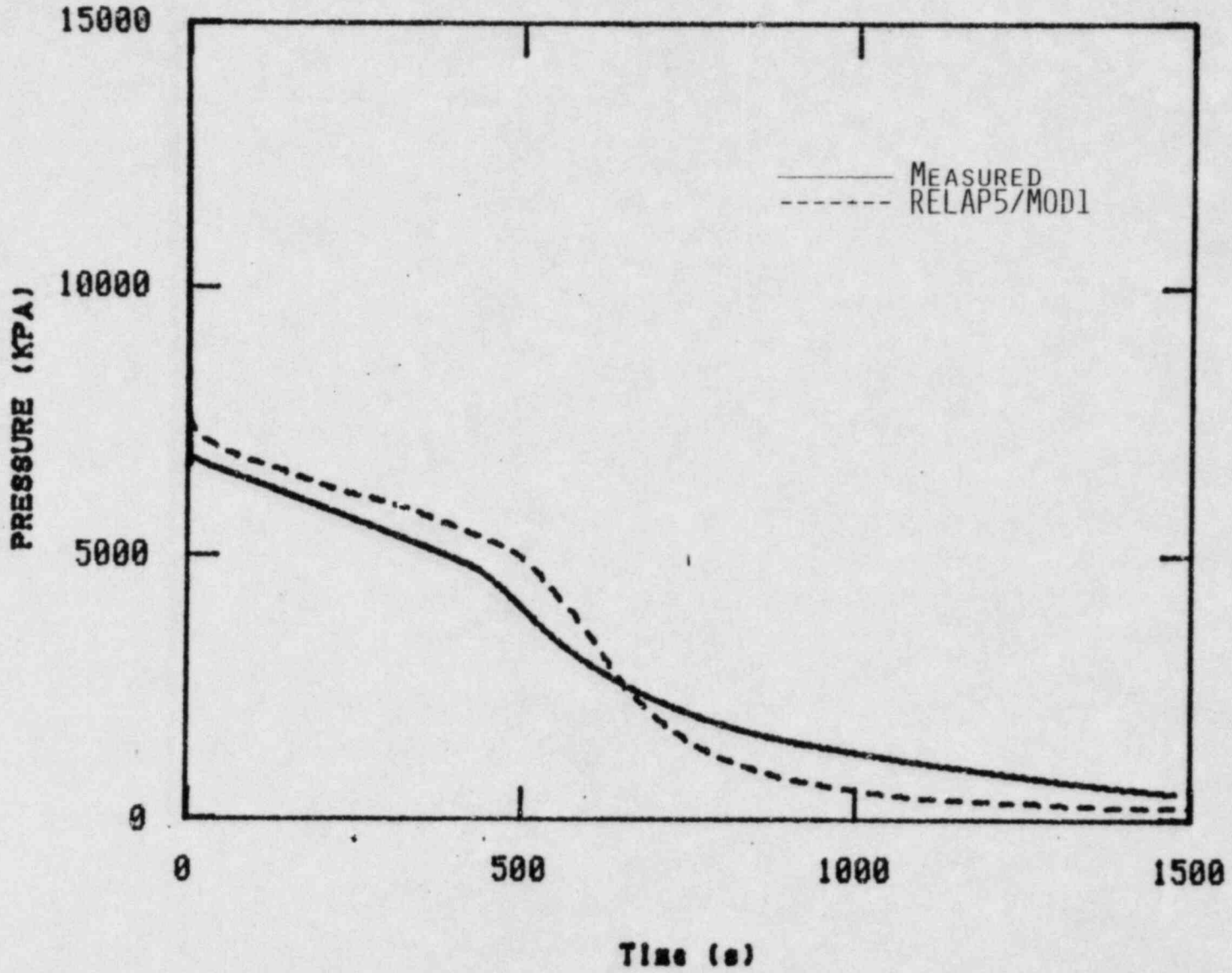

FIGURE 28. MEASUREMENT AND RELAP5/MOD1 CALCULATION OF WYLE SMALL BREAK TEST WSB03R PRESSURE UPSTREAM OF THE BREAK ORIFICE (LARGE MAXIMUM Δt).

time, but with a penalty of increased oscillations. The major parameters such as system pressure and vessel mass inventory are essentially unchanged, however, and an accurate prediction results.

In summary, RELAP5/MOD1 does a reasonable job of predicting the important parameters near and at the break for the Wyle test, which suggests the stratification flow model and its ccupling to the choked flow model are accurate. As with the GE level swell test, care is needed in selection of the user inputted maximum Δt in order to reduce numerical oscillations caused by the interphase drag coupling. In application, it is recommended that some sensitivity of studies be made by reducing or increasing the maximum time step.

2.2 System Tests

2.2.1 Semiscale Mod-3 S-07-6 Posttest Analysis

2.2.1.1 Purpose. Semiscale Mod-3 Test S-07-6[7,8] was the first Semiscale integral blowdown reflood experiment. The test was conducted with a 200% cold leg pipe break and with ECC injection into the cold leg of the intact loop. It is presented here to show the RELAP5/MOD1 comparison to the data during the blowdown portion. The calculation was made from initiation of pipe rupture to 25 seconds after rupture. These results provide an indication of the capability of RELAP5/MOD1 to simulate the behavior of a complex system. The test was first simulated using RELAP5/MOD0, and the results have been previously documented.[9] For this developmental assessment, the test was rerun using RELAP5/MOD1, which has an active accumulator component that was not available in RELAP5/MOD0.

2.2.1.2 Test Description. The Semiscale Mod-3 system[7,8] (Figure 29) is a small scale nonnuclear system containing the major components which comprise a pressurized water reactor. The system includes a vessel with an electrically heated core, an intact loop (includes pressurizer, steam generator, and pump representing three intact loops of a four loop reactor), and a broken loop (includes steam generator, pump, and break assembly representing one loop of a reactor). The core contains 25 full length (3.66 m heated

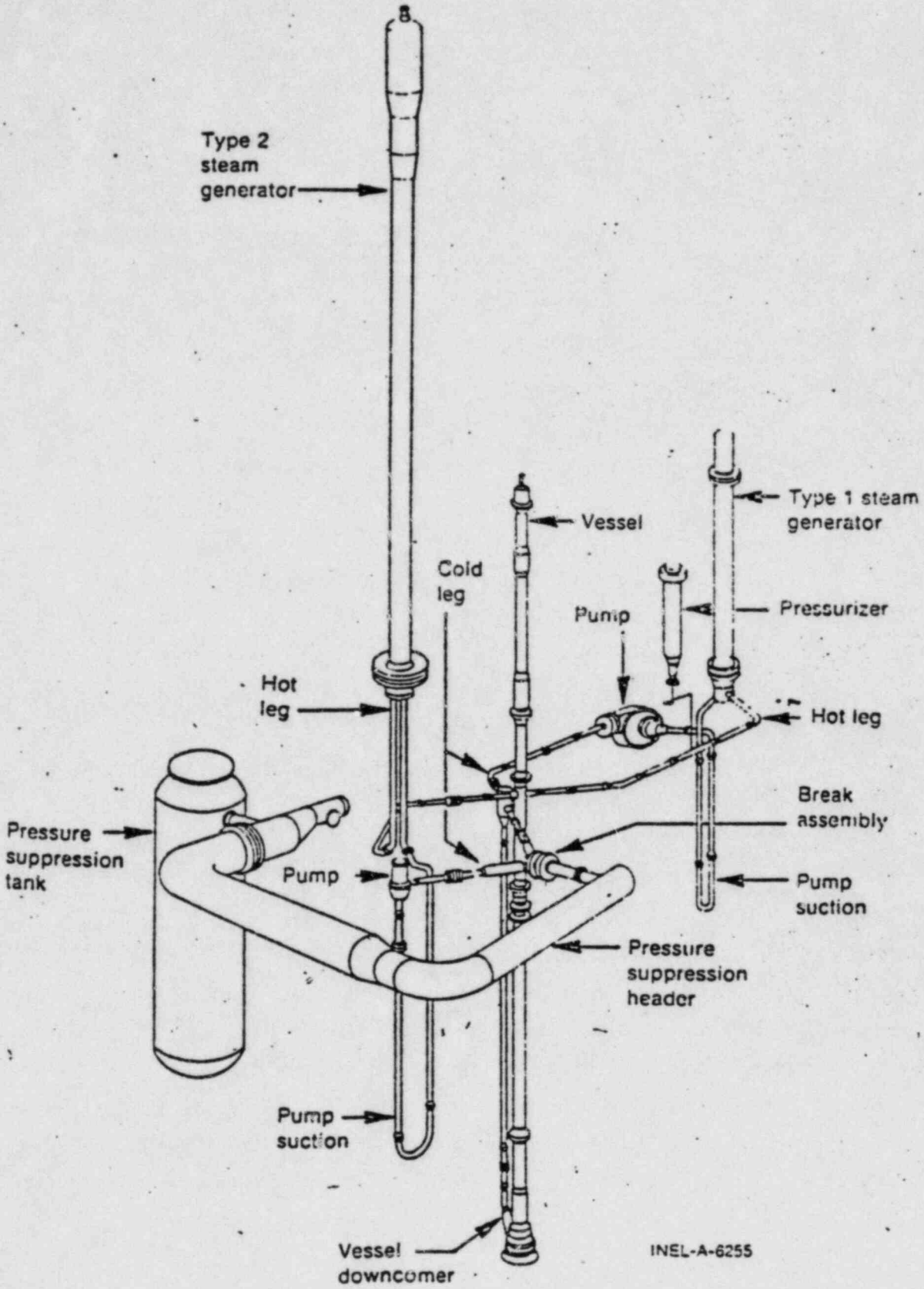

FIGURE 29. SCHEMATIC OF SEMISCALE MOD-3 TEST FACILITY.

section) electrically heated rods. The downcomer is external to the vessel and is comprised of a pipe connecting an external inlet annulus to the lower plenum of the vessel. The breaks are simulated by rupture disc assemblies. The blowdown effluent is discharged into a header that conducts the vapor and water mixture to a collection container. The Mod-3 system is designed with the capability to investigate the influence of upper head ECC injection on the core thermal hydraulics, however, Test S-07-6 had no upper head ECC injection. In the vessel, a support tube and a guide tube connect the upper head region to the upper plenum region.

Test S-07-6 had an initial cold leg fluid temperature of 557 K with a core fluid temperature differential of 37 K and an initial core power of 2.0 MW. The core radial power profile was peaked with 9 high power rods having a peak power of 35 kW/m. Two rods were unpowered for this test. The initial nominal system pressure was 15.51 MPa. ECC fluid at 300 K was injected into the intact loop cold leg by an accumulator, a high-pressure injection system (HPIS), and a low-pressure injection system (LPIS). The blowdown behavior of this test was similar to prior blowdown experiments.

The sequence of the events during the blowdown portion of the test are as follows: (a) The core power decay transient started at the time of blowdown, (b) HPIS injection began at 3 seconds, (c) the pressurizer emptied at 10 seconds, (d) ECC accumulator injection into the intact loop began at 19 seconds.

2.2.1.3 RELAP5 Model. The RELAP5/MOD1 model of the Semiscale Mod-3 facility for Test S-07-6 included 126 fluid control volumes and 129 flow junctions. The system nodalization is illustrated schematically in Figure 30, and the input deck is given in Appendix E. In the model, a total of 93 heat slabs (shown as shaded areas in Figure 30) were used to represent heat transfer in the intact loop and broken loop steam generators, vessel, core barrel, piping system, heater rods, and heat loss to the environment. Twelve slabs were used to represent the high and low power rods.

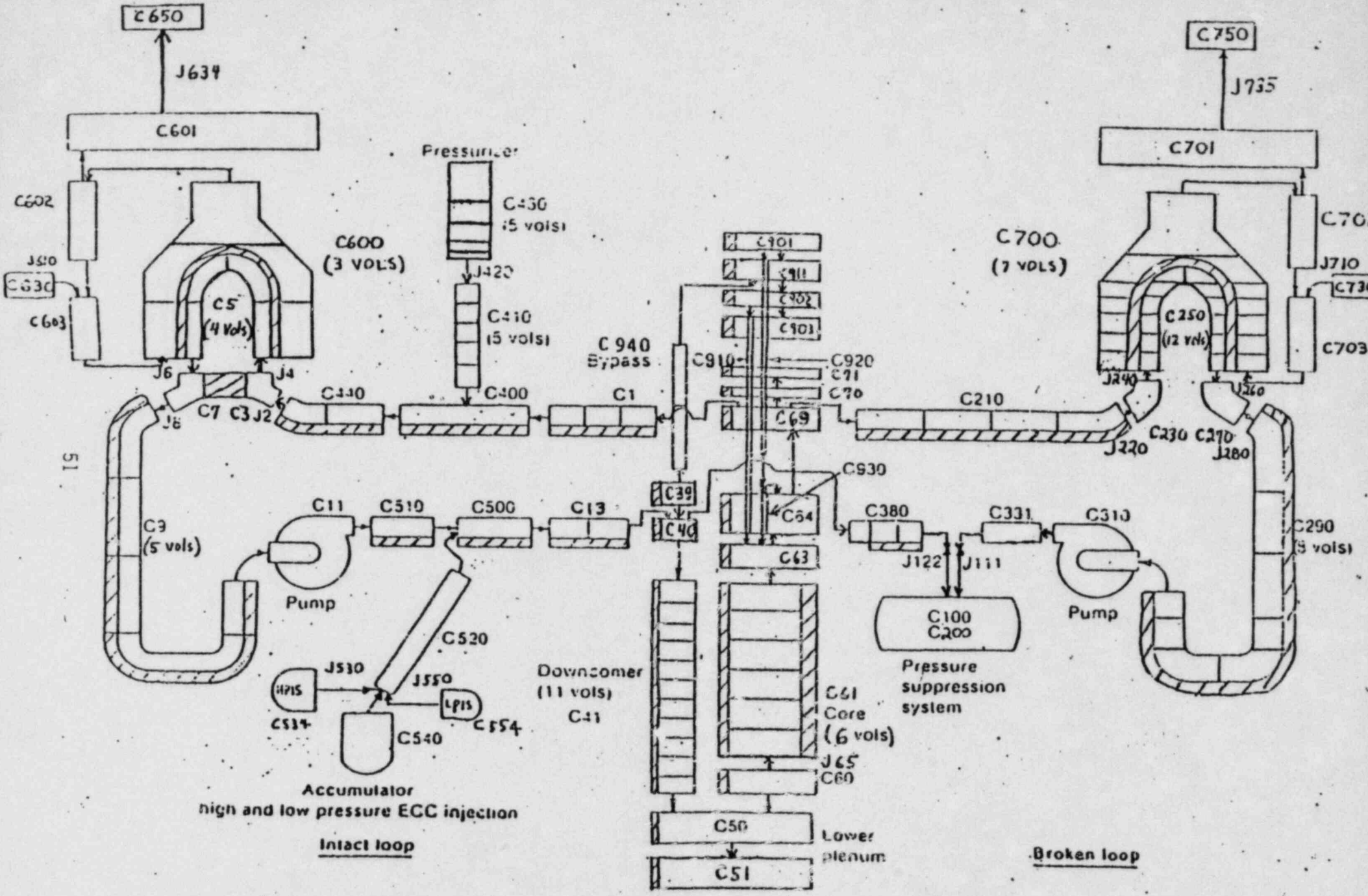

FIGURE 30. RELAP5/MOD1 NODALIZATION FOR SEMISCALE MOD-3 TEST S-07-6.

The input deck given in Appendix E was the first RELAP5 input deck developed for the Semiscale test facility. This deck is somewhat dated, and it does not represent the current deck being used to model Semiscale. More recently, an input deck has been setup for the Semiscale Mod-2A test facility,[10] and an input deck for the Mod-2B test facility has also been developed (not documented yet). The input deck in Appendix E employed a modeling practice for the leak paths that is no longer employed in the current decks. The leak paths are now modeled by using smooth area changes, letting the area at a junction default, and inputting forward and reverse form losses. This way of modeling the leak paths is now the recommended practice. Examples of junctions that should be changed in Appendix E are the junction between components 911 and 940 and the junction between components 940 and 39.

Break flow was calculated routinely by the choked flow model in RELAP5, and a two-phase discharge coefficient of 0.84 and a subcooled discharge coefficient of 1.0 were used. Special considerations for some components are discussed below:

1. The pressurizer component was divided into 5 volumes with a finer nodalization near the bottom so as to define accurately the vapor and liquid interface as the liquid empties. The initial temperature of the vapor and liquid was near the saturation temperature of the system pressure since the fluid heater was immersed in liquid. A slight thermal stratification was assumed.

2. In Test S-07-6, both the intact and broken loop pumps were controlled to follow specified speed versus time curves. The intact loop pump was allowed to coast down to 61% of its initial speed and then was maintained at this speed, while the broken loop pump followed a specified overspeed curve. Thus, instead of calculating the pump speeds using the torque-inertia relation, the measured pump speed data were specified using the time-dependent pump speed option included in RELAP5.

3. A relatively fine nodalization was used in the downcomer (11 volumes) because of the important role it plays in controlling the behavior of the system during the test. Six volumes were used for the core. This differs somewhat from the current modeling practice where the same nodalization is used in the downcomer and core. Six heat structures were used to represent the high power rods, and another six heat structures were used to represent the low power rods.

4. An active accumulator was used. The high and low pressure injections were initiated by pressure trips.

After the input deck was used in this developmental assessment, a 0.1% error in the elevations of the broken loop steam generator was detected. It is our feeling that this error would not significantly affect the results, so the calculation was not rerun with the corrected input deck. The error was found to be in the downcomer (Component 703), and the elevation and length of this component have been changed in Appendix E from 31.9167 ft to 32.0412 ft to reflect this correction. This error can be significant in some cases, particularly when there is mostly liquid present.

2.2.1.4 Simulation Results and Discussion. RELAP5/MOD1/CY=17, with the update listed in Appendix A, was used to simulate the experiment. We found superheating (over 1300 K) in Components 310 and 331 at 12 seconds, but the superheating went away by 14 seconds. This is probably associated with the performance curve of the pump (Component 310), especially since the pump speed from the input table increases from time = 0 seconds to time = 16.5217 seconds. At 16 seconds, the code was updated to repair problems with the accumulator component. This update is listed in Appendix F. In concert with this, the input deck for the accumulator component had to be changed. This renodalization for the accumulator component is listed in Appendix G. The vertical angle had to be changed to 90 degrees, and the energy loss coefficient had to be changed to 449.9. The accumulator began injecting between 16 and 17 seconds. At 21.1881 seconds, the code failed due to a water property error at the minimum time step. Examination of the

temperatures in components 310 and 331 showed them both to be over 1400 K. The calculation of energy dissipation in the pump component was a suspected cause, so the run was restarted at 20 seconds with pump dissipation turned off (added the update in Appendix H to the updates in Appendices F and A). The code was then able to complete the run out to 25 seconds, although the temperature rose to over 1200 K in Component 331.

Another problem was seen by monitoring the volumetric flow rate from the accumulator, where it was found that this flow rate turned off between 20 and 25 seconds (Figure 31). The problem was traced to a pressure spike in the pipe Component 520, and this was traced to a problem with the viscous term in the momentum equations [Equations (232) and (233) in Reference 6] for a branch component (Component 500 in this problem). The viscous term was modified so that it was multiplied by 1/2 $ARAT^2$, where $ARAT=(A_K)_j/A_K$ and $(A_K)_j$ is given by Equation (284) in Reference 6. The code was updated using 1/2 $ARAT^2$ by adding the update of Appendix I to the updates of Appendices H, F, and A. The problem was restarted at 20 seconds and was run out to 25 seconds. As Figure 32 shows, the accumulator volumetric flow rate no longer turned off. Superheating still occurred in Component 331, however, as the temperature rose to over 1300 K, but the code did not fail.

The calculation carried out to 25 seconds required 4083 CPU seconds. A plot of CPU time versus simulated time is shown in Figure 33. As the plot indicates, the code developed run time problems about 3 seconds into the transient, and the problems became worse around 17 seconds when the accumulator turned on. A possible cause of the run time problems may be that the leak paths are not modeled in accordance with current practice. The problem of fluid superheating and slow running are symptamatic of using the abrupt area change model for minor flow paths.

The break flow rate controls the rate at which the system empties, the depressurization rate, and the core flow behavior. Thus, the break flow behavior is very important, especially during the blowdown portion of the test. Figure 34 shows the flow from the side of the break which was fed from the vessel inlet annulus. The calculated mass flow rate was slightly

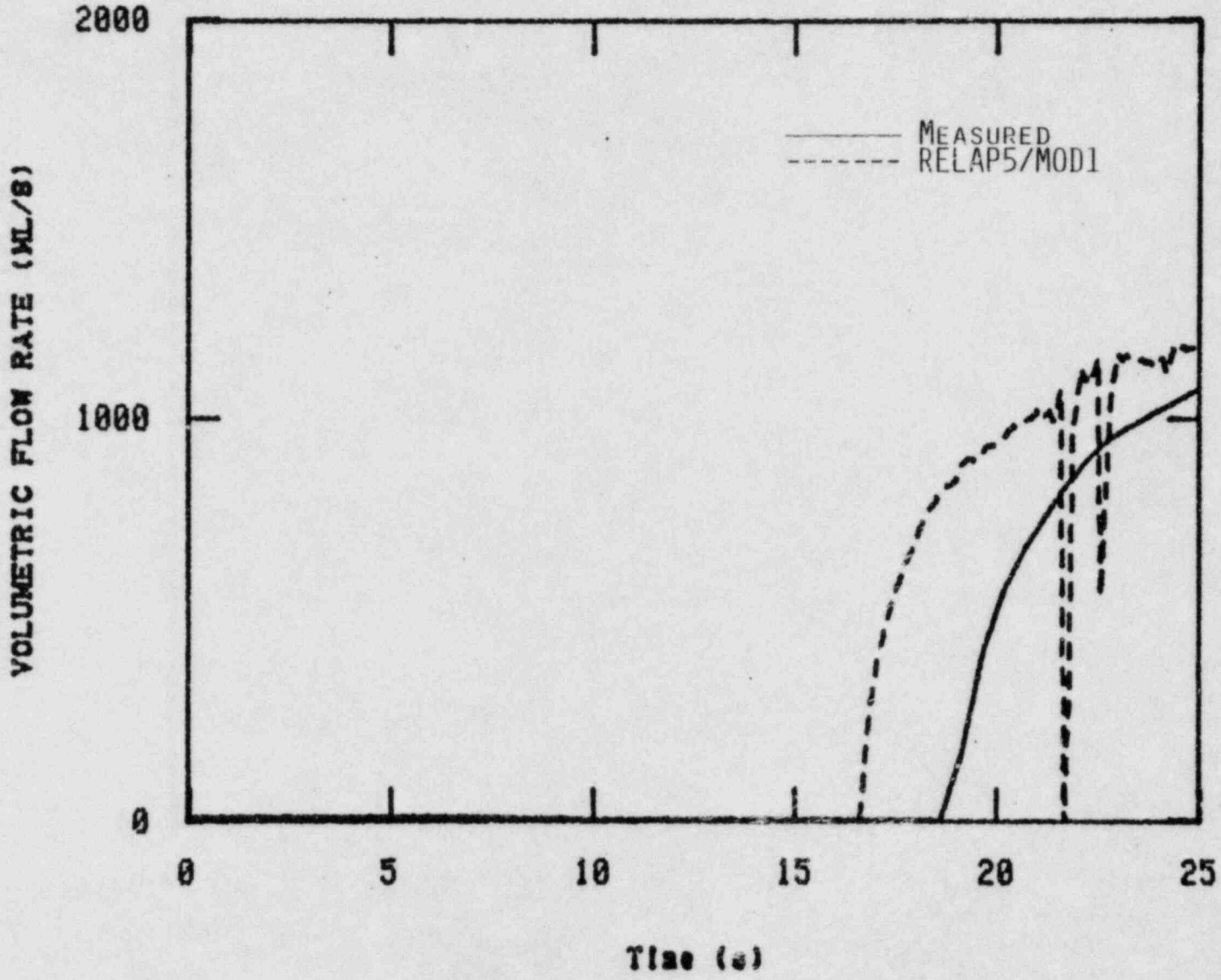

FIGURE 31. MEASUREMENT AND RELAP5/MOD1 CALCULATION OF SEMISCALE MOD-3 TEST S-07-6 VOLUMETRIC FLOW RATE FROM THE ACCUMULATOR (BASE CASE).

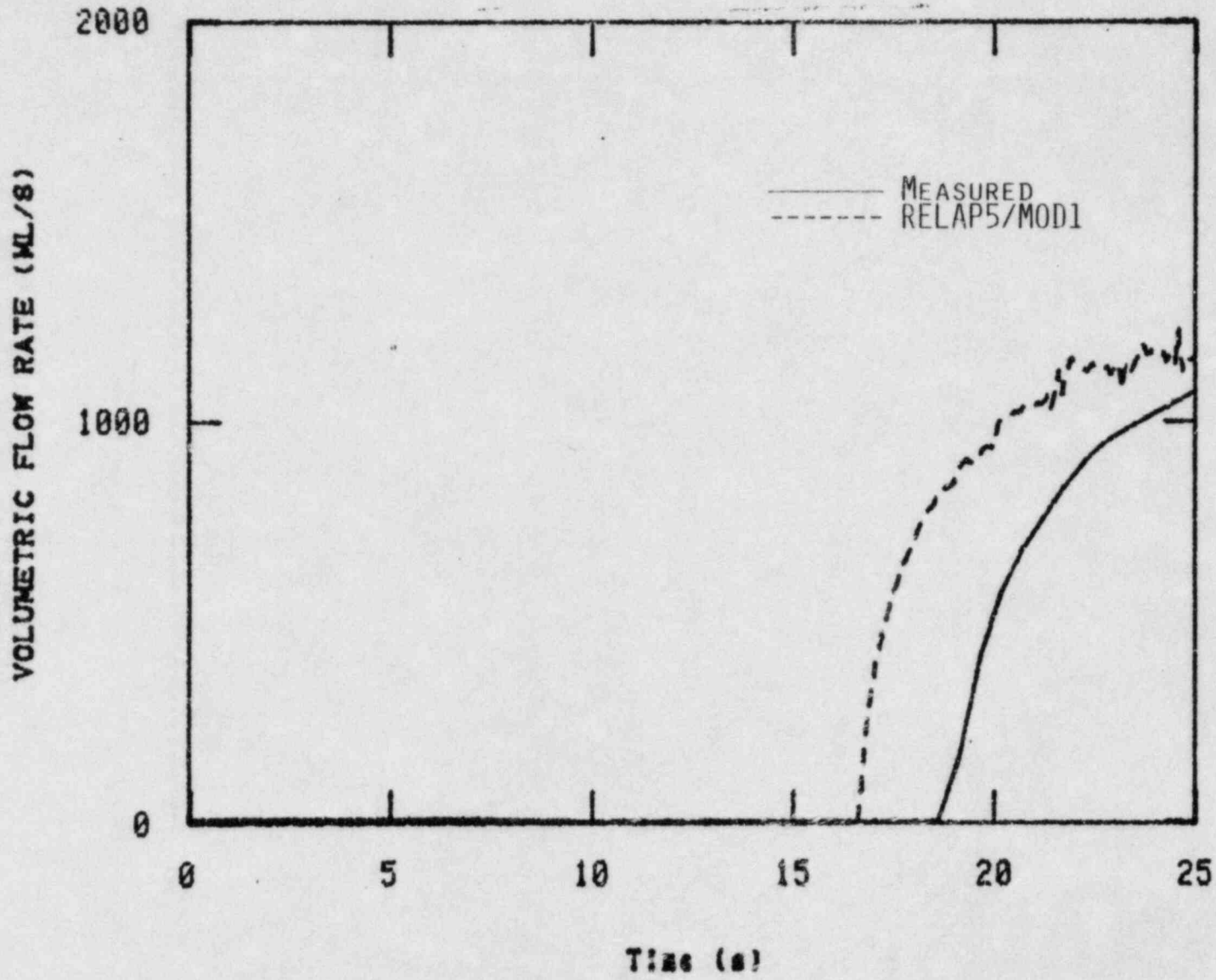

FIGURE 32. MEASUREMENT AND RELAP5/MOD1 CALCULATION OF SEMISCALE MOD-3 TEST S-07-6 VOLUMETRIC FLOW RATE FROM THE ACCUMULATOR (UPDATES VISCOUS TERM).

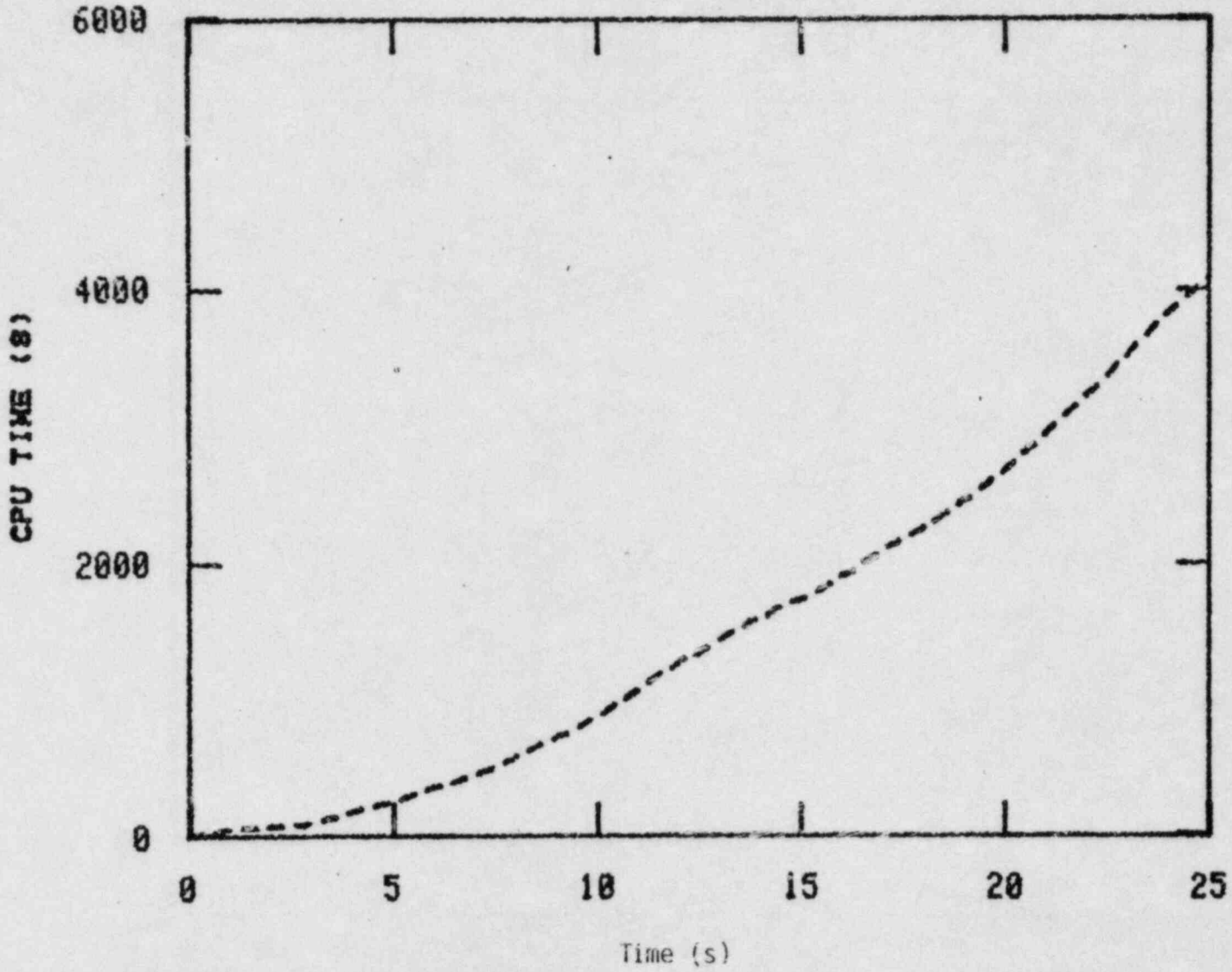

Figure 33. RELAP5/MOD1 CPU time versus simulated time for Semiscale MOD-3 Test S-07-6.

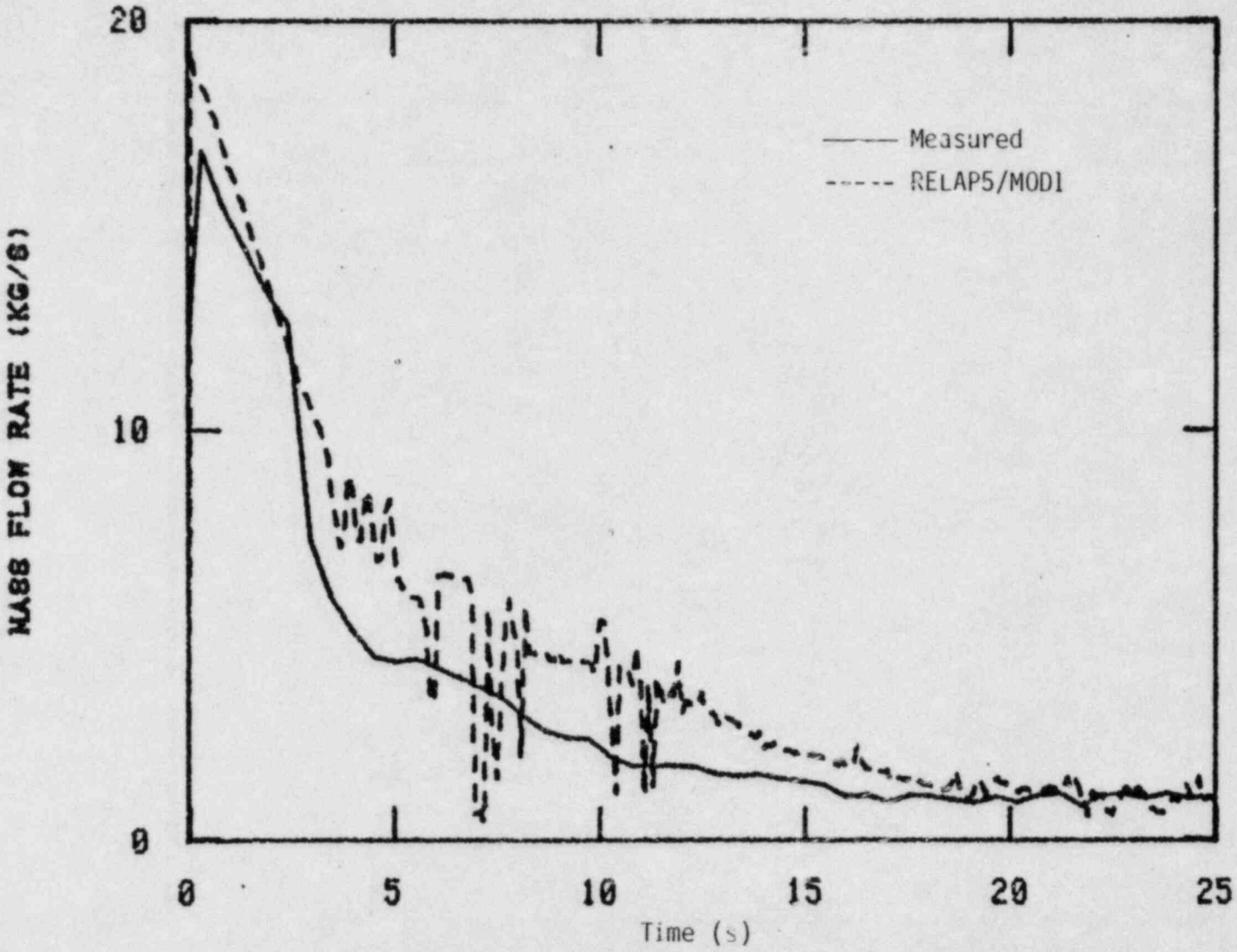

Figure 34. Measurement and RELAP5/MOD1 calculation of Semiscale MOD-3 Test S-07-6 mass flow rate at the vessel side of the break.

higher than the measured mass flow rate during the period of subcooled flow. The transition of break flow to the two-phase flow region was at 3 seconds for both the calculation and the data. The calculated break flow rate in the two-phase region was slightly higher than the data.

The differences in the break flow rate can be traced to differences in fluid conditions in the intact loop cold leg (Figure 35) and in the downcomer (Figure 36) which fed the break flow through the inlet annulus. These differences are due, in part, to the fact that the inlet annulus of the Mod-3 system has a very complex geometry. The inlet annulus is characterized as a cone-shaped annular structure feeding the downcomer at the bottom and having cold leg pipes connected horizontally on the side and separated by 180 degrees. The downcomer is a single pipe separated from the vessel in the Mod-3 system. This complex structure and associated flow field were modeled in RELAP5 by a simple branch component.

The calculated mass flow rate in the intact loop cold leg at a point just downstream of the ECC injection point agreed well with the test data (Figure 35) until 17 seconds into the transient, when the accumulator ECC injection occurs and oscillations develop. The mass flow rate in the lower part of the downcomer (positive downward), shown in Figure 36, indicated that the flow immediately reversed direction after rupture and surged up the downcomer toward the inlet annulus. The comparisons agree well up to 2 seconds, where the calculation goes to zero faster than the measured value. Similar behavior was observed in the core inlet flow. The mass flow rate in the upper plenum (positive upward) is shown in Figure 37. Here, the calculation develops some negative flows (downward), while the data remains positive.

The mass flow on the pump side of the break is given in Figure 38. The agreement was good up to 20 seconds, but a discrepancy developed for times greater than 20 seconds, which in part is due to low flow instrumentation inaccuracy. The slightly higher calculated total break mass flow rate (the sum of that shown in Figures 34 and 38) resulted in slightly more

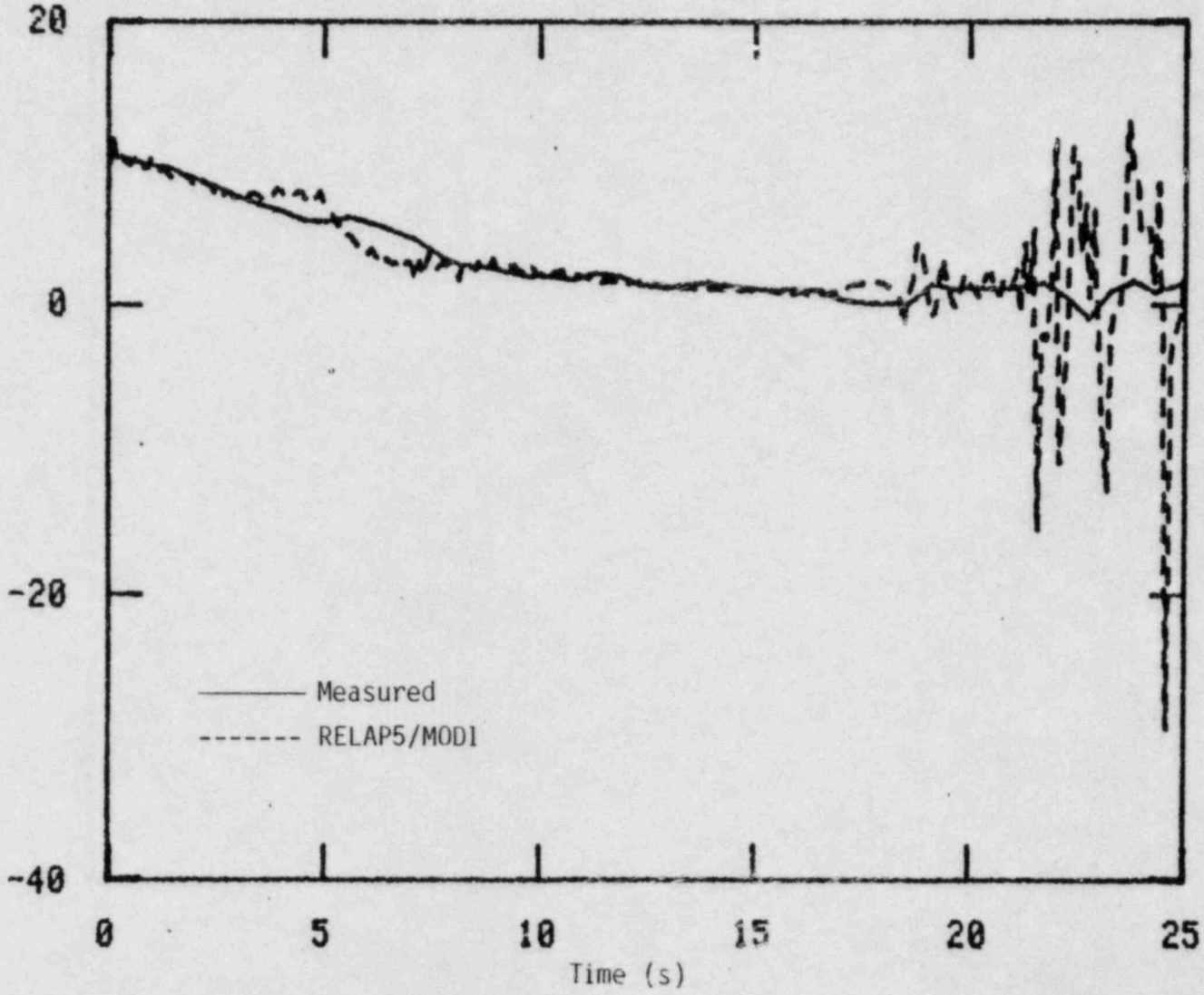

Figure 35. Measurement and RELAP5/MOD1 calculation of Semiscale MOD-3 test S-07-6 mass flow rate in the intact loop cold leg just downstream of the ECC injection point.

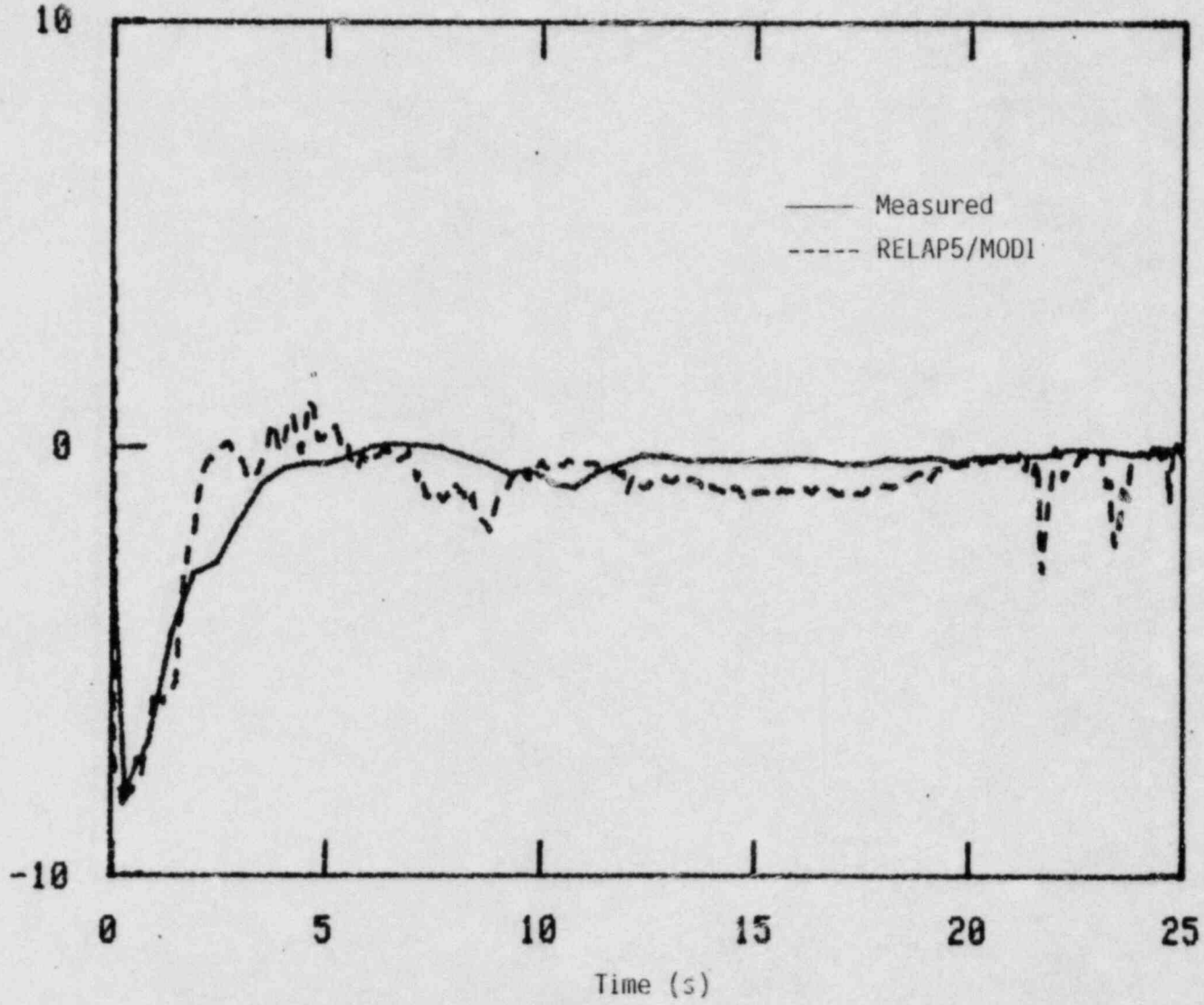

Figure 36. Measurement and RELAP5/MOD1 calculation of Semiscale MOD-3 Test S-07-6 mass flow rate in the lower part of the downcomer.

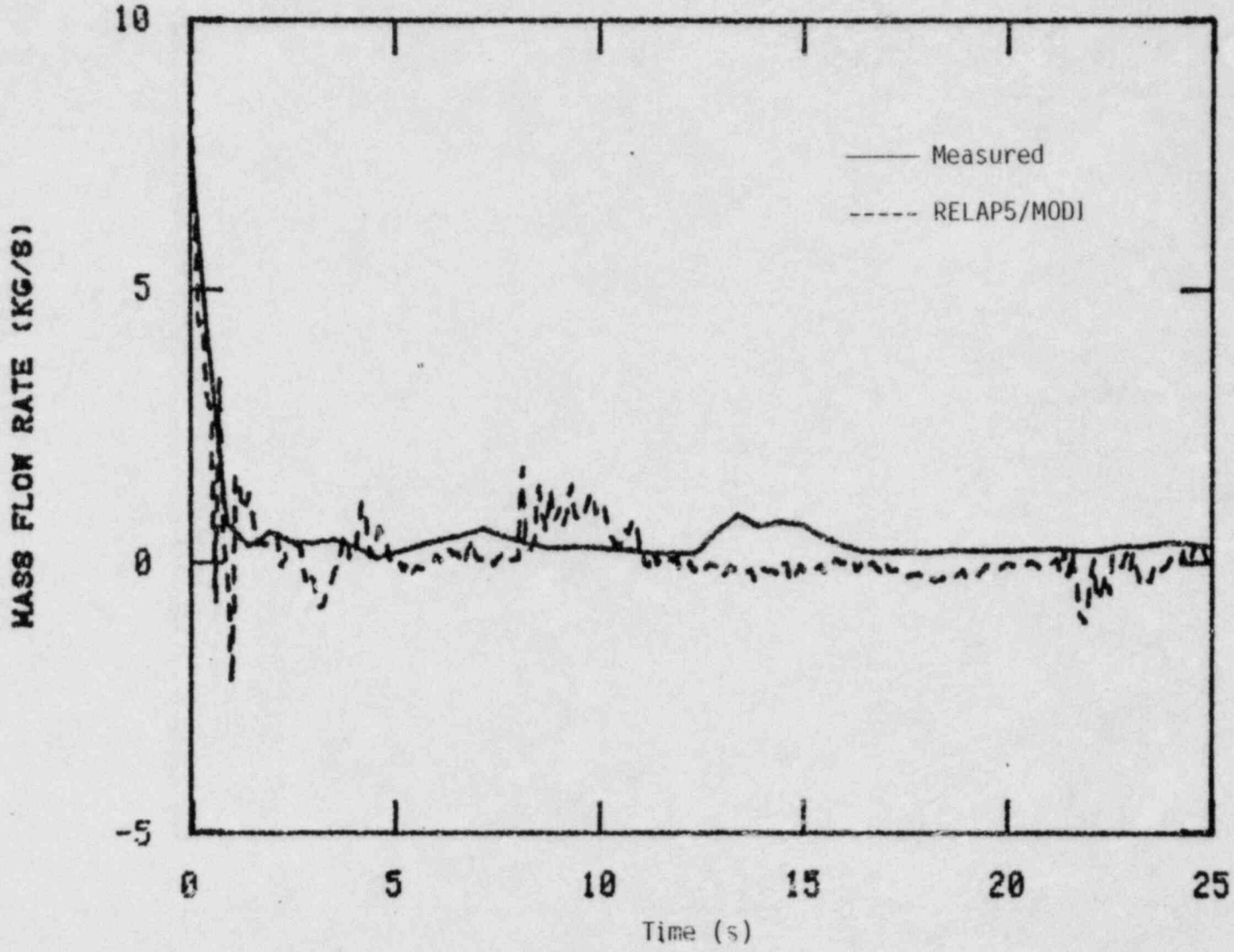

Figure 37. Measurement and RELAP5/MODi calculation of Semiscale MOD-3 Test S-07-6 mass flow rate in the upper plenum.

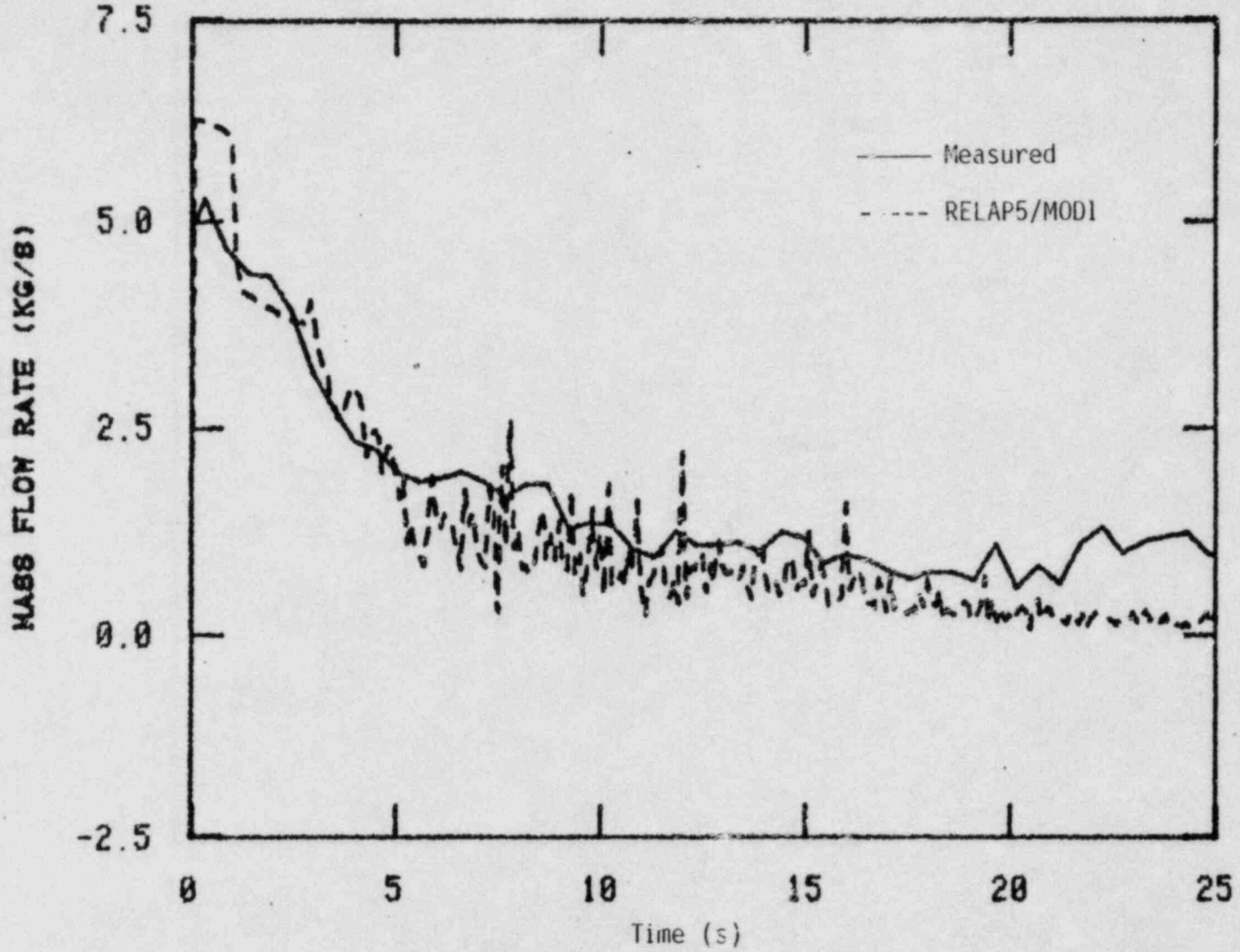

Figure 38. Measurement and RELAP5/MOD1 calculation of Semiscale MOD-3 Test S-07-6 mass flow rate at the pump side of the break.

rapid depressurization of the Mod-3 primary system. Figure 39 shows a representative primary system pressure comparison (the pressure in the vessel upper plenum). The calculated pressure was higher than shown by the test data before 5 seconds and lower from 14 to 25 seconds. The low pressure in the primary system is also the result of poor coupling between the primary and secondary system. The comparisons of the secondary system pressure as seen in the intact loop steam dome and broken loop steam dome are shown in Figures 40 and 41, respectively.

In spite of slight discrepancies, the RELAP5 calculation of the blowdown behavior of the Mod-3 system was good. This was reflected in the core heater temperature. Figure 42 shows the rod temperature during the blowdown in the hot channel at 184 cm above the bottom of the core. The calculated temperature was at the surface of the rod while the measured temperature was taken at slightly under the surface (80 K difference existed at the initial steady state conditions). Calculated temperatures reached a peak of 1100 K, which agreed with the test data. The decrease in heater rod temperature beginning at about 12 seconds after rupture was a result of water draining from the upper head into the core. The RELAP5 calculated core temperature responded to the draining of upper head water into the core at about the same time.

The RELAP5 simulation of the phenomenon associated with accumulator ECC injection when the system pressure reached 4.14 MPa will be discussed next. The volumetric flow rate from the accumulator was previously shown in Figure 32. The calculation shows the injection beginning at 17 seconds while the data shows the injection beginning at 19 seconds. The early injection is the result of lower calculated primary system pressure (Figure 39). The density downstream of the ECC injection point and just before the inlet annulus is given in Figure 43. Density increased sharply as shown in plots when ECC injection occurred. In general, the calculation agrees well with the data, except for the oscillations in this density (Figure 43) as well as the mass flow rate (Figure 35) downstream of the ECC injection point after the injection began. It is our feeling that these

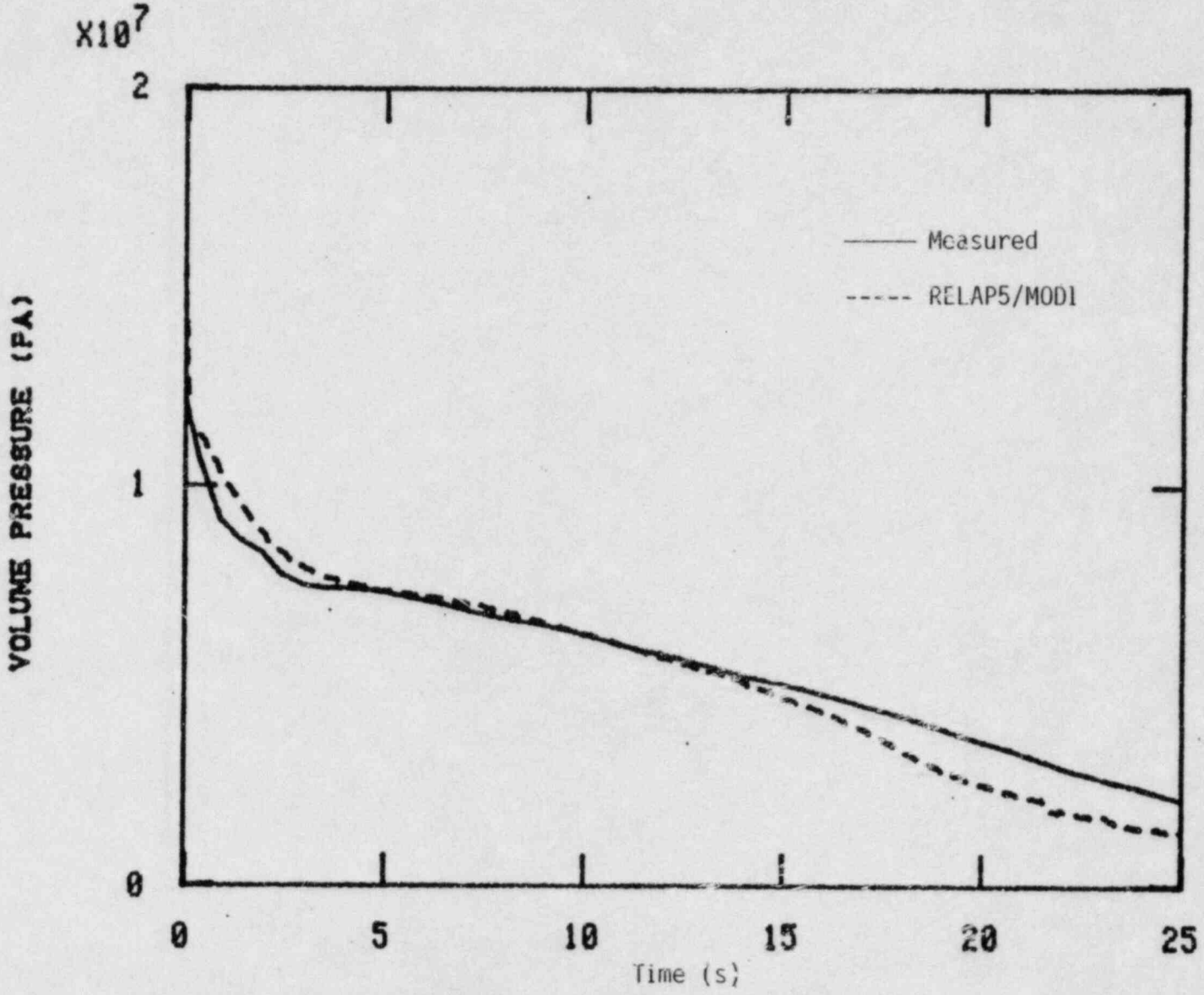

Figure 39. Measurement and RELAP5/MOD1 calculation of Semiscale MOD-3 Test S-07-6 pressure in the vessel upper plenum.

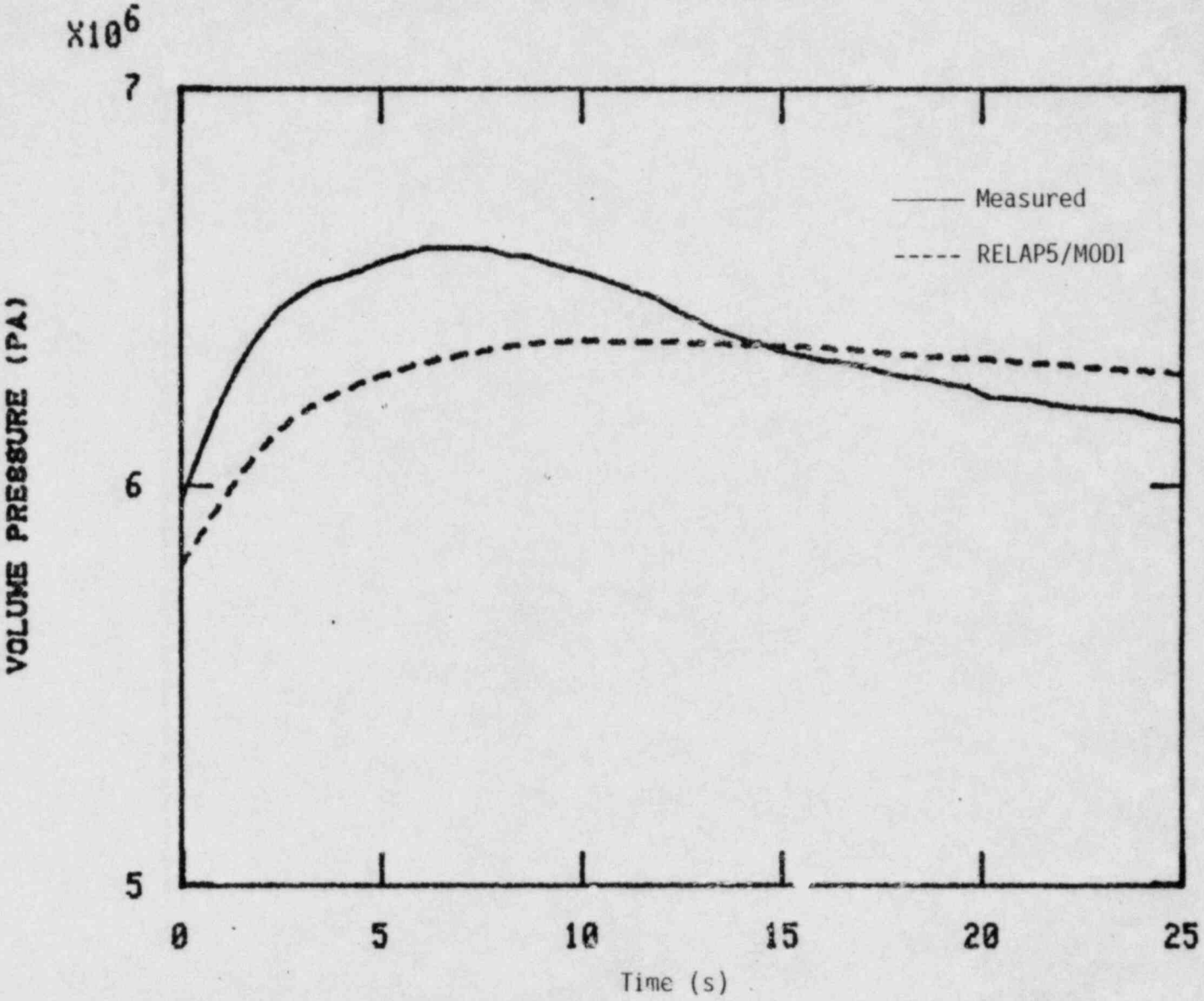

Figure 40. Measurement and RELAP5/MOD1 calculation of Semiscale MOD-3 Test S-07-6 pressure in the intact loop steam dome.

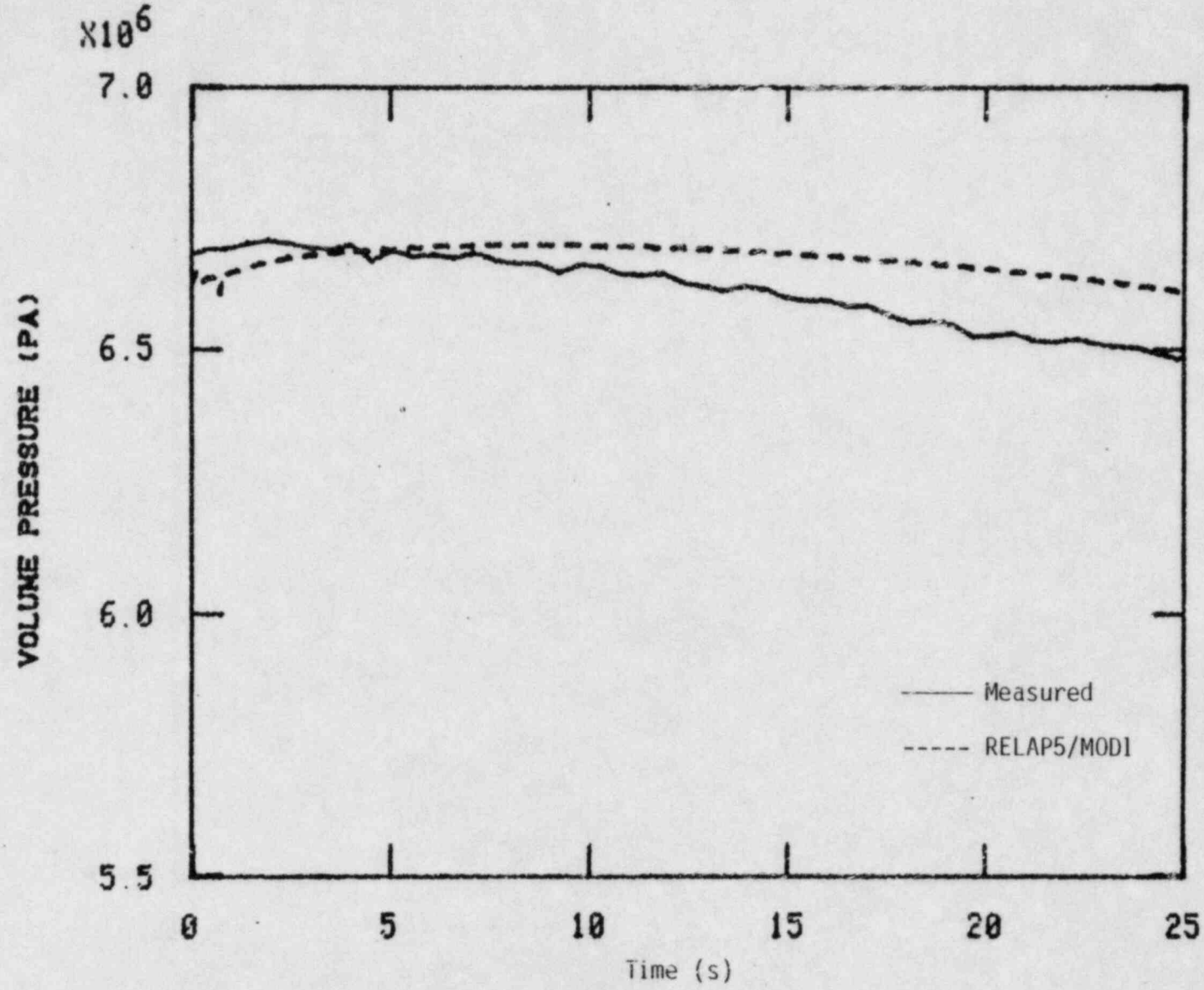

Figure 41. Measurement and RELAP5/MOD1 calculation of Semiscale MOD-3 Test S-07-6 pressure in the broken loop steam dome.

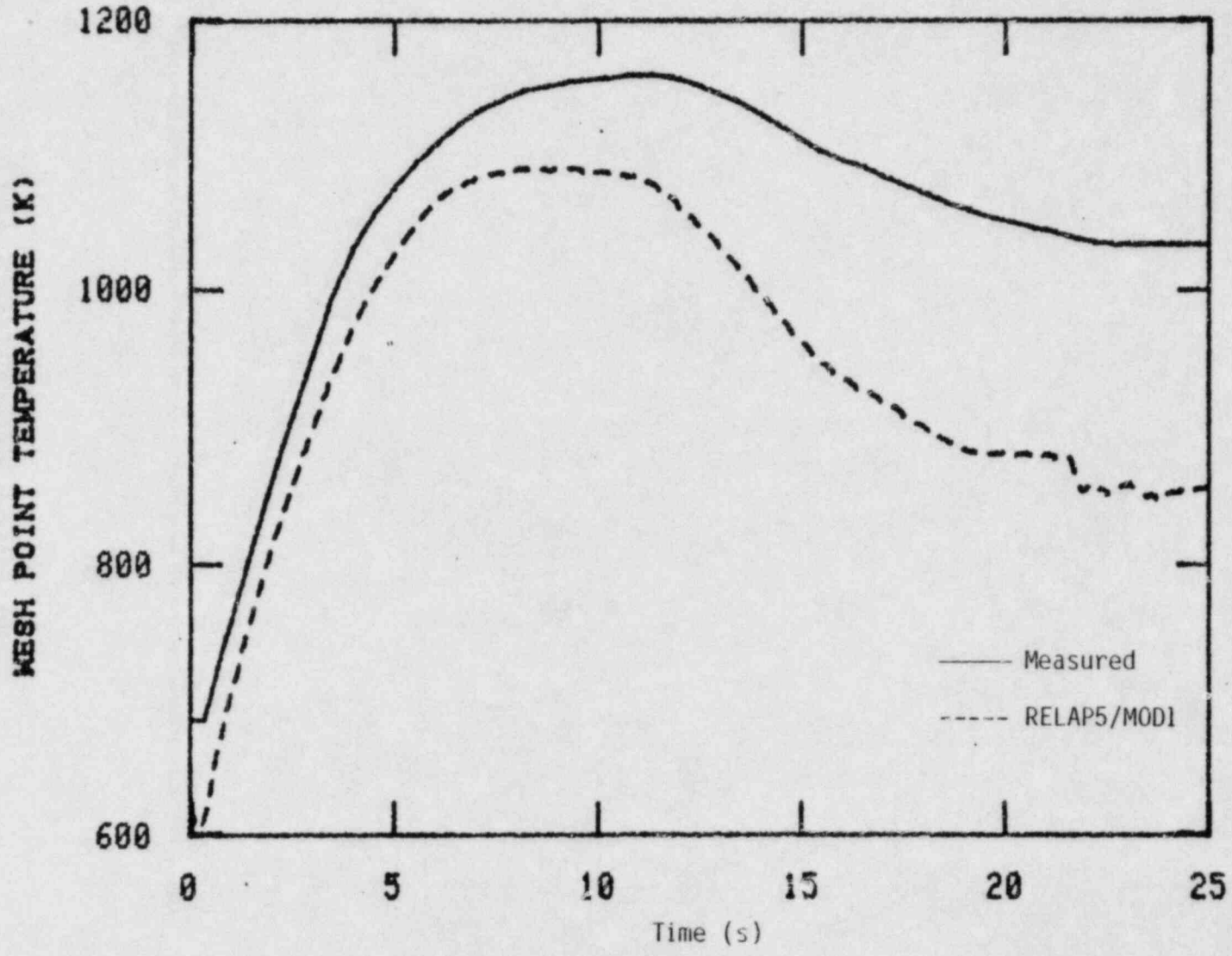

Figure 42. Measurement and RELAP5/MOD1 calculation of Semiscale MOD-3 Test S-07-6 heater rod temperature in the hot channel at 184 cm above the bottom of the core.

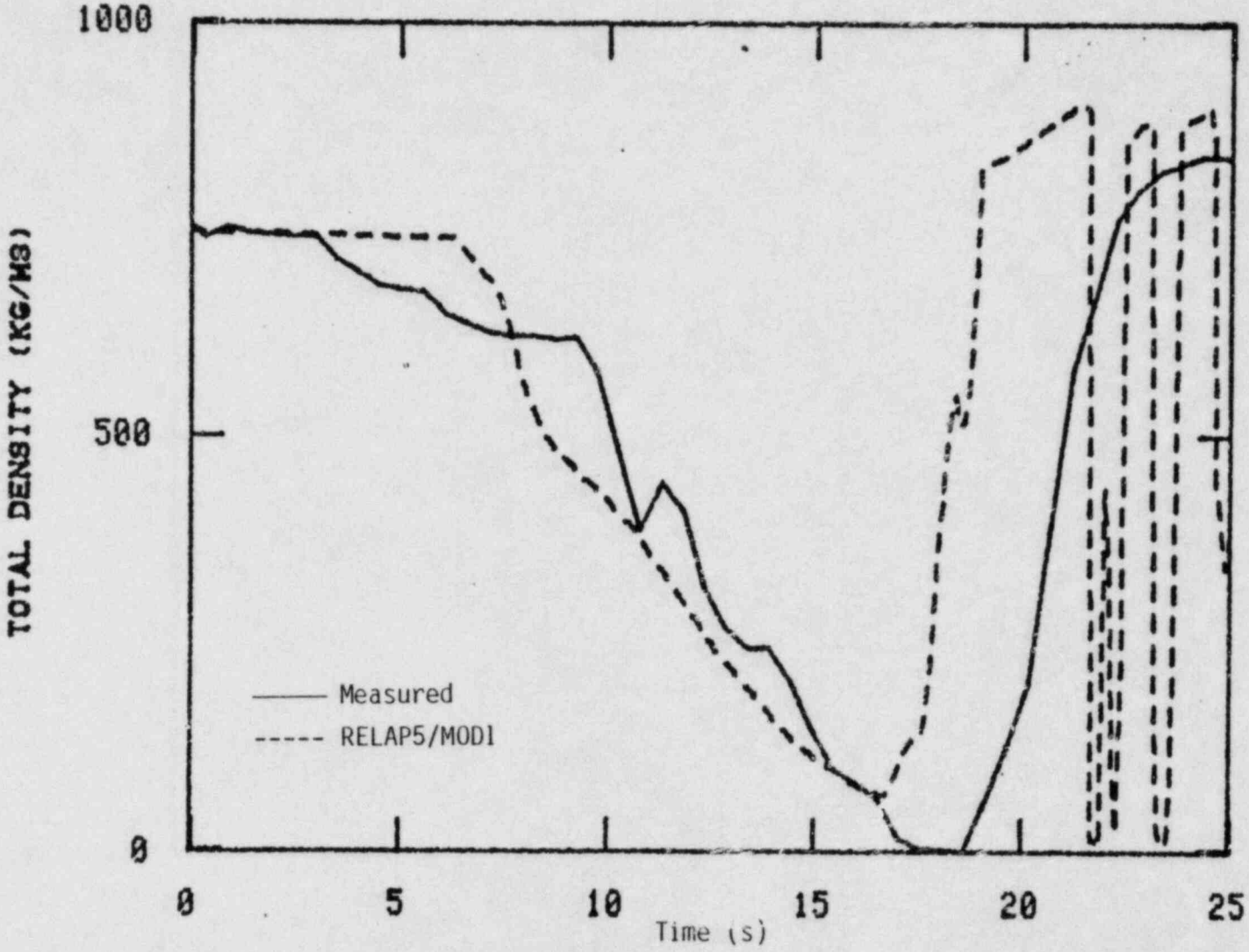

Figure 43. Measurement and RELAP5/MOD1 calculation of Semiscale MOD-3 Test S-07-6 density in the intact loop cold leg just before the inlet annulus.

oscillations in the cold leg are probably due to the high condensation rate characteristic of the MOD1 interphase mass transfer model (based on condensation values in bubbly flow).

In summary, RELAP5/MOD1 does a good job of calculating most of the key parameters for Semiscale Mod-3 Test S-07-6. On the other hand, the calculation has run time problems (163 times slower than real time out to 25 seconds) and some discrepancies develop in the mass flow rate calculations. The run time problems may have been due to noncurrent modeling of the leak paths. In addition, the calculated primary system pressure becomes too low which causes early accumulator ECC injection. After this injection, oscillations develop in the downstream mass flow rate and density. No work was done to refine the model and to explain the reasons for the poor run time as it was felt these issues were outside the scope of this report.

2.2.2 LOFT L3-7 Posttest Analysis

2.2.2.1 Purpose. The Loss-of-Fluid Test (LOFT) Facility[11] is a 50 MW(t), volumetrically scaled, pressurized water reactor (PWR) system. The LOFT facility was designed to study the engineered safety features in a commercial PWR system as to their response to a postulated loss-of-coolant accident (LOCA).

The LOFT Test L3-7[12] was performed to analyze the effects of a single-ended offset shear break of a small [1-in. (2.54 cm) diameter)] pipe connected to the cold leg of a four-loop large PWR. The test was conducted at 49 MW, yielding a maximum linear heat generation rate of 52.8 kW/m.

The LOFT Test L3-7 is presented here to demonstrate the ability of RELAP5/MOD1 to calculate the important parameters in a small break transient for a full system test.

2.2.2.2 Test Description. The LOFT facility[11] is a 50 MW(t) PWR intended to simulate the major behavioral aspects of generic 3000 MW(t) PWR's in carefully conducted experiments. The nuclear core is approximately

1.68 m in length and 0.61 m in diameter and is composed of nine fuel assemblies containing 1300 fuel rods of representative PWR design. Three unbroken PWR coolant loops are simulated by using a volume/power ratio scaled by the single circulating (intact) loop in the LOFT primary system, and the postulated broken PWR loop is simulated by the scaled LOFT blowdown (broken) loop (Figure 44).

The LOFT broken loop is orificed to simulate various break sizes and contains steam generator and pump simulators to model the hydraulic resistance of these components in the broken PWR loop. Either hot leg (reactor vessel outlet piping) or cold leg (reactor vessel inlet piping) breaks can be simulated by relocating the steam generator and pump simulators. Quick-opening valves (with opening times adjustable from approximately 20 to 50 ms) simulate the initiation of primary coolant piping ruptures. Primary blowdown effluent is collected in a blowdown suppression tank which can model the significant portions of the various PWR containment back-pressure transients.

An emergency core cooling (ECC) system is provided to model the loss-of-coolant engineered safety features in PWRs. The ECC is supplied by a high-pressure injection system (HPIS) positive displacement pump, a low-pressure injection system (LPIS) centrifugal pump, and a nitrogen pressurized accumulator. LPIS and accumulator discharge lines are orificed as required to simulate the delivery characteristics of various PWR emergency coolant injection systems. The accumulator is equipped with an adjustable height "standpipe" which allows the liquid and gas volumes to be varied. Five ECC injection points are built into the primary coolant system. These injection points are located in the intact loop hot leg, intact loop cold leg, upper plenum, lower plenum, and vessel downcomer.

Fluid pressure, temperature, velocity, and density are monitored by extensive instrumentation at key locations in the primary coolant, emergency core coolant, blowdown, and secondary coolant systems. Thermocouples monitor fuel rod cladding temperatures and support tube temperatures at 196 core

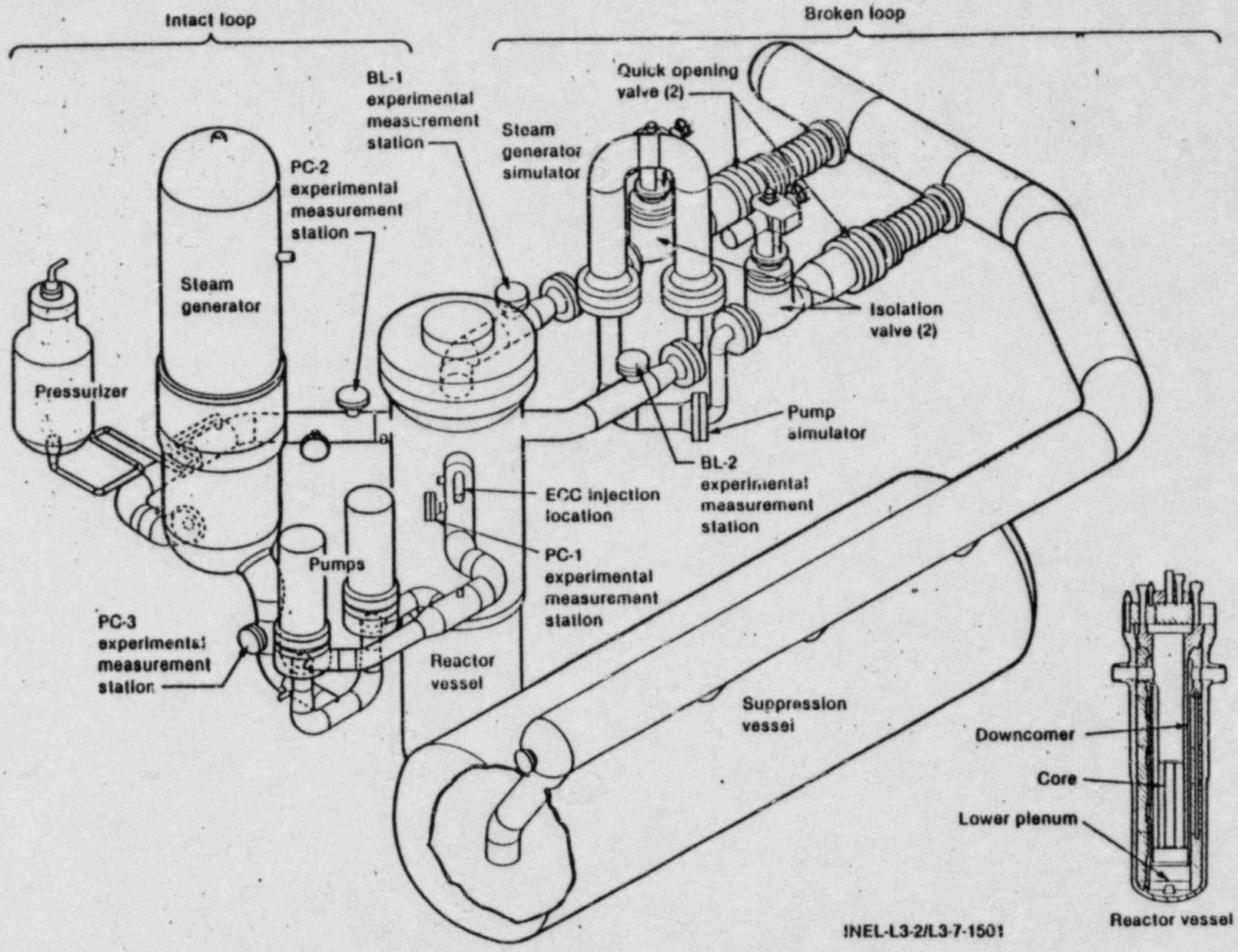

Figure 44. Schematic of LOFT test facility.

locations. Four fixed nuclear detectors and a four-location traversing in-core nuclear detector system determine core power profiles and transient response.

The primary objectives of Test L3-7[12] were to establish a break flow approximately equal to HPIS flow when the primary pressure was in the range of 6.9 MPa, to establish conditions for steam generator reflux cooling, to isolate the break and stabilize the plant at cold shutdown conditions, and to analyze the data obtained to investigate associated phenomena.

Prior to the break, the nuclear core was operating at a steady state maximum heat generation rate of 52.8 ± 3.7 kW/m. Other significant initial conditions for Test L3-7 were: system pressure, 14.90 ± 0.25 MPa; core outlet temperature, 576.1 ± 0.5 K; and intact loop flow rate, 481.3 ± 6.3 kg/s. Table 1, which is taken from Reference 12, contains a more complete list of initial conditions. Table 2, which also is taken from Reference 12, contains the sequence of major events for the test, and Figure 45 shows the measured primary system pressure and indicates some of these events. At 36 s after the break occurred, the reactor scrammed on a low system pressure signal. Within 10 s after scram verification, the pumps were manually tripped and coasted down. Pump coastdown was followed by the inception of natural loop circulation. Between 1800 (30 min) and 5974 s (1 hr. 40 min), the HPIS was turned off to hasten the loss-of-fluid inventory and to establish the conditions considered favorable for reflux flow in the primary loop. Starting at 3600 s (1 hr), operator-controlled steam bleeding (opening the main steam bypass valve early and the main steam valve later in the transient) and steam generator feeding (using both the auxiliary and main feedwater systems) were used to decrease primary system pressure. Steam generator secondary feed and bleed maintained an effective heat sink throughout the experiment.

Later in the experiment, at 7302 s (2 hr. 2 min), the blowdown isolation valve was closed, which isolated the break. System mass depletion stopped, and all decay heat energy not lost to the environment was removed

TABLE 1. INITIAL CONDITIONS FOR EXPERIMENT L3-7

Parameter	Specified Value[a]	Measured Value[b]
Primary Coolant System		
Mass flow rate (kg/s)	478.8 ± 8.8	481.3 ± 6.3
Hot leg pressure (MPa)	14.95 ± 0.34	14.90 ± 0.25
Cold leg temperature (K)	556.8 ± 2.2	556 ± 3
Hot leg temperature (K)	--	576.1 ± 0.5
Boron concentration (ppm)	As required to maintain temperature	726 ± 15
Reactor Vessel		
Power level (MW)	50 ± 1	49 ± 1
Maximum linear heat generation rate (kW/m)	--	52.8 ± 3.7
Control rod position (above full-in position) (m)	1.372 ± 0.013	1.373 ± 0.010
Pressurizer		
Steam volume (m^3)	--	0.30 ± 0.05
Liquid volume (m^3)	--	0.63 ± 0.05
Water temperature (K)	--	615.0 ± 0.3
Pressure (MPa)	14.95 ± 0.34	14.90 ± 0.04
Liquid level (m)	1.13 ± 0.18	1.10 ± 0.02
Broken Loop		
Cold leg temperature near reactor vessel (K)	--	557.7 ± 2.5
Hot leg temperature near reactor vessel (K)	--	561.4 ± 2.5
Steam Generator Secondary Side		
Water level (m)[c]	0.25 ± 0.05	0.25 ± 0.06
Water temperature (K)	--	544.0 ± 0.2
Pressure (MPa)	--	5.576 ± 0.012
Mass flow rate (kg/s)	--	28.0 ± 0.4
Accumulator A		
Liquid level (m)	1.85 ± 0.05	1.85 ± 0.01
Liquid volume (m^3)	--	2.60 ± 0.03
Gas volume (m^3)	--	1.19 ± 0.03
Pressure (MPa)	4.22 ± 0.17	4.31 ± 0.06
Temperature (K)	305.4 ± 5.6	306.6 ± 0.7
Boron concentration (ppm)	>3000	3405 ± 15

TABLE 1. (continued)

Parameter	Specified Value[a]	Measured Value[b]
HPIS		
Initial flow rate (L/s)	0.32 ± 0.13	0.32 ± 0.02
Initiation pressure (MPa)	13.16 ± 0.19	13.35 ± 0.24

a. The specified value tolerance is an indicated operating band.

b. The measured value tolerance is the uncertainty in the measurement.

c. The water level is defined as 0.0 at 2.95 m above the top of the tube sheet.

TABLE 2. SEQUENCE OF EVENTS FOR EXPERIMENT L3-7

Event	Time after LOCE Initiation (s)
LOCE initiated	0
Reactor scrammed	36.0 ± 0.1
Control rods reached bottom	38.1 ± 0.1
Primary coolant pumps tripped	39.3 ± 0.5
Primary coolant pump coastdown completed	56.2 ± 0.1
Core natural circulation first indicated	60.8 ± 0.5
HPIS injection initiated	65.6 ± 0.1
SCS auxiliary feed initiated	75 ± 3
Pressurizer emptied	264 ± 7
Upper plenum reached saturation pressure	382 ± 6
End of subcooled break flow	1037 ± 10
SCS auxiliary initial feed terminated	1800 ± 5
HPIS flow terminated	1805.3 ± 0.1
SCS steam bleed initiated	3603 ± 1
HPIS flow reinstated	5974.2 ± 0.1
Accumulator injection initiated	6028 ± 5
Break isolated	7302.0 ± 0.1
Primary system fluid became subcooled	7915 ± 20
Pressurizer refill initiated	8680 ± 10
Purification system recirculation initiated	18 180 ± 60
Pressurizer refill terminated[a]	19 900 ± 100
Experiment completed[b]	29 500 ± 100

a. The level at which pressurizer refill terminated was 1.4 m.

b. The experiment was finished when the PCS temperature dropped to 366.5 K.

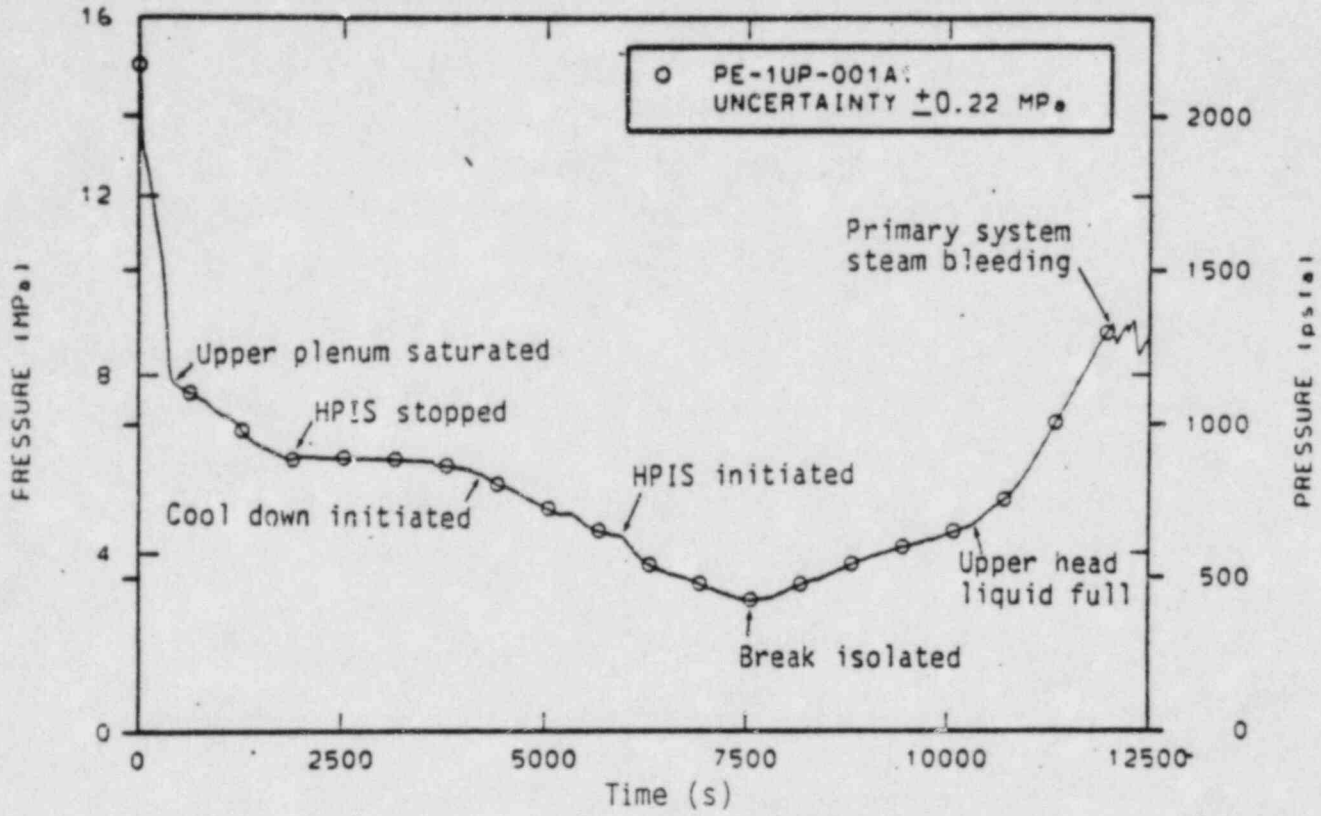

Figure 45. Measured primary system pressure for LOFT test L3-7.

by the steam generator. Primary system pressure gradually increased, causing the fluid in the system to become subcooled. Subsequently, the purification system was used to bring the reactor to a cold shutdown condition, and the experiment terminated.

2.2.2.3 RELAP5 Model. The RELAP5/MOD1 model of the LOFT facility for Test L3-7 included 105 fluid control volumes and 108 flow junctions. The system nodalization is illustrated schematically in Figure 46, and the input deck used to run the transient is given in Appendix J. In the model, a total of 65 heat slabs (shown as shaded areas in Figure 46) were used to represent heat transfer in the intact loop steam generator vessel, core, and pressurizer. The value of the two-phase and subcooled discharge coefficients for the break used in the input deck were both 1.0.

This input deck is practically the same as the one used in the LOFT program's posttest analysis[13] for L3-7, which in turn was developed from the LOFT base deck developed during 1980.[14] As with the Semiscale input deck used in this report, this LOFT input deck is somewhat dated and does not represent the current deck being used to model LOFT. Unfortunately, no documentation is available at this time for the current deck. The input deck in Appendix J also employed the old way of modeling leak paths. As with Semiscale, the current LOFT input deck now models leak paths by using smooth area changes, letting the area at a junction default, and inputting forward and reverse form losses. This way of modeling the leak paths is now the recommended practice. The junction connecting components 245 and 200 is such a leak path in this problem. The LOFT posttest analysis deck was changed to incorporate Component 520 into Component 500, which is in keeping with the current LOFT method of modeling the separator. In the process of doing this, an error was made in connecting Component 515 to Component 500, which resulted in a 20% error in the elevations of the intact loop steam generator. (For Card 5003101, the "to connection" code was incorrectly entered as 500000000 instead of 500010000.) Unfortunately, this error was not detected until after the transient simulation run was completed. We reran the corrected input deck for the steady state

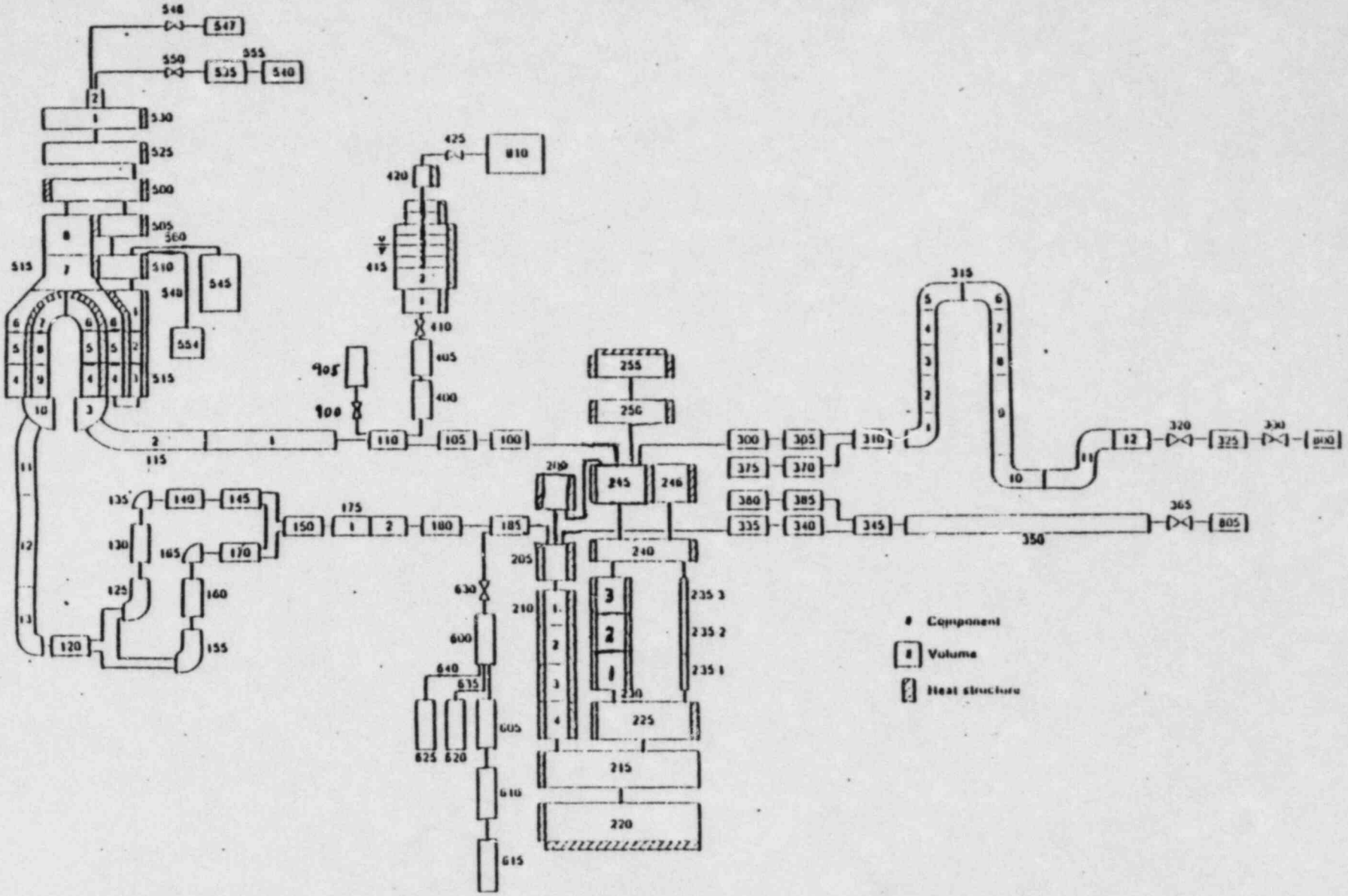

Figure 46. RELAP5/MOD1 nodalization for LOFT test L3-7.

initialization and found no difference with the previous steady state run. Thus, rather than rerun the transient out to 5900 seconds, we felt the results would be unaffected and decided to accept the results. This correction has been incorporated in the deck shown in Appendix J.

After the transient was completed, a missing card was found in the deck which was also missing from the deck used in the LOFT posttest analysis. Heat structure-geometry 2100 was found to be missing Card 12100502, which resulted in heat structure number 2100002 being connected to Volume 210030000 rather than 210020000. It was felt that this missing card would not significantly affect the results, so the transient was not rerun. This card has been incorporated into the deck included as Appendix J.

Finally, an error was found after the transient was completed in the volumetric heat capacity of Inconnel 600 (composition number 6). The table had values of the order 10^5, but the correct values are of the order 10^6. This error was also in the deck used in the LOFT posttest analysis. Again it was felt this error would not adversely affect the results, so the transient was not rerun. This correction also has been incorporated into the input deck in Appendix J.

The first attempt to run the transient was made using the LOFT project posttest analysis deck (which was used with RELAP5/MOD1/CY=10) on RELAP5/MOD1/CY=17 using only the standard LOFT update to the pump for a variable inertia model (Appendix K). Slow run time was encountered, until the updates included in Appendix A were added. This LOFT L3-7 test simulation, as well as the other tests in this developmental assessment, has been made using the update in Appendix A. The simulation was run out to 245 seconds and the results compared to data. The simulation was stopped at 245 seconds because important changes between calculated and measured pressure had occurred by this time (the initial conditions were the same as those used in the LOFT posttest analysis). Figures 47 and 48 show the comparison between the data and RELAP5 for pressure in the primary system and secondary system, respectively. The primary system calculated

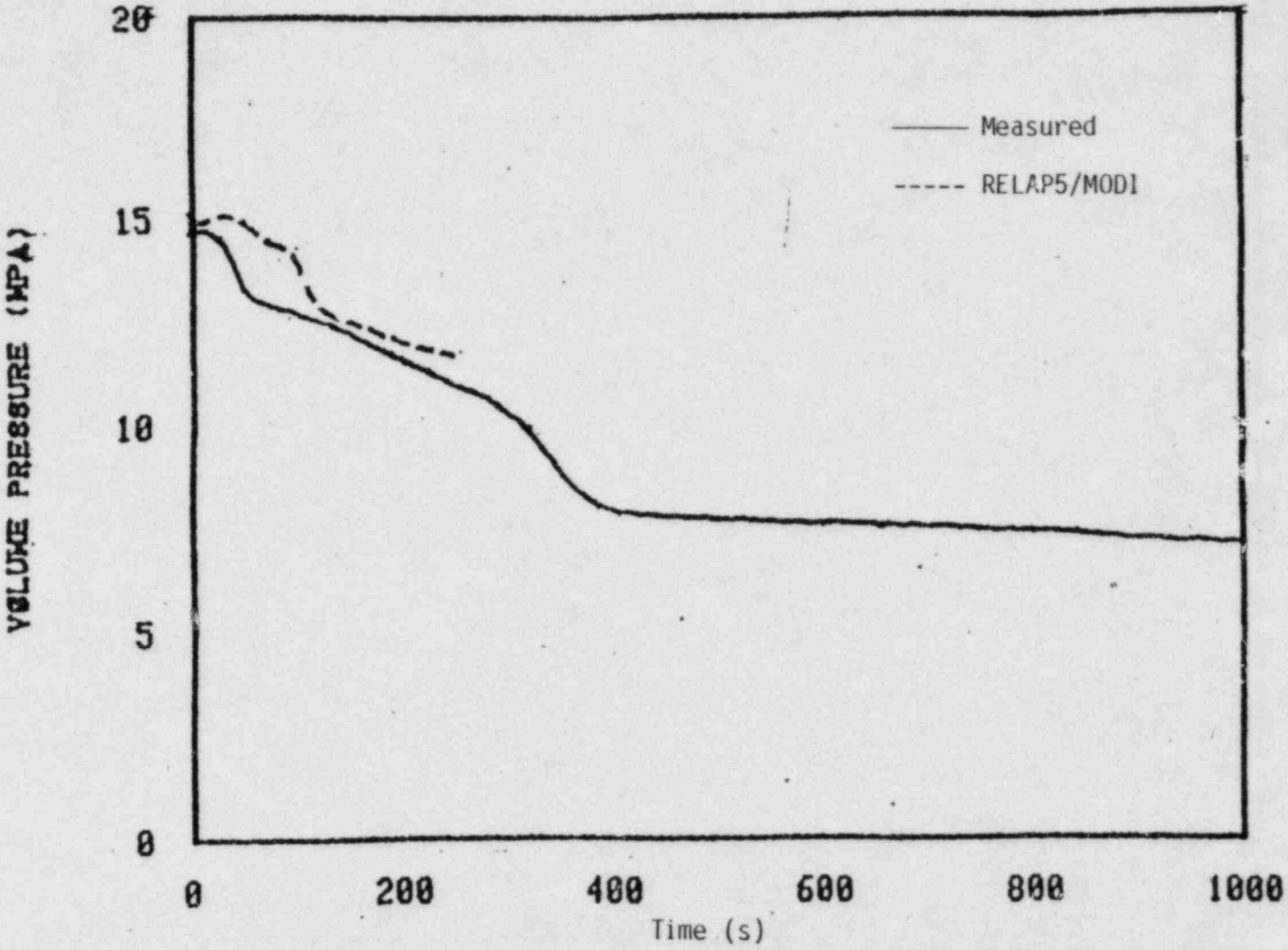

Figure 47. Measurement and RELAP5/MOD1 calculation of LOFT test L3-7 primary system pressure (original deck).

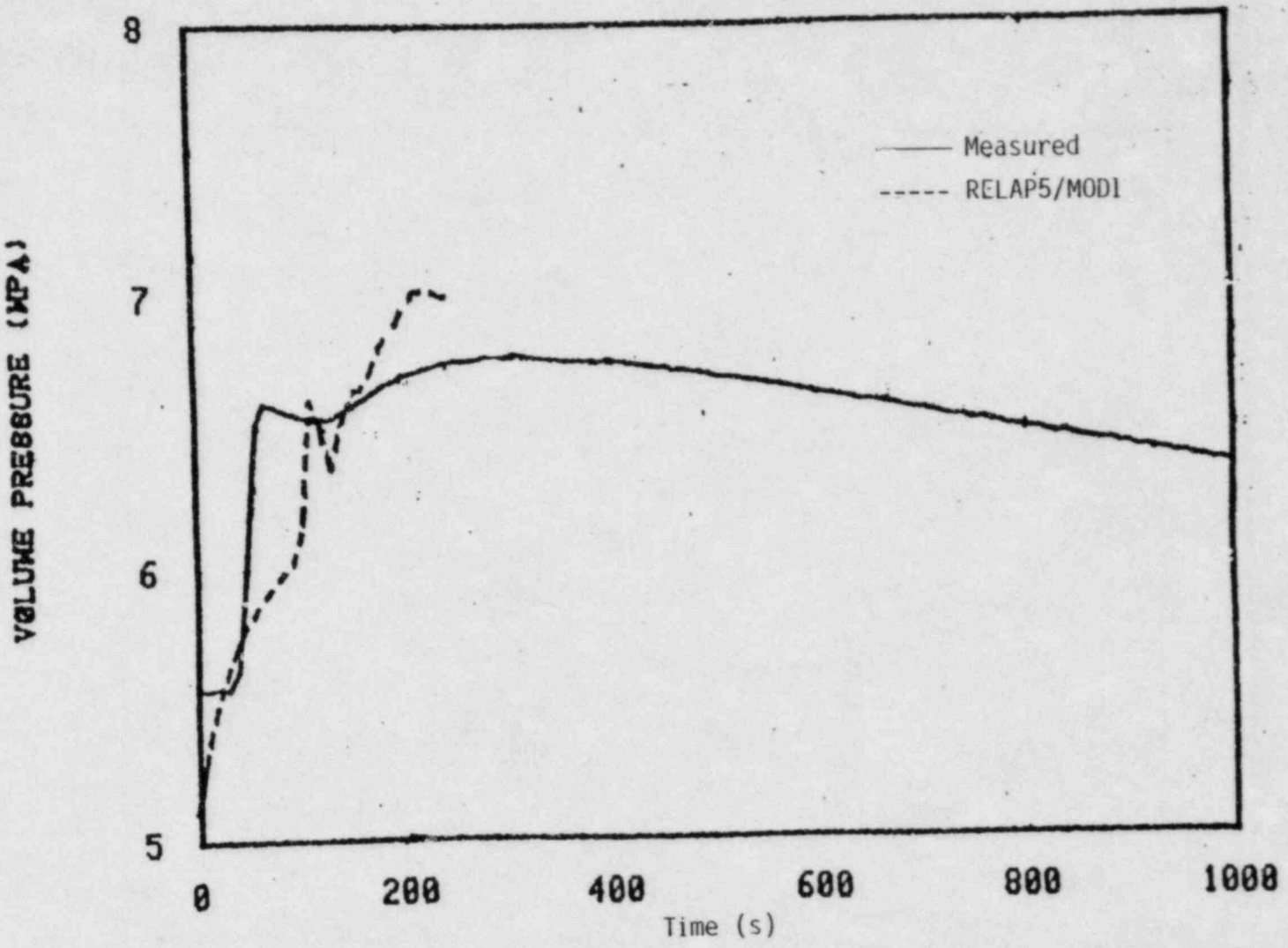

Figure 48. Measurement and RELAP5/MOD1 calculation of LOFT test L3-7 secondary system pressure (original deck).

pressure actually increases initially, and the secondary system calculated pressure is in poor agreement with the data. It was suspected that these differences were caused by changes to the code between Cycles 10 and 17 that rendered the steady-state initialization invalid. Therefore, it was decided to run a steady-state initialization using Cycle 17 with updates from Appendices A and K, following the normal LOFT procedures. For this calculation, most of the outer heat structures were removed, the break was closed, and the broken loop was made intact. The area for the steam control valve (Component 550) was adjusted slightly (final value of 0.00485 m^2) to obtain reasonable mass flow rates in the secondary side. The steady state was run for 210 seconds, and representative plots of the primary system pressure, secondary system pressure, primary system hot leg temperature, secondary system temperature, and steam control valve mass flow rate are shown in Figures 49-53. The normal LOFT initialization procedure was followed. The RELAP5 output file from this steady state run was saved, then this file and the steady-state deck were run through LOFT's PYGMALION[15] program, to obtain a new deck initialized to the conditions at the end of the steady-state run. The outer heat structures were then replaced, the break was replaced, dead end pressures and energies were initialized to values in connected components, dead end velocities were zeroed out, the pressurizer pressures and qualities were sharpened to match initial conditions, and the broken loop temperatures were reset to specifications. This procedure established the input deck used to run the transient, which is essentially the deck listed in Appendix J. As mentioned earlier, this deck was corrected after the simulation was completed to incorporate errors found in Component 500, heat structure-geometry 2100, and Inconnel 600 heat capacity.

2.2.2.4 Simulation Results and Discussion. RELAP5/MOD1/CY=17, with the updates listed in Appendices A and K, was used to simulate the experiment. Since the accumulator was expected to begin injection around 6000 sec, the code was updated at 5500 sec to repair problems with the accumulator and branch components as was done with Semiscale Test S-07-6. These updates are listed in Appendices F and I. In concert with this, the input deck for the accumulator component had to be changed. For the LOFT

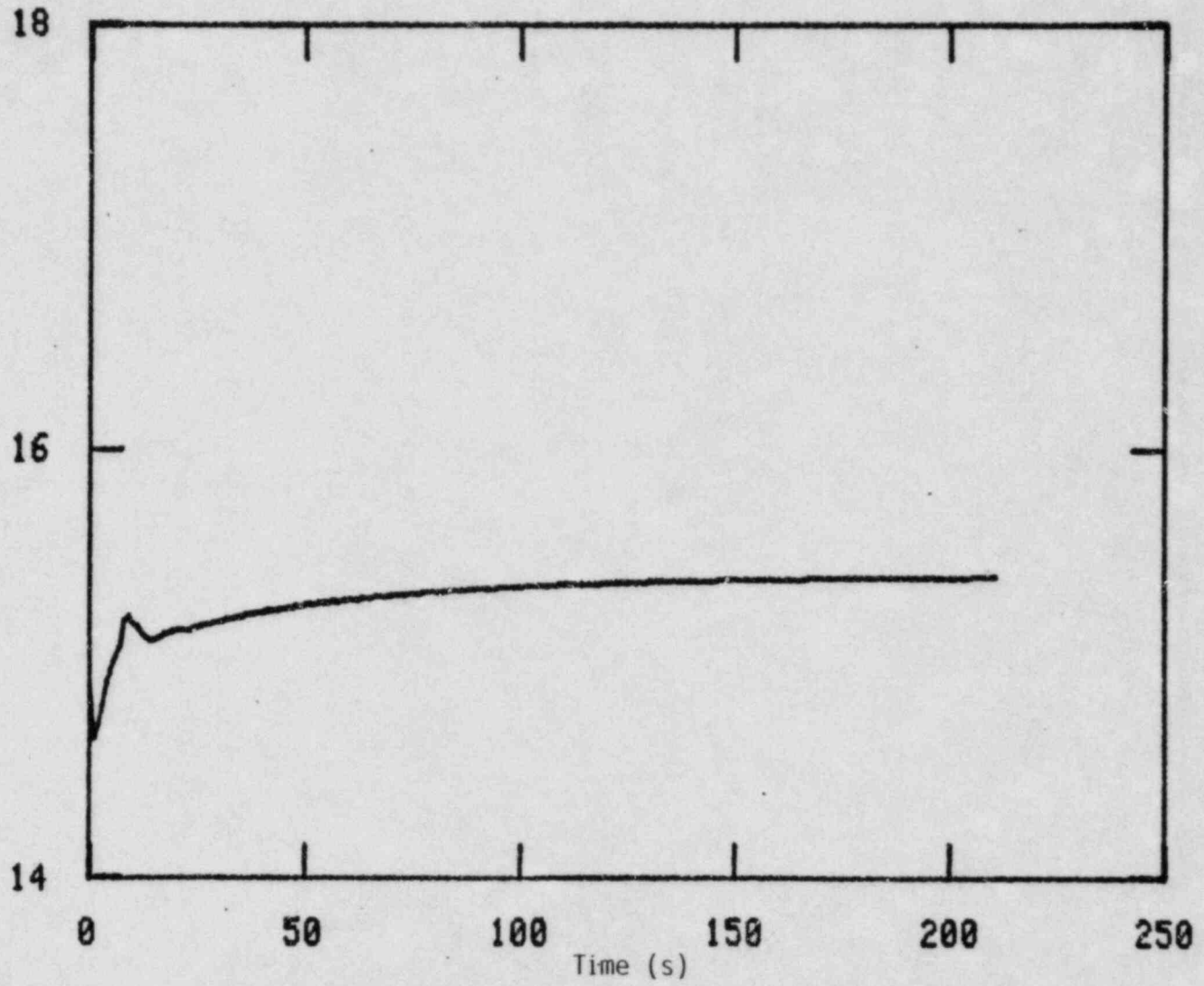

Figure 49. RELAP5/MOD1 steady state calculation of LOFT test L3-7 primary system pressure.

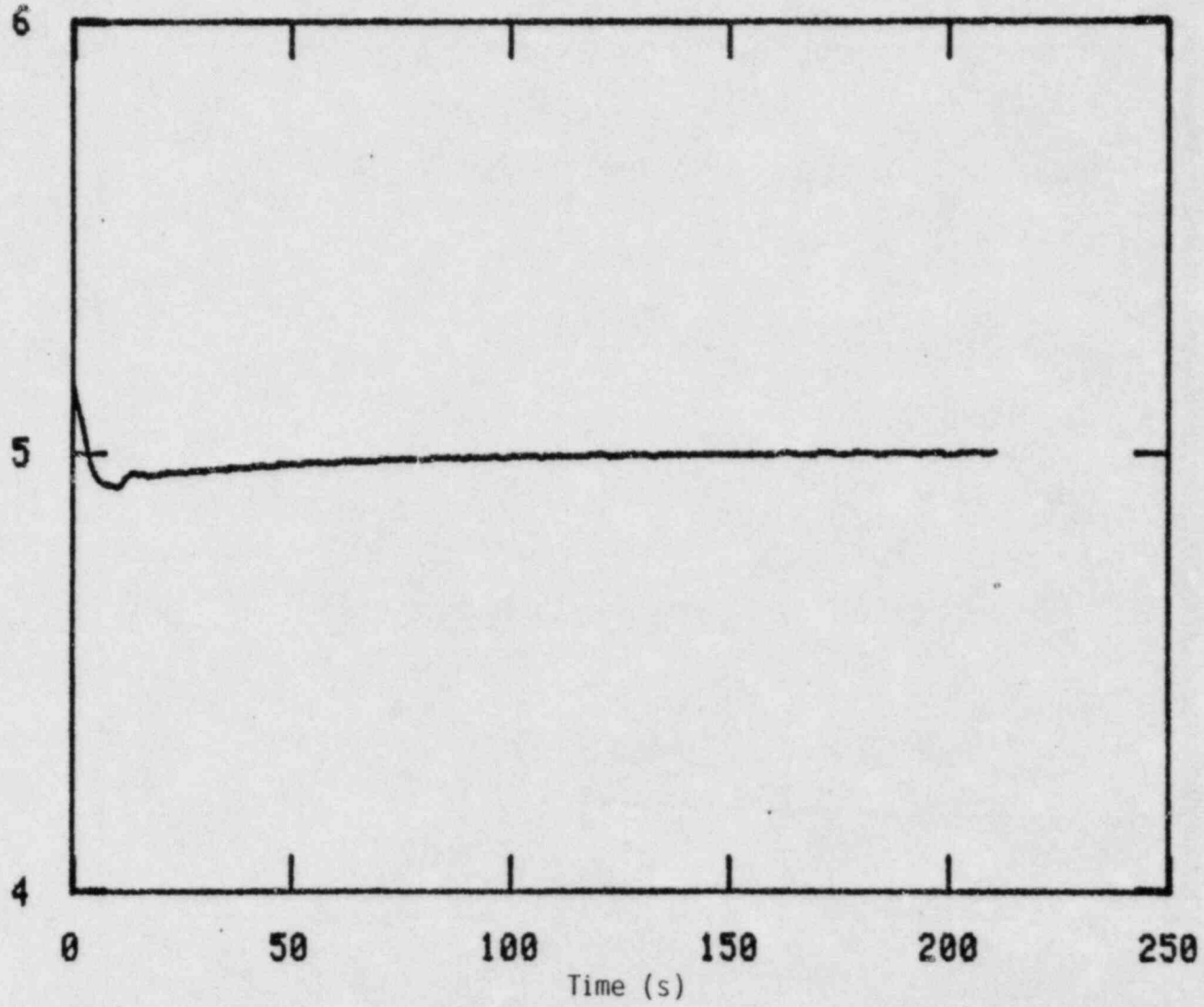

Figure 50. RELAP5/MOD1 steady state calculation of LOFT test L3-7 secondary system pressure.

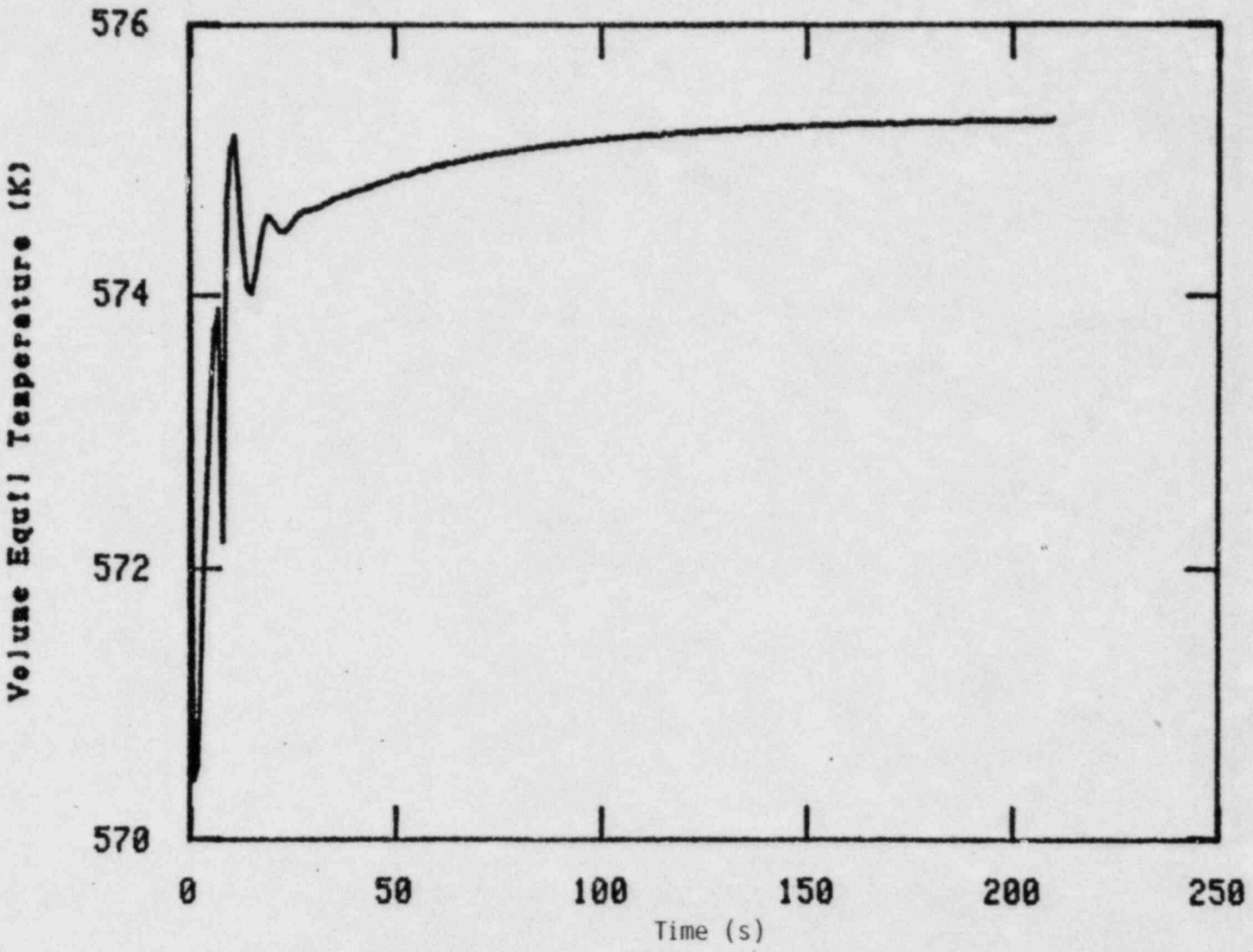

Figure 51. RELAP5/MOD1 steady state calculation of LOFT test L3-7 primary system hot leg temperature.

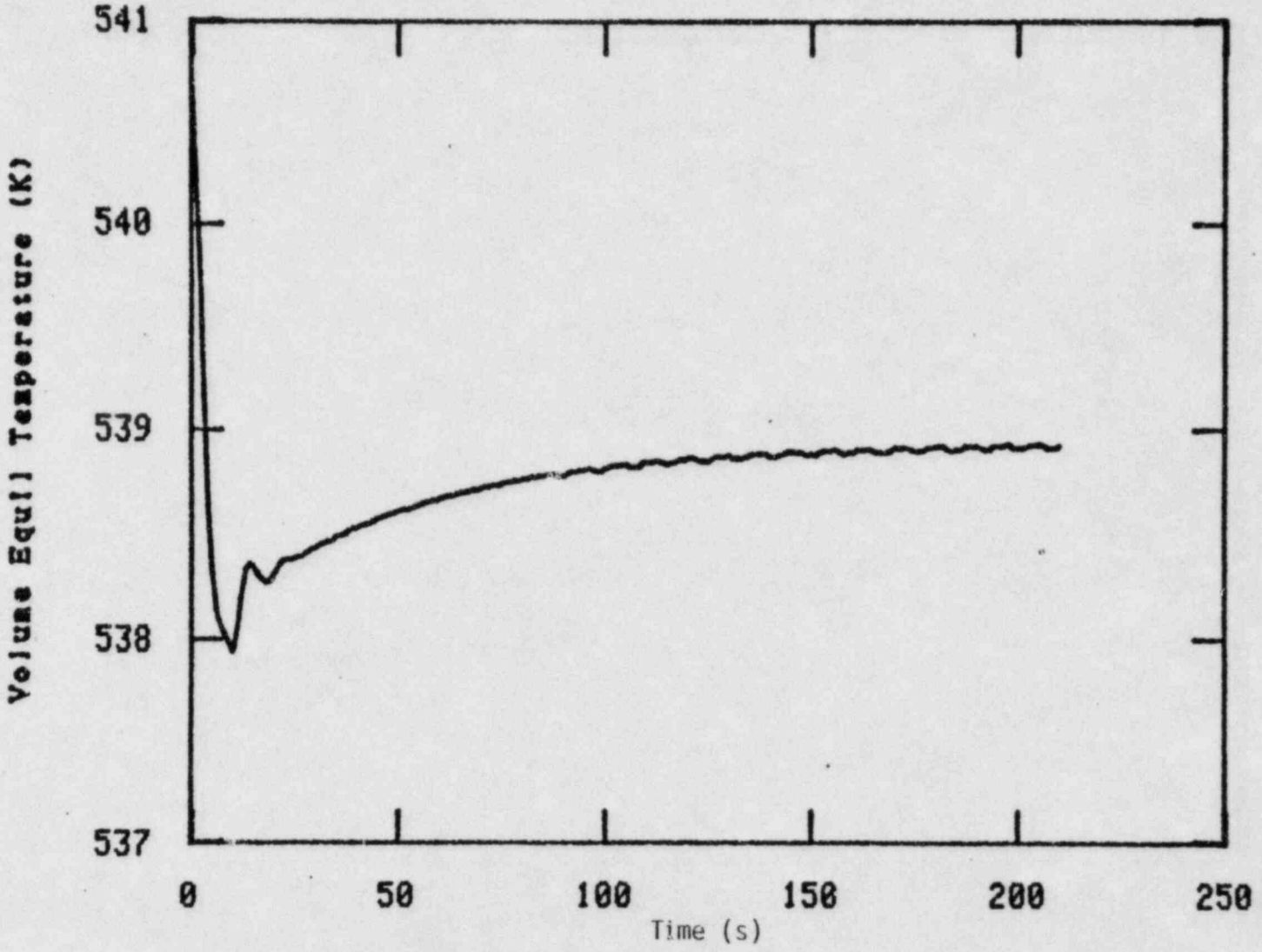

Figure 52. RELAP5/MOD1 steady state calculation of LOFT test L3-7 secondary system temperature.

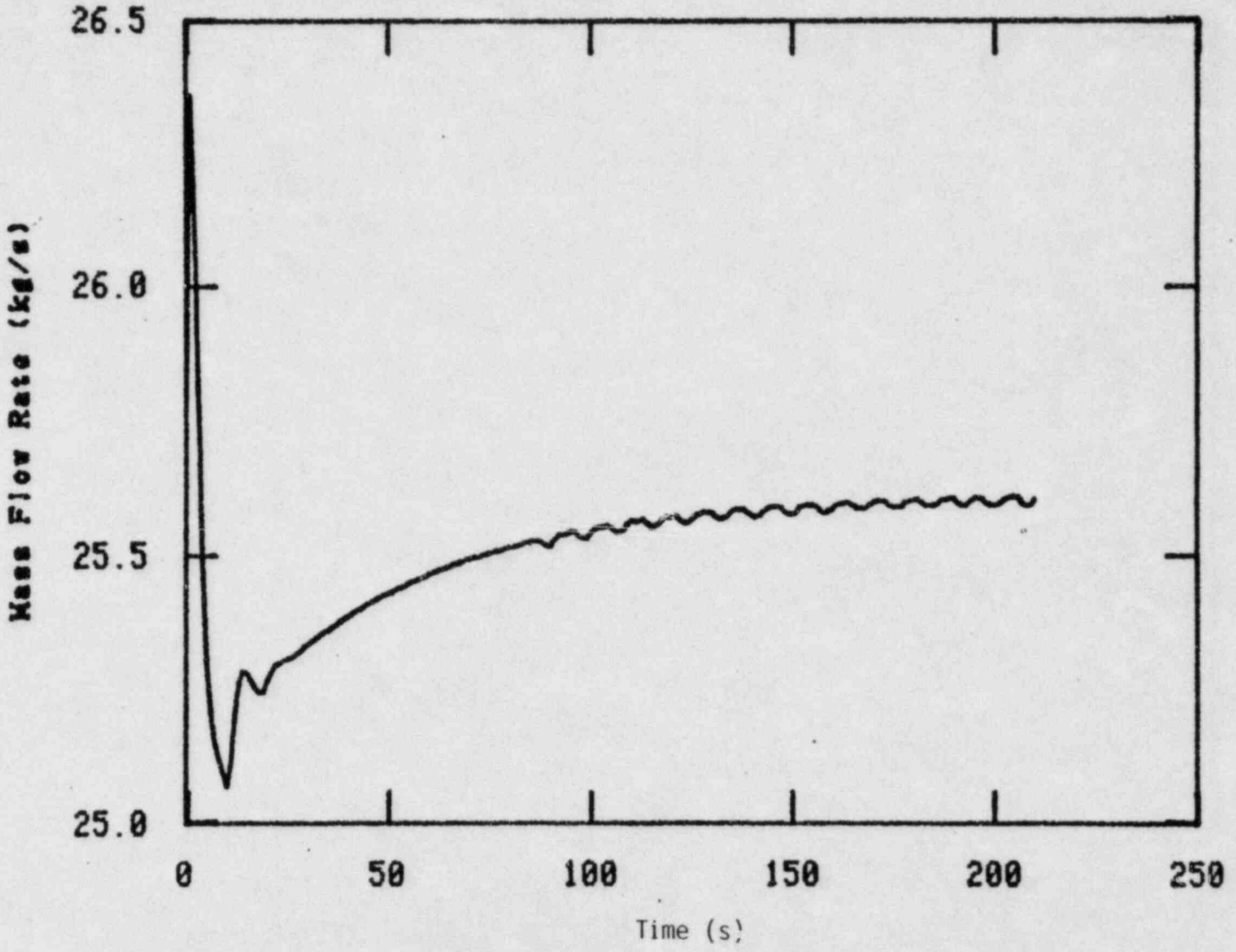

Figure 53. RELAP5/MOD1 steady state calculation of LOFT test L3-7 steam control valve mass flow rate.

test, extensive changes had to be made due to errors found in the original deck for the ECC System. These changes were made in conjunction with the LOFT group.[16] The renodalization deck is listed in Appendix L, and a nodalization diagram for the revised ECC system is given in Figure 54. Changes included removing Volume 605, inserting a valve (also numbered 605) between 610 and 600, correcting lengths and elevations, and correcting the energy loss coefficients. The accumulator began injecting between 5680 and 5690 seconds. The mass flow rate through the accumulator valve 605 was monitored and, unfortunately, this flow rate turned off and on between 5700 and 5900 seconds (Figure 55), even though the update in Appendix I was included. This update modified the momentum equations for a branch and was successful in eliminating the oscillation problem in Semiscale Test S-07-6. Due to lack of time, it was decided to terminate the run at 5900 seconds and to leave this problem as unresolved. No data for the accumulator flow rate were available due to an instrument failure.

To carry the calculation out to 5900 seconds required 9832 CPU seconds. Plots of the CPU time versus simulated time are shown in Figures 56 and 57, for both the run of this report (Cycle 17) as well as the run of the LOFT project posttest analysis (Cycle 10). Figure 56 shows the run out to 2000 seconds of simulated time, and it shows that the later cycle runs faster except in the first part. Figure 57 shows the whole run out to 5900 seconds, and it indicates the CPU time is significantly improved and half that of the earlier cycle.

The first comparisons that will be presented are for primary system pressure. Figure 58 is for the short term and Figure 59 is for the long term, both for Cycle 17. Figure 60 shows the same comparisons taken from the LOFT posttest analysis report[13] (Cycle 10), for both the short and long terms. The Cycle 17 run pressure stays high at 400 seconds rather than dropping with the data as does the Cycle 10 run. The reason for this is that the primary system cold leg temperature for Cycle 17 begins at 557 K while the temperature for Cycle 10 begins at 556 K. This 1 K temperature increase, which is the result of slightly different steady state end conditions, is enough to start the pressure out higher and to

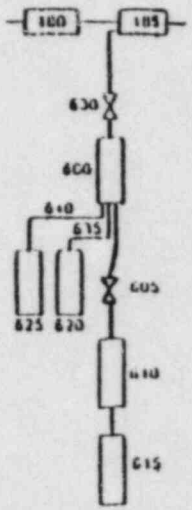

Figure 54. RELAP5/MOD1 renodalization for LOFT test L3-7 ECC system.

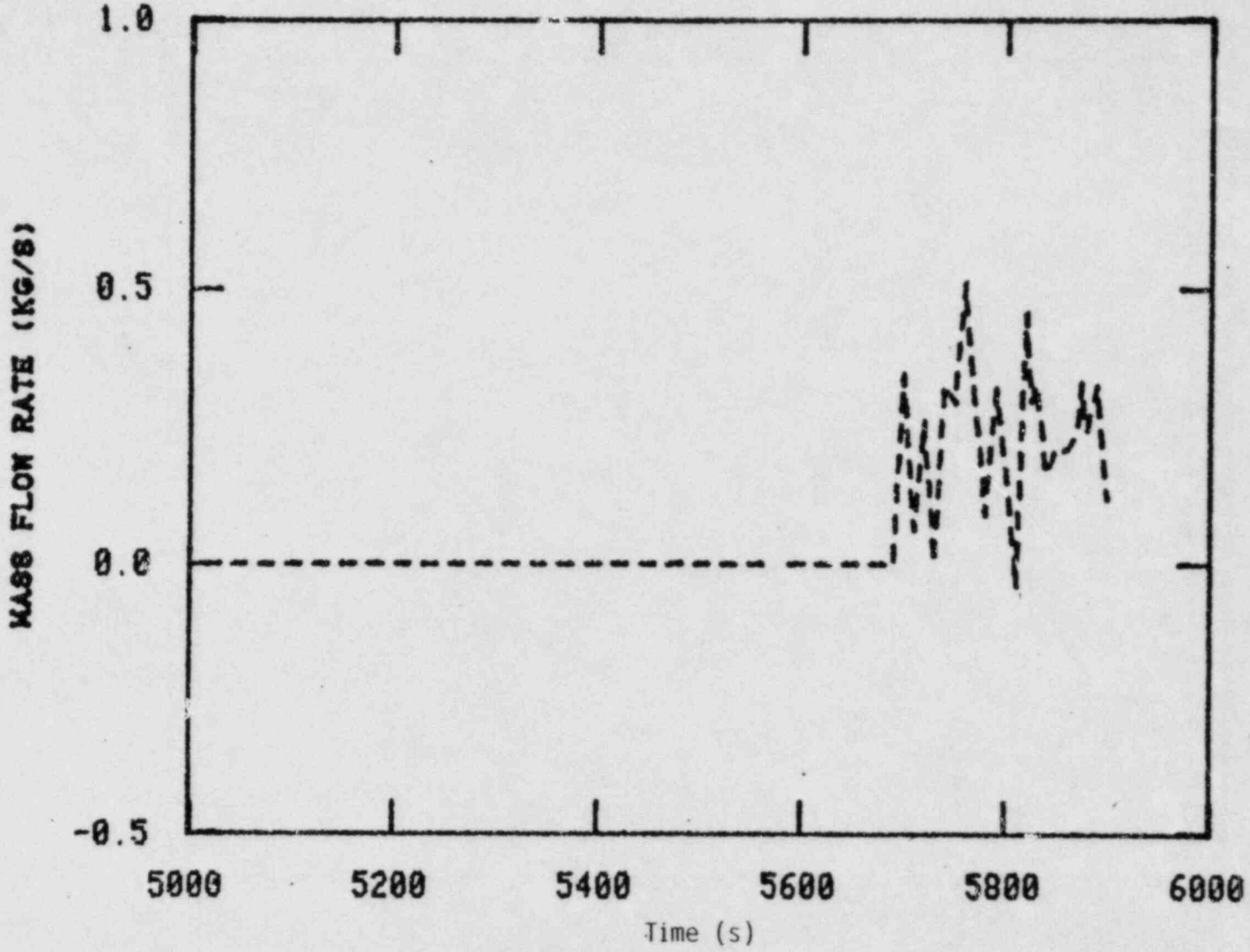

Figure 55. RELAP5/MOD1 calculation of LOFT test L3-7 mass flow rate through the accumulator valve.

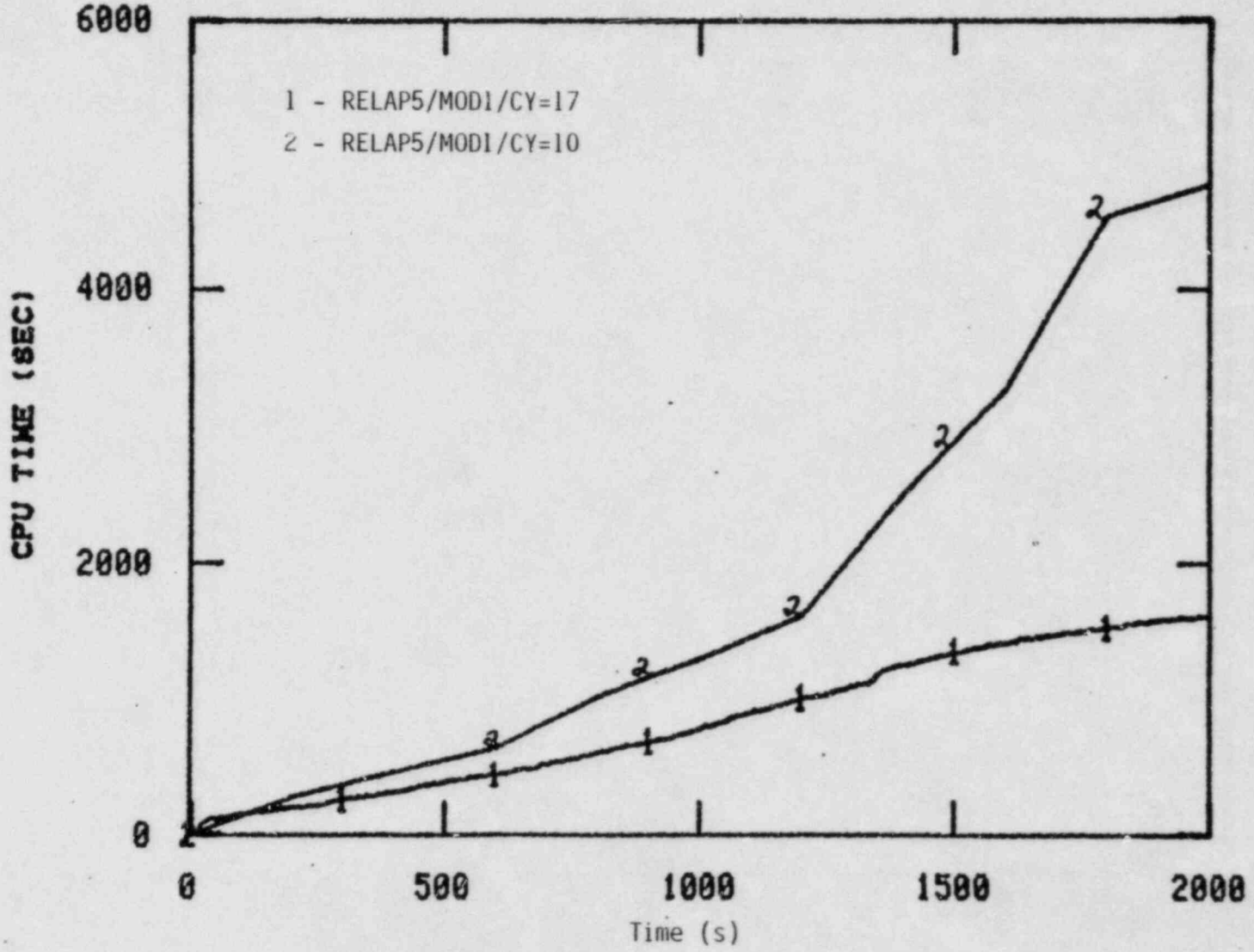

Figure 56. RELAP5/MOD1 CPU time versus simulated time for LOFT test L3-7 (short term).

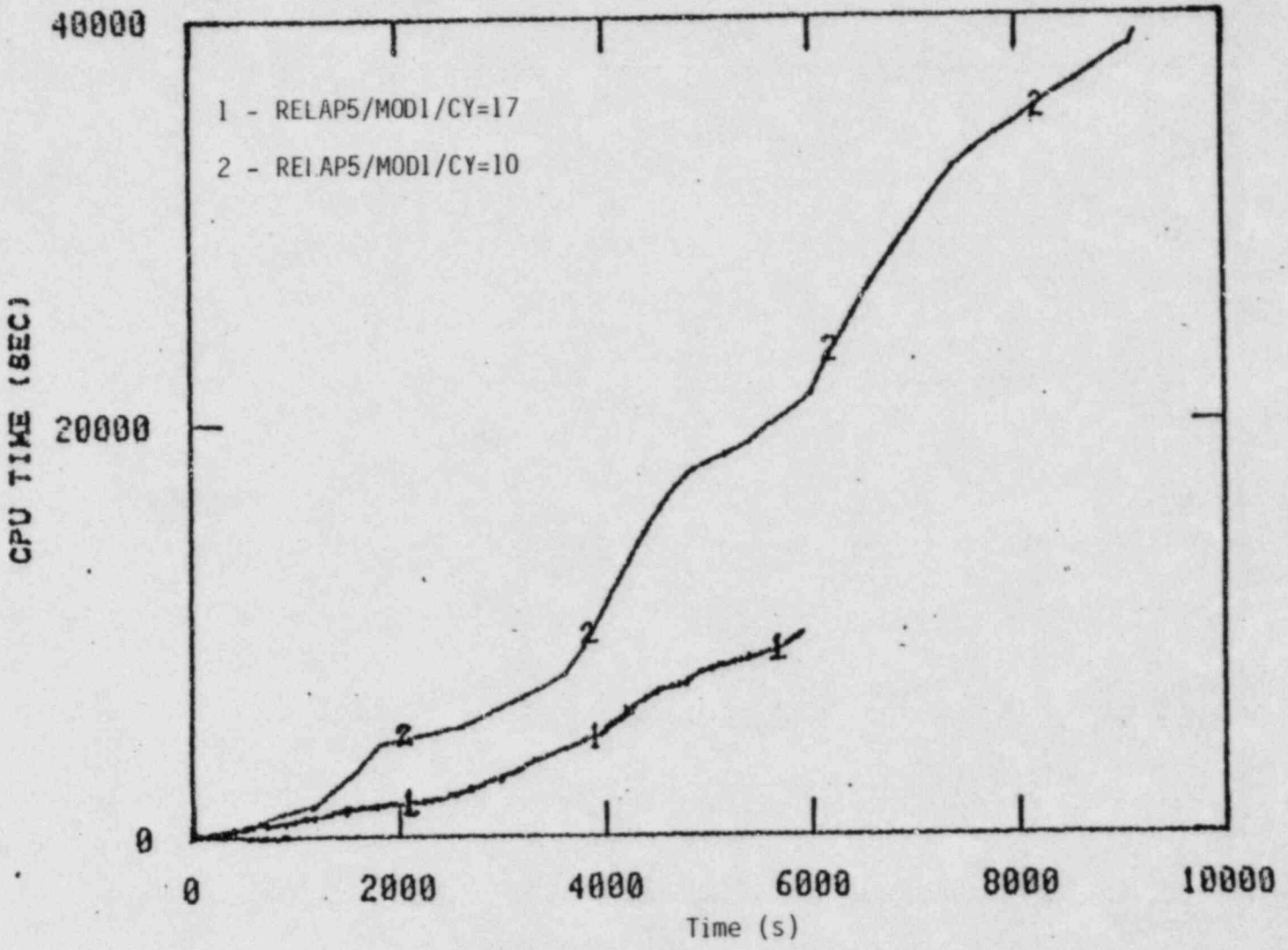

Figure 57. RELAP5/MOD1 CPU time versus simulated time for LOFT test L3-7 (long term).

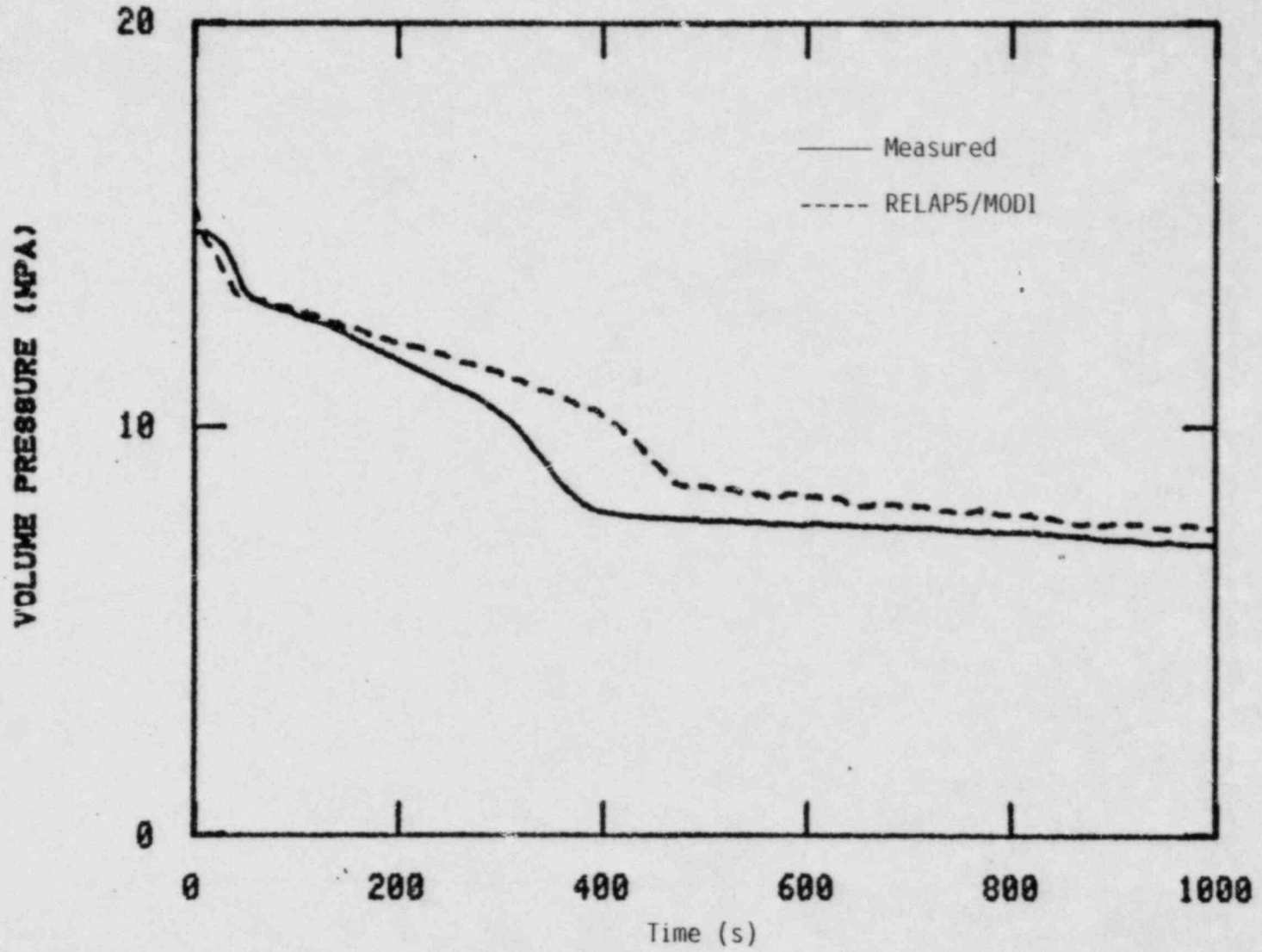

Figure 58. Measurement and RELAP5/MOD1 calculation of LOFT test L3-7 primary system pressure (short term).

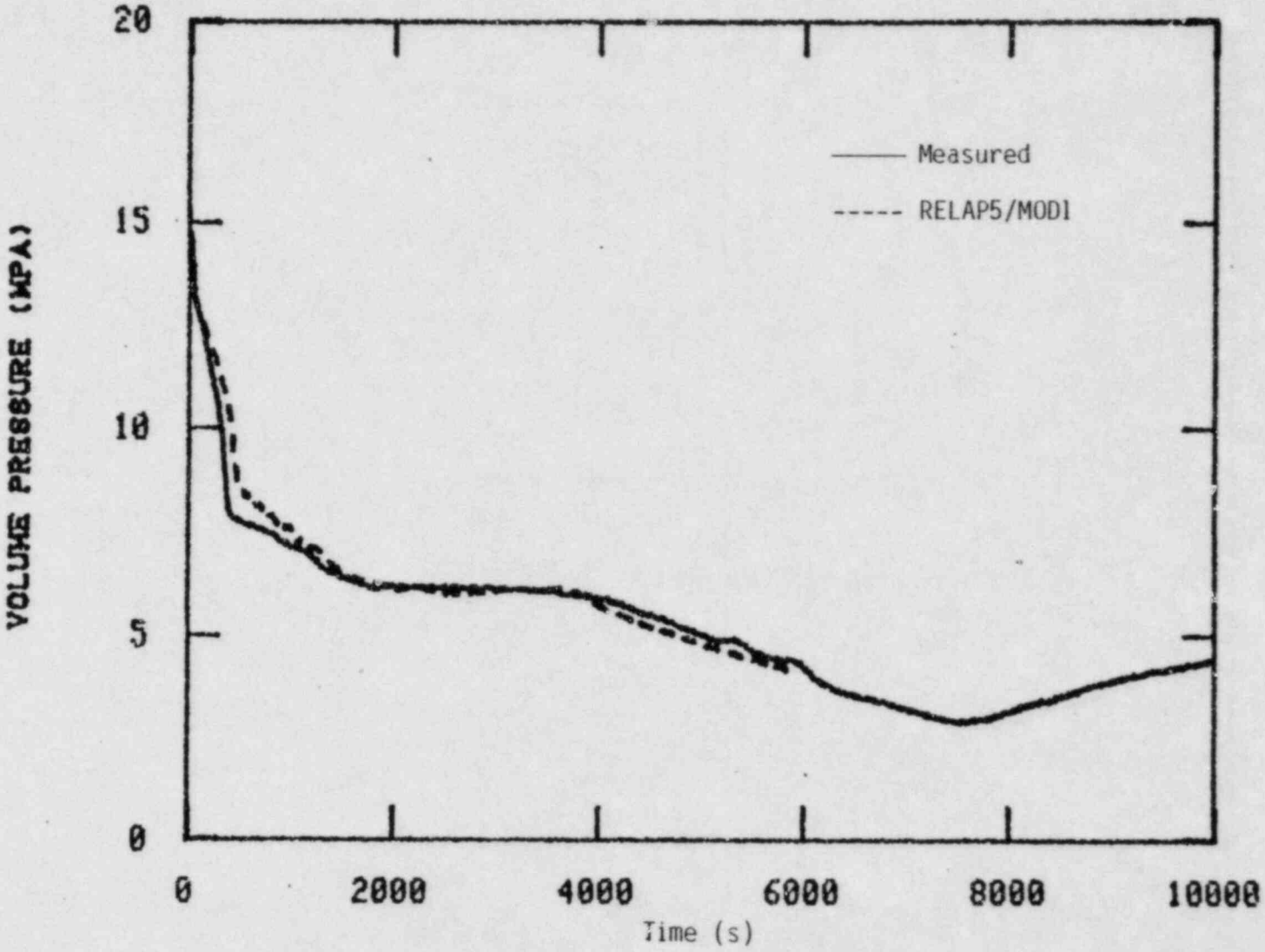

Figure 59. Measurement and RELAP5/MOD1 calculation of LOFT test L3-7 primary system pressure (long term).

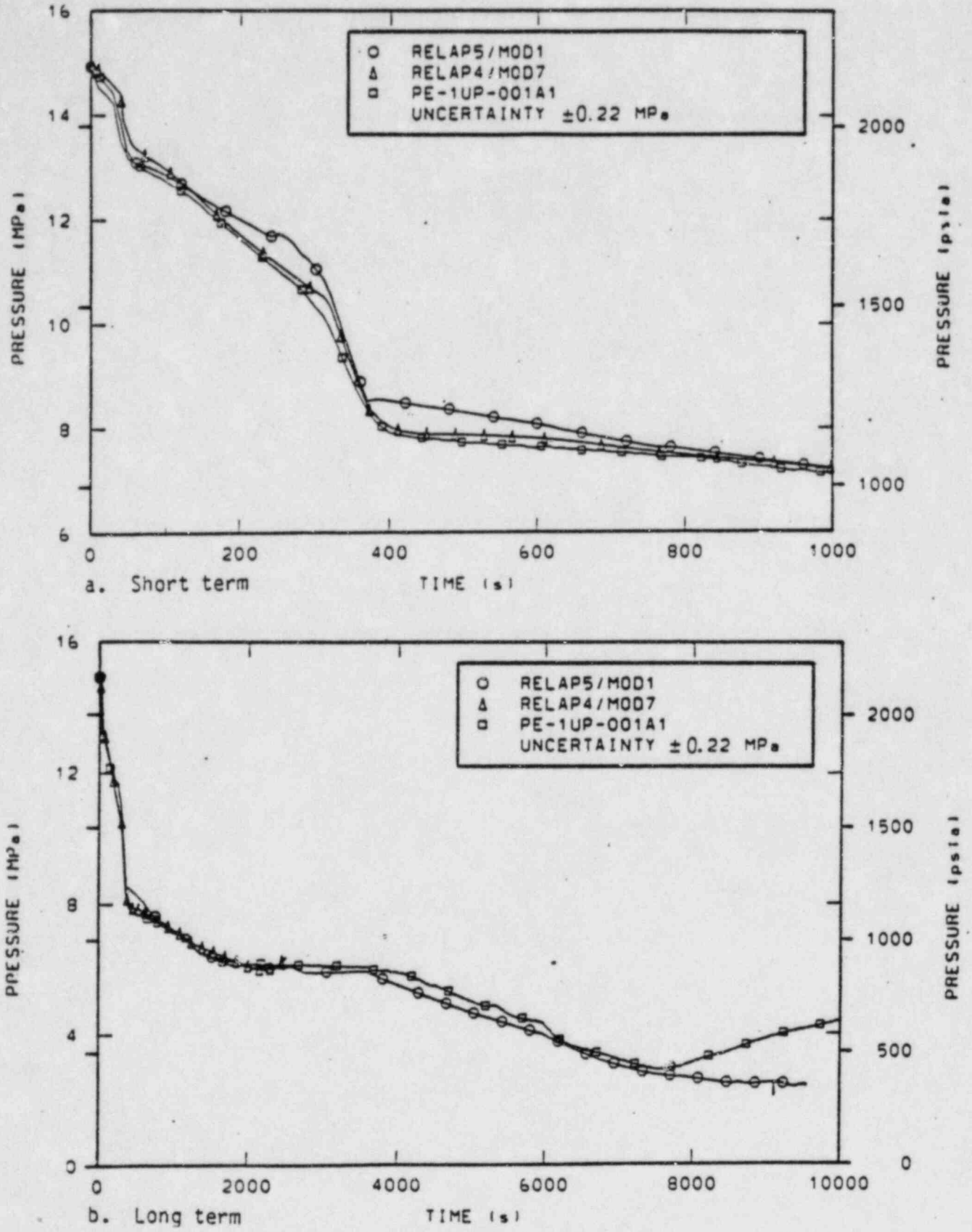

Figure 60. Comparison of posttest calculated to measured primary system pressure for LOCE L3-7.

keep it higher during the early part of the transient. In addition, when the drop does occur, it is late because of a high calculated temperature in the upper head. LOFT currently uses a different model, and this problem does not occur. Later on in the transient, Cycle 17 compares very well to the data and is similar to Cycle 10. The objective of this report was not to exactly match the data, and thus the slightly different steady state is acceptable. For a LOFT posttest analysis, this inaccuracy would be of more concern and its source would be investigated, i.e. core power, flows, heat transfer effective areas.

The next comparisons are for the secondary system pressure. Figure 61 is for the short term and Figure 62 is for the long term, both for Cycle 17. Figure 63 shows the same comparisons taken from the LOFT posttest analysis report (cycle 10), for short and long terms. The Cycle 17 calculation is much closer to the data than Cycle 10, although both show a decrease at 2000 seconds that is greater than the data (no explanation is evident for this behavior).

The next parameters of interest are the intact loop hot leg velocities for both vapor and liquid (Figures 64 and 65). The data presented for both velocities are the same pulsed-neutron-activation velocity measurements. During single-phase natural circulation early in the transient, the calculated velocities agree well with the data. The code then calculates a smooth transition from single-phase to two-phase natural circulation, and the calculated velocities during two-phase natural circulation were nearly double the measured values. The comparisons presented here using Cycle 17 are very similar to the results using Cycle 10.

Finally, other parameters of interest are core temperature difference, mass flow rate at the break, and density in the intact loop hot leg. These are shown in Figures 66, 67, and 68. The calculated core temperature difference using Cycle 17 was similar to that using Cycle 10, in that while the code calculated smooth transitions between natural circulation modes, the time of transition did not agree with the measured data. The break

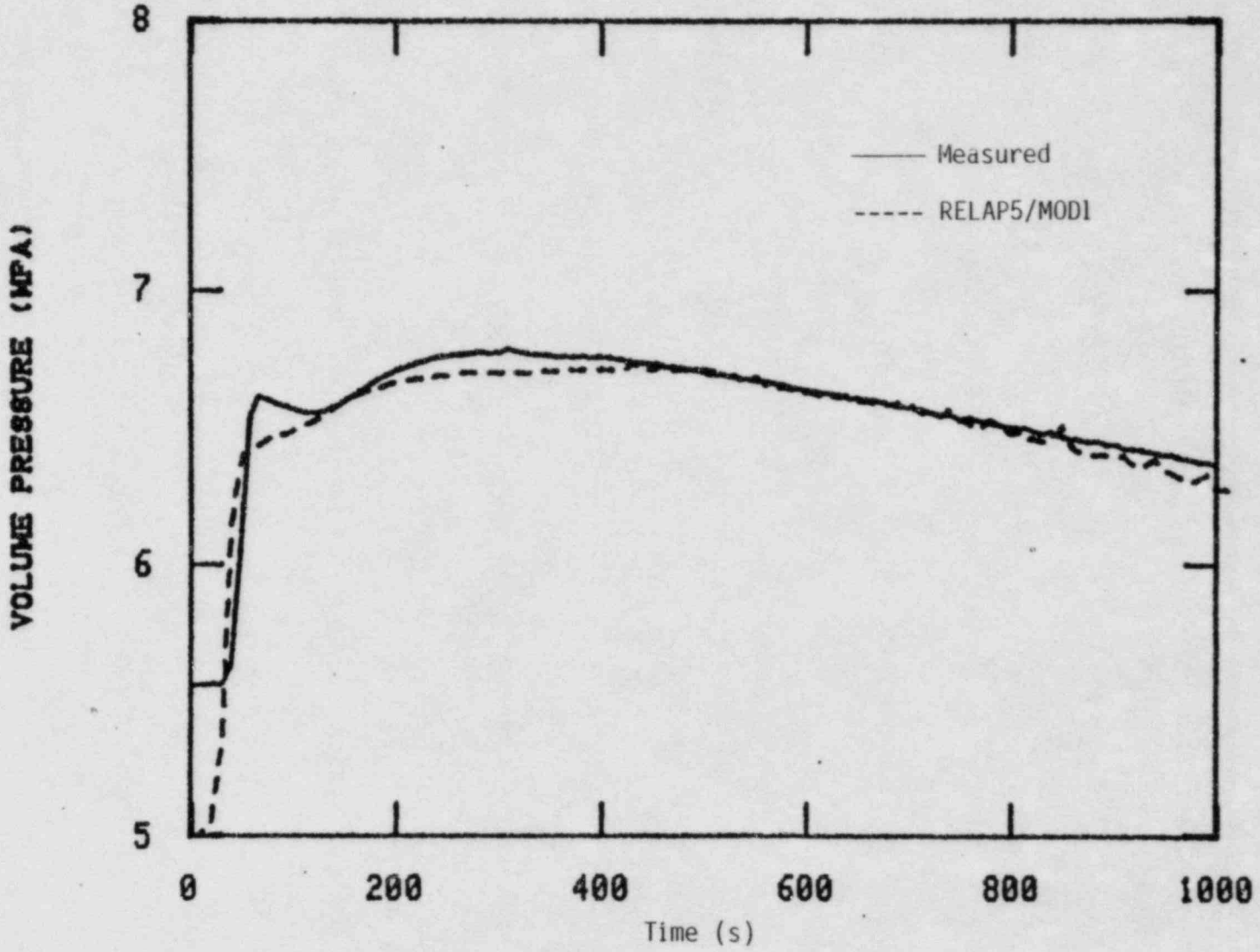

Figure 61. Measurement and RELAP5/MOD1 calculation of LOFT test L3-7 steam generator secondary pressure (short term).

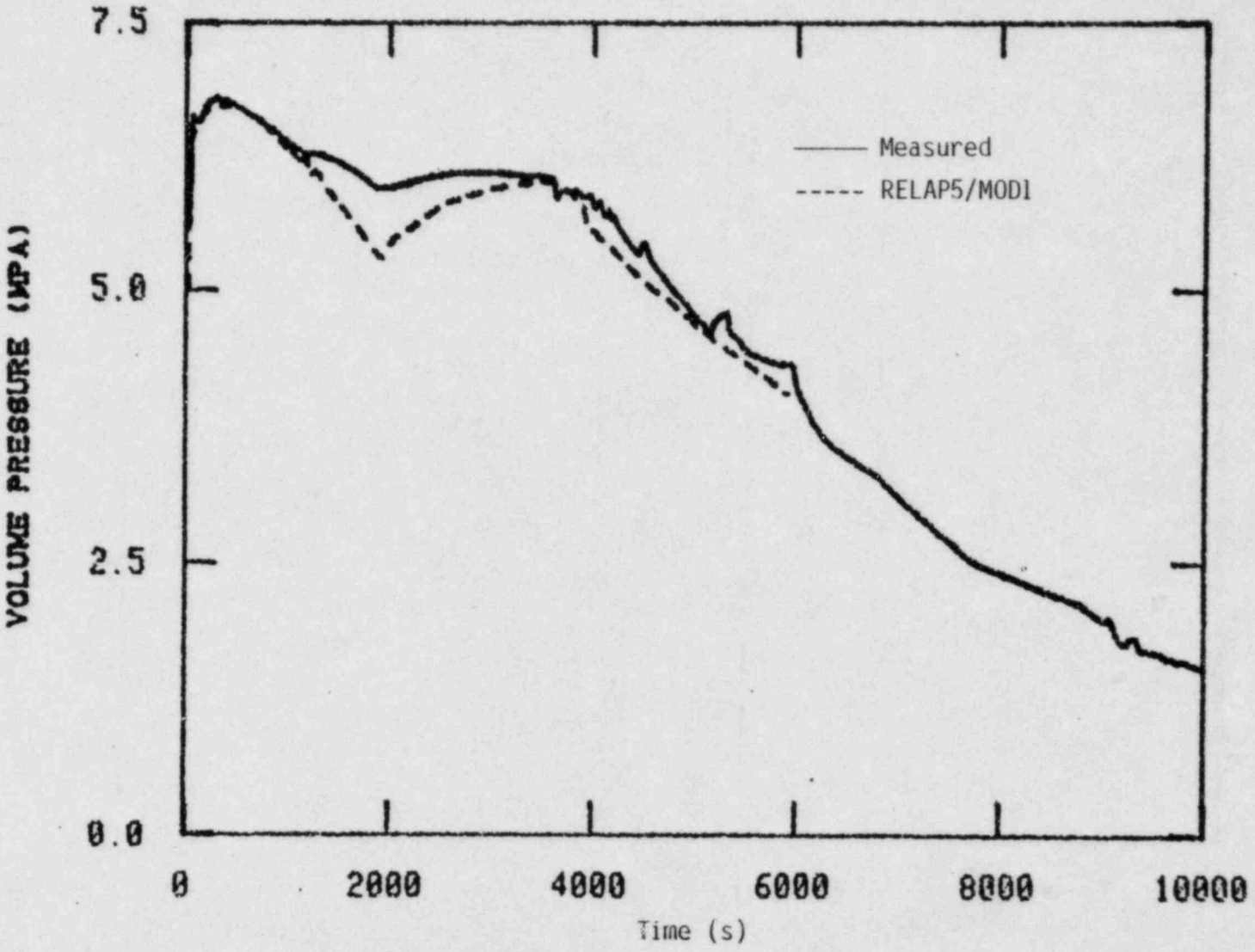

Figure 62. Measurement and RELAP5/MOD1 calculation of LOFT test L3-7 steam generator secondary pressure (long term).

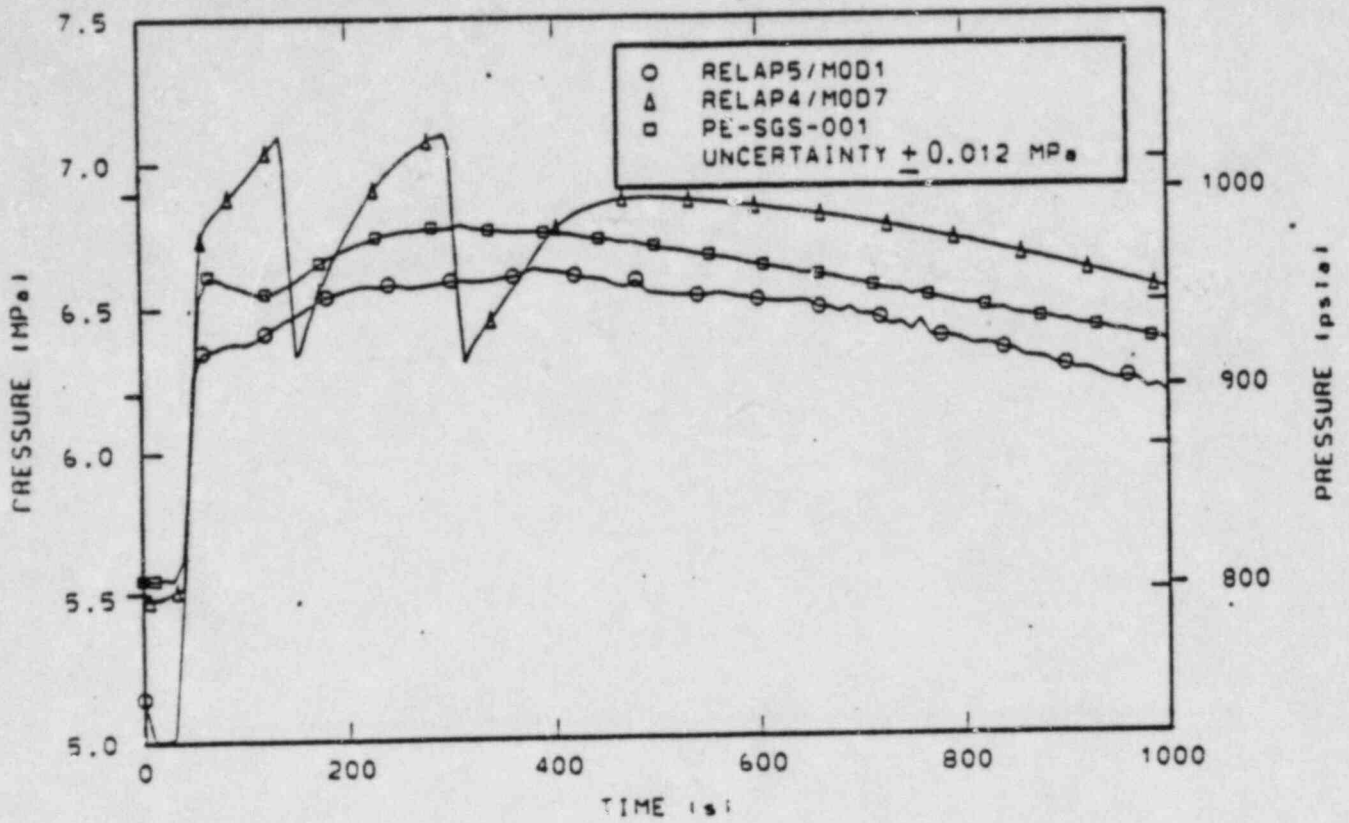

a. Short term

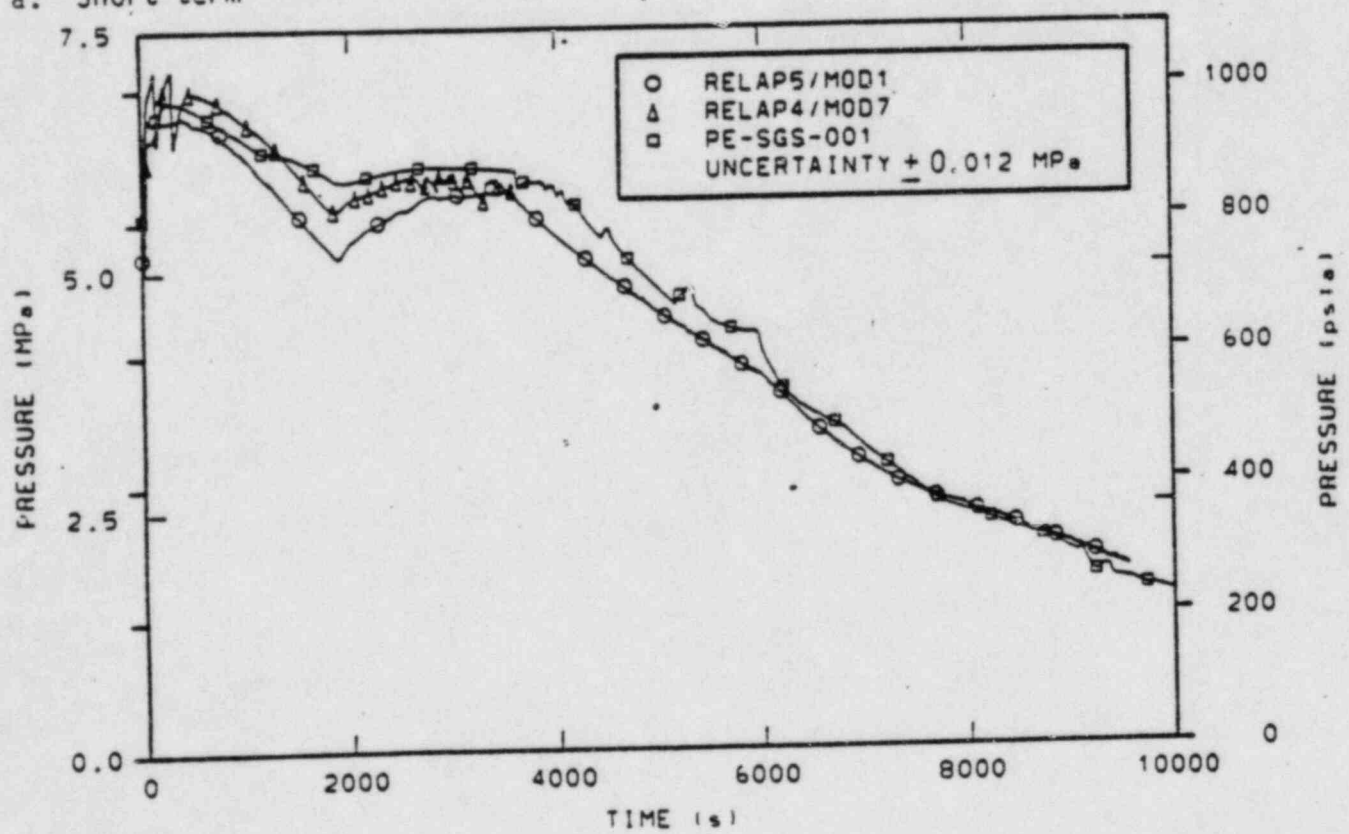

b. Long term

Figure 63. Comparison of posttest calculated to measured steam generator secondary pressure for LOCE L3-7.

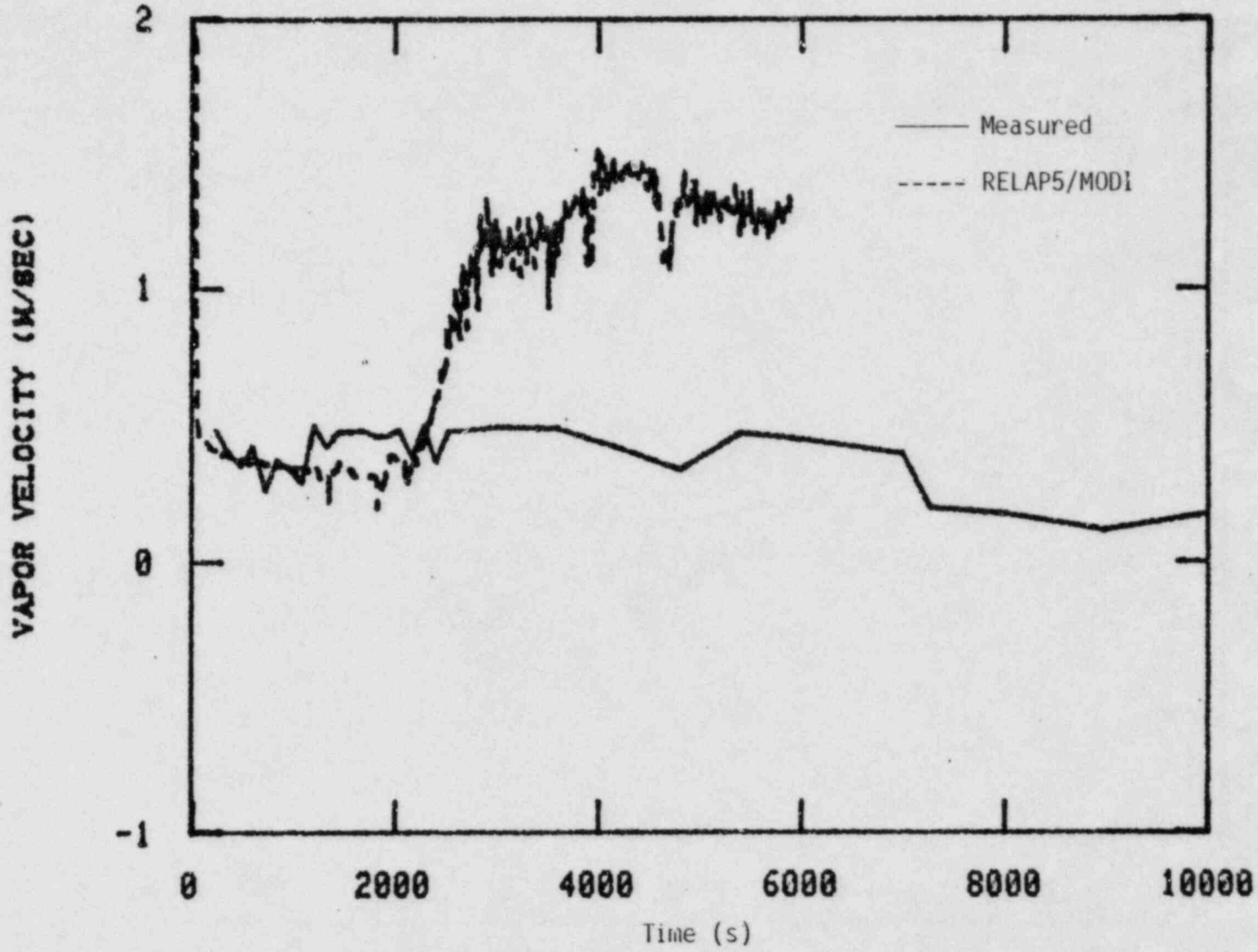

Figure 64. Measurement and RELAP5/MOD1 calculation of LOFT test L3-7 intact loop hot leg vapor velocity.

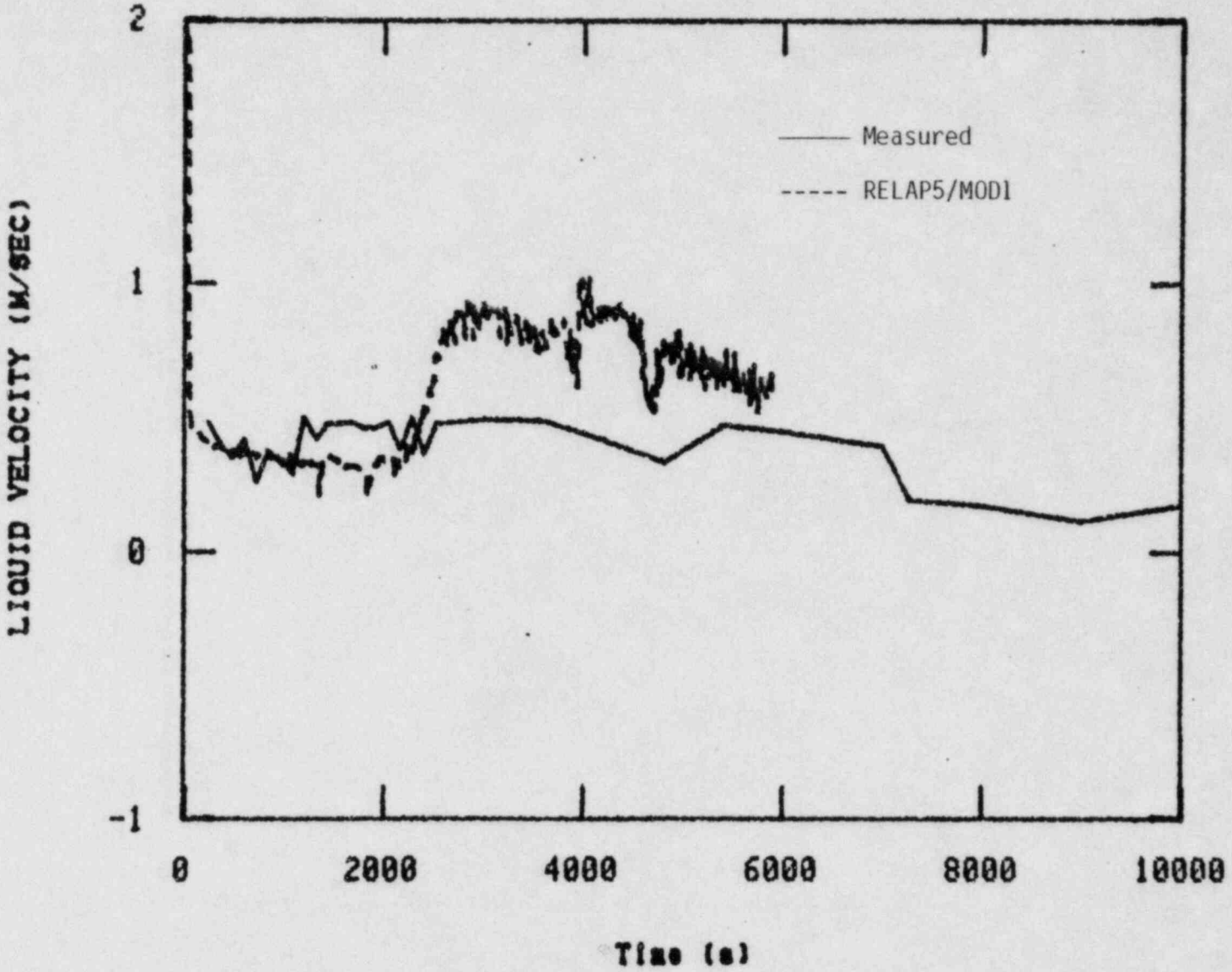

Figure 65. Measurement and RELAP5/MOD1 calculation of LOFT test L3-7 intact loop hot leg liquid velocity.

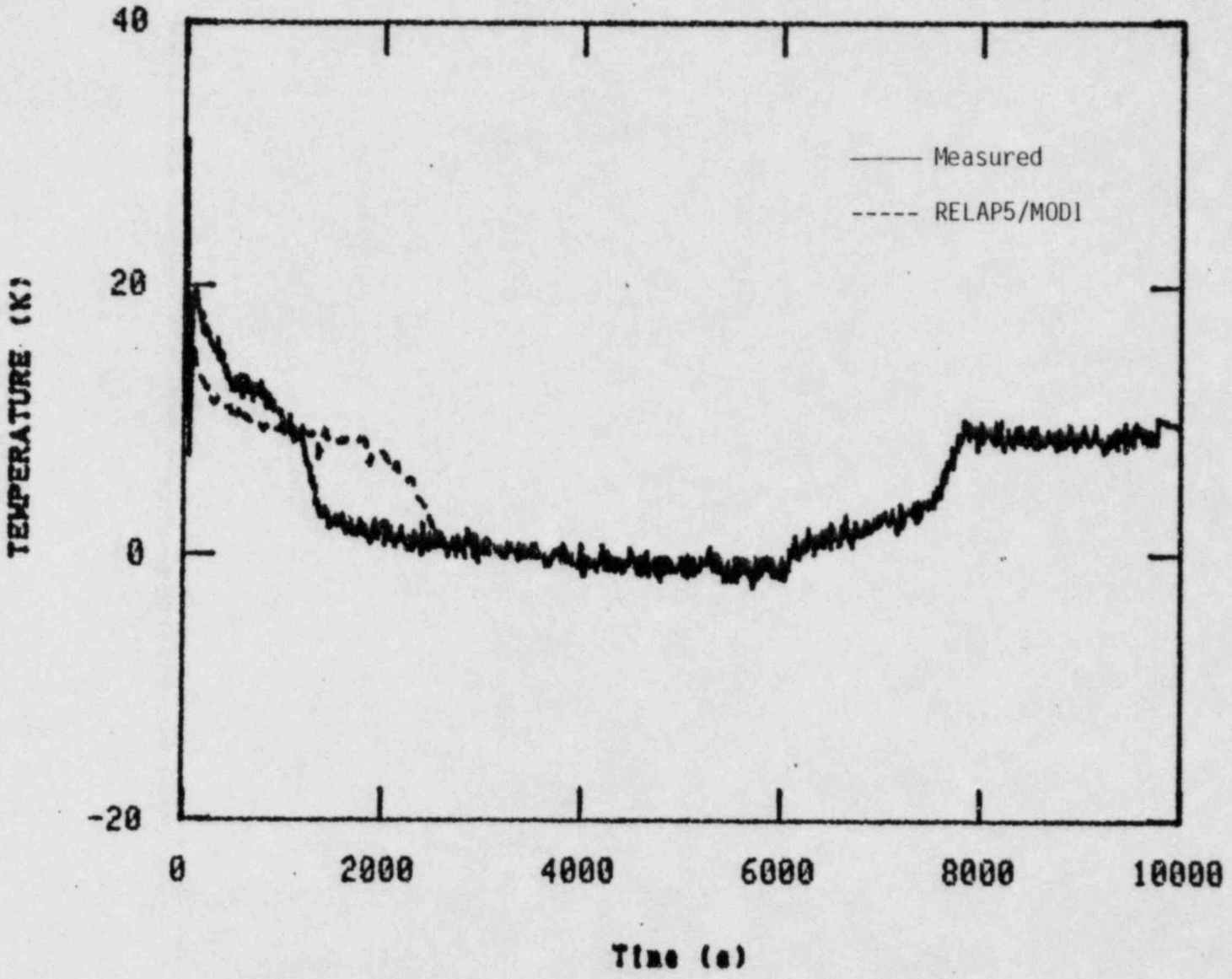

Figure 66. Measurement and RELAP5/MOD1 calculation of LOFT test L3-7 core temperature difference.

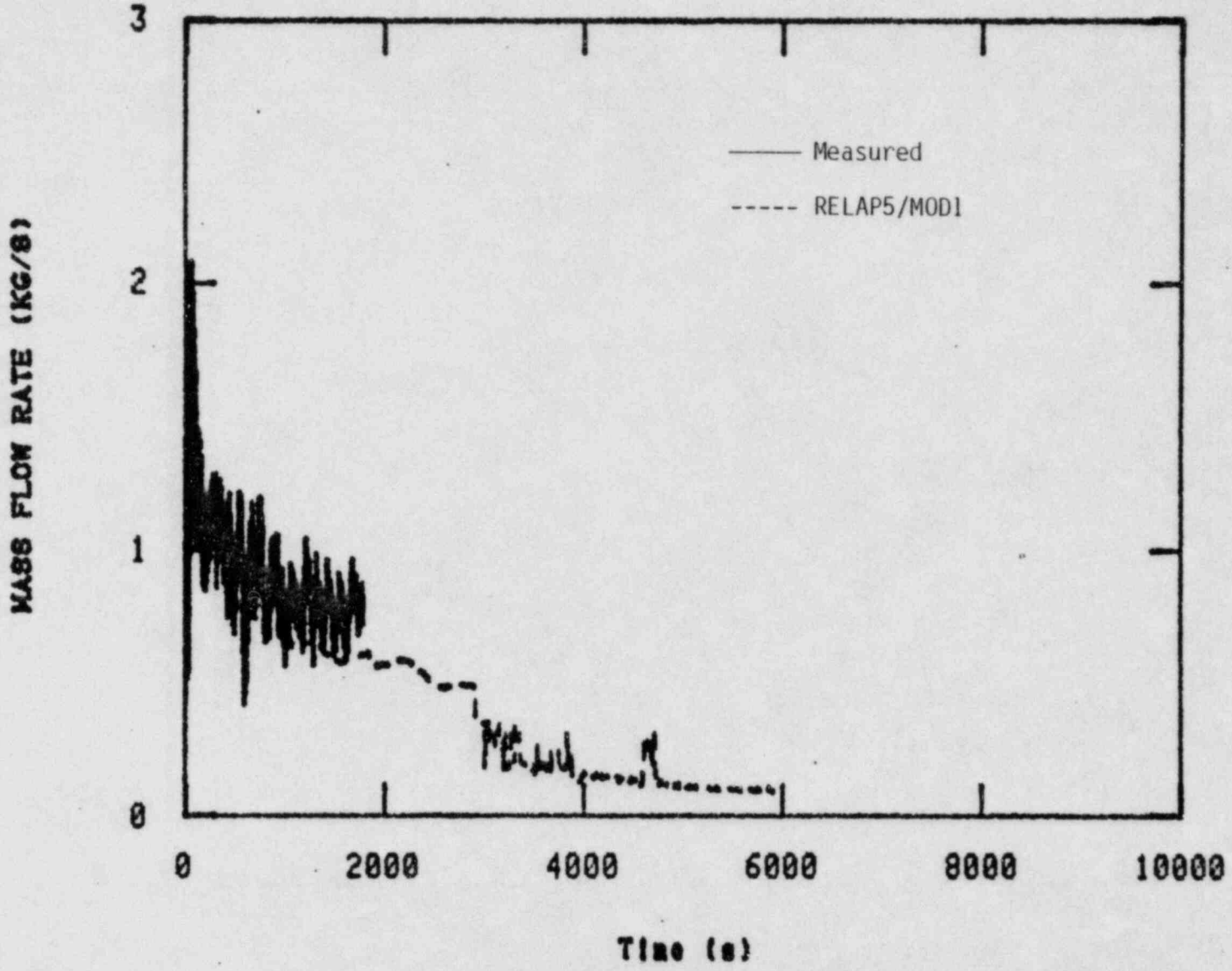

Figure 67. Measurement and RELAP5/MOD1 calculation of LOFT test L3-7 mass flow rate at the break.

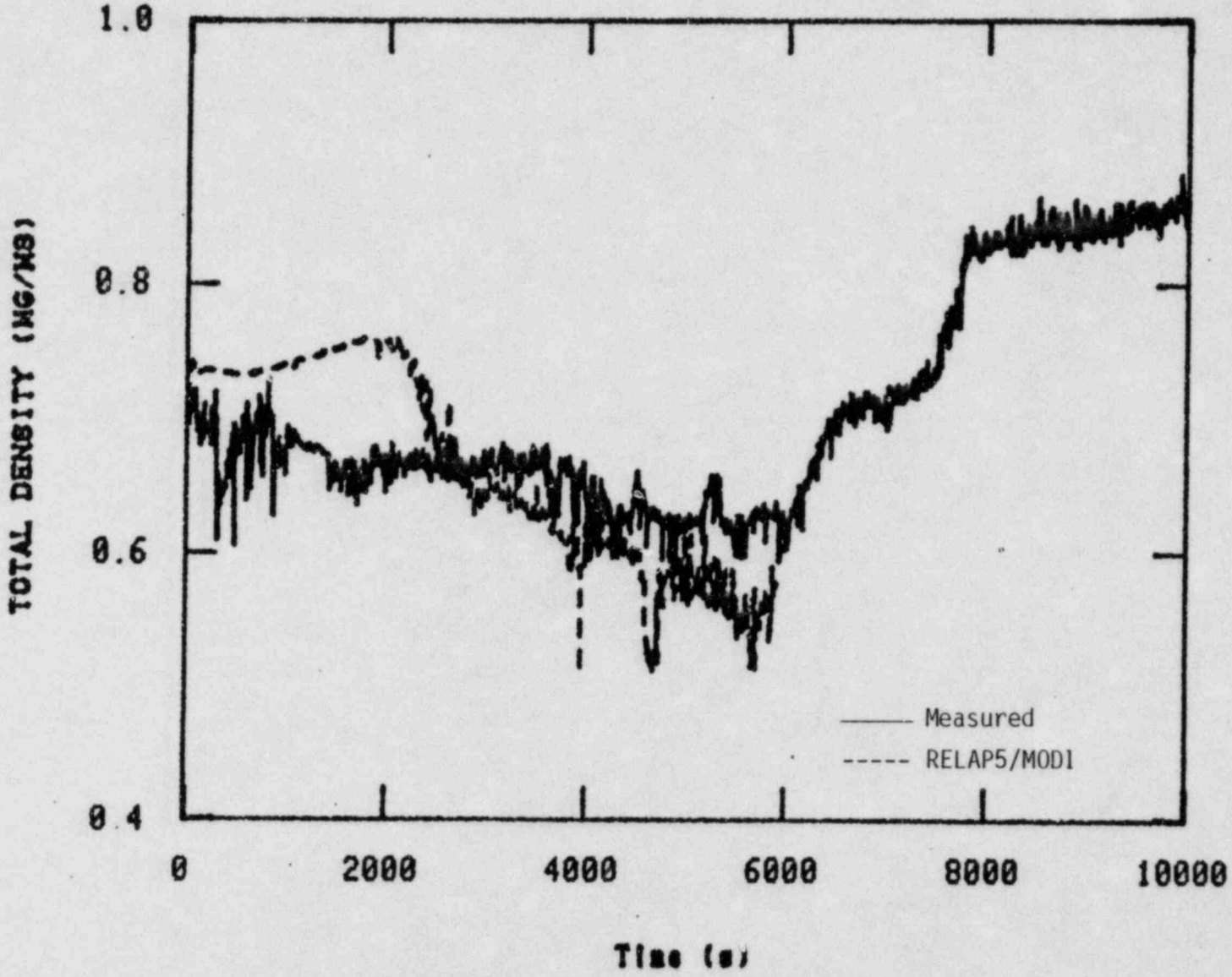

Figure 68. Measurement and RELAP5/MOD1 calculation of LOFT test L3-7 density in the intact loop hot leg.

mass flow rate and intact loop hot leg density comparisons were not presented in the LOFT L3-7 posttest analysis report using Cycle 10, but we present them here because they are usually important parameters for a break analysis. The code agrees well with the measured break mass flow rate, but unfortunately, the data ended shortly before 2000 seconds. With regard to intact loop hot leg density, the calculation was high during single-phase natural circulation (0 → 2000 seconds) and low during two-phase natural circulation (>2000 seconds).

In summary, RELAP5/MOD1 simulates many of the important parameters for the LOFT Test L3-7 quite well qualitatively. Quantitatively, the primary system pressure was too high early in the transient due to the approximate nature of the steady state. Also, the intact loop velocities were higher than the data in two-phase natural circulation, while the time of core temperature difference transitions did not agree with the data. The code run time was decreased two-fold from Cycle 10 to Cycle 17. The accumulator behavior remains in question and it was not clear whether modeling errors or code errors were responsible for the erratic behavior. Some continued effort will be required to resolve this.

3. CONCLUSIONS

This volume of the RELAP5/MOD1 documentation has been written to provide to users of the code: (a) information concerning applicability of the code, (b) examples of accepted modeling practice, and (c) some quantification of the code accuracy. A comprehensive assessment of the code capabilities is beyond the scope of this effort, but it should complement results from the independent assessment efforts. The results of the example problems are presented and both the highlights and the inadequacies of the code are discussed in order to present a balanced summary of the code capabilities.

In general, the test comparisons collaborate the nonhomogeneous modeling (interphase drag) in the code although the maximum time step requires user constraint in some cases to achieve a converged result. This was evident in both the General Electric Test 1004-3 and the Wyle small break Test WSB03R applications. It is recommended that the user perform at least a limited test for convergence by reducing/increasing the maximum permitted time step.

The integral experiment applications of the code indicate that the key system parameters are calculated for large and small break blowdown of a loss-of-coolant accident. The code execution time compared to transient simulation time varies widely depending upon the system model detail and the type of accident. For the case of the Semiscale S-07-6 test, the code ran quite slow, while for the LOFT L3-7 small break test, the code ran at twice real time. However, because of the differing time scales of interest (25 s for S-07-6 compared to 6000 s for L3-7) the overall calculational times for the two transients were comparable. The accumulator model cycled on and off during injection for Test L3-7. This behavior was not shown by the data and a brief review did not reveal modeling errors or errors in the accumulator model. Resolution of this discrepancy was beyond the scope of this task. Caution should be exercised in the use of the accumulator model. The predicted and measured core temperature difference for Test L3-7 showed a difference in transition to natural circulation. This difference could not be accounted for.

RELAP5/MOD1 represents a significant advance in modeling realism compared to its predecessors. However, there remain several areas of potential improvement in the basic physical model and in added component modeling capabilities. These areas are being addressed in the continued development. RELAP5/MOD2 will contain complete pressurized water reactor modeling capability and limited boiling water reactor capability. The physical models will also be substantially improved so that known limitations of the MOD1 version will be removed.

4. REFERENCES

1. J. A. Findlay, G. L. Sazzi, BWR Refill-Reflood Program--Model Qualification Task Plan, EPRI NP-1527, NUREG/CR-1899, GEAP-24898, October 1981.

2. N. Abauf, O. C. Jones, Jr., B. J. C. Wu, Critical Flashing Flow in Nozzles with Subcooled Inlet Conditions, BNL Informal Report, BNL-NUREG-27512, 1980.

3. L. Ericson, L. Gros d'Aillon, K. Kilpi, O. Sandervag, R. Schultz, J. Vidarsson, The Marviken Full-Scale Critical Flow Tests Interim Report; Results from Test 24, MXC-224, May 1979.

4. J. C. Lin, G. E. Gruen, W. J. Quapp, "Critical Flow in Small Nozzles for Saturated and Subcooled Water at High Pressure," Basic Mechanisms in Two-Phase Flow and Heat Transfer Symposium at the Winter Annual Meeting of the American Society of Mechanical Engineers, Chicago, Illinois, pp. 9-17, November 16-21, 1980.

5. H. H. Kuo, H. Chow, V. H. Ransom, "RELAP5 Horizontal Stratified Flow Model with Application to a Wyle LOFT Nozzle Calibration Experiment," ANS Specialists Meeting on Small Break Loss-of-Coolant Accident Analyses in LWRs, Monterey, California, pp. 6.91-6.110, August 25-27, 1981.

6. V. H. Ransom et al., RELAP5/MOD1 Code Manual, Volume 1, NUREG/CR-1826, EGG-2070, March 1982.

7. M. L. Patton, Semiscale Mod-3 Test Program and System Description, TREE-NUREG-1212, July 1978.

8. V. Esparza, K. E. Sackett, K. Stanger, Experiment Data Report for Semiscale Mod-3 Integral Blowdown and Reflood Heat Transfer Test S-07-6 (Baseline Test Series), NUREG/CR-0467, TREE-1226, January 1979.

9. H. H. Kuo, V. H. Ransom, D. M. Snider, "Calculated Thermal-Hydraulic Response for Semiscale Mod-3 Test using RELAP5-A New LWR System Analysis Code," Proceedings of the ANS/ASME/NRC International Topical Meeting on Nuclear Reactor Thermal-Hydraulics, Saratoga Springs, New York, volume 1, pp. 117-128, NUREG/CP-0014, October 5-8, 1980.

10. M. T. Leonard, RELAP5 Standard Model Description for the Semiscale MOD-2A System, EGG-SEMI-5692, December 1981.

11. D. L. Reeder, LOFT System and Test Description (5.5 ft. Nuclear Core/LOCEs), NUREG/CR-0247, TREE-1208, July 1978.

12. D. L. Gillas, J. M. Carpenter, Experimental Data Report for LOFT Nuclear Small Break Experiment L3-7, NUREG/CR-1570, EGG-2049, August 1980.

13. W. H. Grush, G. E. McCreery, Posttest Analysis of Loss-of-Fluid Tests L3-2 and L3-7, EGG-LOFT-5632, October 1981.

14. E. J. Kee, P. J. Schally, L. Winters, Base Input for LOFT RELAP5 Calculation, EGG-LOFT-5199, July 1980.

15. W. H. Grush, private communication, 1982.

16. T. H. Chen, private communication, 1982.

Flyer sheet

APPENDIX A
UPDATE USED IN ALL SIMULATIONS

APPENDIX B

INPUT DECK FOR GE LEVEL SWELL TEST 1004-3

APPENDIX C

INPUT DECK FOR MARVIKEN TEST 24

APPENDIX D

INPUT DECK FOR WYLE SMALL BREAK TEST WSB03R

APPENDIX E

INPUT DECK FOR SEMISCALE MOD-3 S-07-6 POSTTEST ANALYSIS

APPENDIX F

UPDATE USED FOR SEMISCALE MOD-3 S-07-6 AND LOFT L3-7 POSTTEST ANALYSES THAT UPDATES ACCUMULATOR COMPONENT

APPENDIX G
RENODALIZATION DECK FOR SEMISCALE MOD-3 S-07-6 POSTTEST ANALYSIS

APPENDIX H

UPDATE USED FOR SEMISCALE MOD-3 S-07-6 POSTTEST ANALYSIS THAT TURNS PUMP DISSIPATION OFF

APPENDIX I

UPDATE USED FOR SEMISCALE MOD-3 S-07-6 AND LOFT L3-7 POSTTEST ANALYSES THAT MULTIPLIES VISC TERM BY 1/2 $ARAT^2$

APPENDIX J

INPUT DECK FOR LOFT L3-7 POSTTEST ANALYSIS

APPENDIX K

UPDATE USED FOR LOFT L3-7 POSTTEST ANALYSIS THAT UPDATES THE PUMP COMPONENT

APPENDIX L
RENODALIZATION DECK FOR LOFT L3-7 POSTTEST ANALYSIS